Research Programme of the Research Fund for Coal and Steel

Steel RTD

Project carried out with a financial grant of the

Research Programme of the Research Fund for Coal and Steel

Draft Final Report

Technical Report No: 6

Period of Reference: 01/07/2008 – 30/06/2011

Technical Group: TGS8 "Steel products and applications for buildings, construction and industry"

Robustness of car parks against localised fire

Project acronym: ROBUSTFIRE

Grant Agreement Number: Contract N° RFSR-CT-2008-00036

Beneficiaries: University of Liège - ULGG (Belgium)
Imperial College of science, technology and medicine – ICST (United Kingdom)
Faculdade de Ciencias e Tecnologia da Universidade de Coimbra – FCTUCOIMBRA (Portugal)
Arcelormittal Belval & Differdange – ARCELORPROFIL (Luxembourg)
Centre Scientifique et Techinique du Bâtiment - CSTB (France)
Greisch Ingénierie – GREISCH (Belgium)
Centre Technique Industriel de la Construction Métallique – CTICM (France)

Location: ULGG, Place du 20 août, 7 4000 Liège Belgium
ICST, South Kensington Campus, SW7 2 AZ, London, UK
FCTUCOIMBRA, Rua Silvio Lima, Universidade de Coimbra Polo I, 3030-790 Coimbra, Portugal
ARCELORPROFIL, Rue de Luxembourg, 66, 4221 Esch-sur-Alzette, Luxembourg
CSTB, Avenue Jean Jaurès, 84, 77420 Champs sur Marne, France
GREISCH, Allée des Noisetiers, 25, 4031 Liège, Belgium
CTICM, Espace Technologique l'Orme des MPessieurs, Immeuble Apollo, 91193 Saint-Aubin, France

Co-ordinator: Jean-Pierre Jaspart, University of Liège

Authors: Jean-François Demonceau (ULGG)

Clara Huvelle (ULGG)

Ludivine Comeliau (ULGG)
Long Van Hoang (ULGG)
Jean-Pierre Jaspart (ULGG)
Cheng Fang (ICST)
Bassam Izzuddin (ICST)
Ahmed Y. Elghazouli (ICST)
David A. Nethercot (ICST)
Bin Zhao (CTICM)
Nicolas Taillefer (CSTB)
Dhionis Dhima (CSTB)
Frédéric Gens (GREISCH)
Cécile Haremza (FCTUCOIMBRA)
Aldina Santiago (FCTUCOIMBRA)
Luis Da Silva (FCTUCOIMBRA)
Renata Obiala (ARCELORPROFIL)

Commencement Date: 01/07/2008

Completion Date: 31/06/2011

I. Distribution list

TGS8 members:

- CHAIRMAN: **Louis–Guy CAJOT**, Arcelormittal Belval & Differdange S.A.
  lg.cajot@arcelormittal.com
- **Nancy BADDOO**, The Steel Construction Institute
  n.baddoo@steel-sci.com
- **Darko BEG**, Univerza V Ljudljana
  dbeg@fgg.uni-lj.si
- **Anthony KARAMANOS**, A.S. Karamanos & Associates
  karama@otenet.gr
- **Andrzej KLIMPEL**, Silesian University of Technology – Politechnika Slaska
  andrzej.klimpel@polsl.pl
- **Mr Jouko KOUHI**, Finnish Constructional Steelwork Association
  jouko.kouhi@fcsa.fi
- **Joaquín ORDIERES MERE**, Universidad De La Rioja
  joaquin.ordieres@unirioja.es
- **Walter SALVATORE**, Universita Di Pisa – Dipartemento Di Ingegneria Strutturale
  walter@ing.unipi.it
- **Adam BANNISTER**, Corus UK LTD – Swinden Technology Centre
  adam.bannister@corusgroup.com
- **Thierry BRAINE-BONNAIRE**, Arcelor France S.A.
  thierry.brainebonnaire@arcelormittal.com
- **Giuseppe DEMOFONTI**, Centro Sviluppo Materiali SPA
  g.demofonti@c-s-m.it
- **Gerhard KNAUF**, Salzgitter Mannesmann Forschung GmbH
  g.knauf@du.szmf.de
- **Antonio Augusto FERNANDES**, Faculdade De Engenharia Da Universidade Do Porto
  aaf@fe.up.pt

II. Table of contents

III. Abstract

The increase of the market shares for steel and composite car parks in Europe is somewhat limited by the lack of information on how these structures behave under exceptional localised fire resulting from the burning of cars. In the present project, a general philosophy for the design of robust structures against exceptional events is developed and practical design guidelines for its application to car parks under localised fire are derived.

To achieve it, the following project objectives were had been identified:

- Review current practice and state of the art in the design and assessment of car parks subject to localised fire, and propose potentially robust structural schemes for subsequent investigation.
- Develop and validate detailed numerical models as well as simplified analytical models of the fire response of critical structural components, including columns, connections and beams.
- Propose a system level approach for simplified analytical modelling of steel composite car parks under localised fire, and verify against validated numerical modelling.
- Develop a robustness assessment approach for steel composite car parks under fire, to be event independent as far as possible, and propose relevant and practical design guidance.
- Demonstrate using a real case study the accuracy and practicality of the developed analytical models, robustness assessment approach and corresponding design guidance.

In the present report, it is demonstrated how these objectives have been achieved, using experiences gained from previous or ongoing RFCS projects related to various individual aspects (temperature distribution, joint behaviour …) and performing new and innovative experimental, numerical and analytical developments.

IV. Project overview

CATEGORY OF RESEARCH:	STEEL
TECHNICAL GROUP:	TGS 8
REFERENCE PERIOD:	01/07/2008 – 30/06/2011
GRANT AGREEMENT N°:	Contract N° RFSR-CT-2008-00036
PROJECT N°:	
TITLE:	ROBUSTFIRE – Robustness of car parks against localised fire
BENEFICIARIES:	University of Liège (Belgium) Imperial College of science, technology and medicine (United Kingdom) Faculdade de Ciencias e Tecnologia da Universidade de Coimbra (Portugal) Arcelormittal Balval & Differdange (Luxembourg) Centre Scientifique et Techinique du Bâtiment (France) Greisch Ingenierie (Belgium) Centre Technique Industriel de la Construction Métallique (France)
COMMENCEMENT DATE:	01/07/2008
COMPLETION DATE:	30/06/2011
NEW COMPLETION DATE:	NO
WORK UNDERTAKEN:	- Realisation of benchmark studies for the validation of numerical tools - Experimental, numerical and analytical investigations on structural elements - Numerical investigations on structures or substructures - Development of sophisticated and simplified numerical and analytical models - Design of a study case and investigation of its behaviour under the considered scenario

MAIN RESULTS:	- All the deliverables are available - Experimental test results on joints at elevated temperature available - Proposal of a multi-level approach for numerical analyses of car park structures under the considered scenario - Proposal of a simplified analytical model to predict the response of car park structures under the considered scenario
FUTURE WORK TO BE UNDERTAKEN:	- The importance of the plastic elongation of the connections and members at the beam extremities for the derivation of the membrane effects in the floors has been pointed out. In the project, realistic values have been taken from literature; but extra research investigations aiming at developing an analytical prediction would be required.
ON SCHEDULE (*YES /NO)*:	YES
PROBLEMS ENCOUNTERED:	Delays have been encountered for the finalisation of WP2 and WP3 due to a delay in the realisation of the experimental tests
CORRECTION – ACTIONS *(USE OF A TABLE IS RECOMMENDED)*:	-
BUDGET INFORMATION PER PARTNER:	See the table here below
TOTAL BUDGET (EURO) :	1266395.05 euro

PUBLICATIONS – PATENTS :	*Published:* Fang, C., Izzuddin, B.A., Elghazouli, A.Y., Nethercot, D.A. (2011) Robustness of Steel-composite Building Structures Subject to Localised Fire. Fire Safety Journal, 46(6), pp. 348-363. Cécile Haremza, Aldina Santiago and Luís Simões da Silva. Experimental behaviour of heated composite joints subject to variable bending moments. Eurosteel, 6th European Conference on Steel and Composite Structures, Proceedings of the conference edited by László Dunai et al., Budapest, Hungary, August 2011. C. Haremza, A. Santiago and L. Simões da Silva. Behaviour of heated composite joints - Preliminary numerical studies. University of Coimbra. ASFE, Application of Structural Fire Design, COST Action TU0904, Prague, April 2011. J.F. Demonceau, C. Comeliau and J.P. Jaspart. « Robustness of building structures – Recent developments and adopted strategy », Eurosteel 2011 "6th International conference on Steel and Composite Structures", Budapest, Hungary, pp. 2475-2480. J.F. Demonceau, L. Comeliau and J.P. Jaspart. « Robustness of building structures – recent developments and adopted strategy », Steel Construction journal, Vol. 3, September 2011, pp. 166-170 (paper selected amongst the Eurosteel 2011 paper) *Accepted:* Fang, C., Izzuddin, B.A., Obiala, R., Elghazouli, A.Y., Nethercot, D.A. (2012) Robustness of Multi-Storey Car Parks under Vehicle Fire. Journal of Constructional Steel Research. *Under preparation:* Haremza, C., Santiago, A. and Simões da Silva, L., "Numerical simulation of a composite steel-concrete joint subject to bending moments", YIC2012, First ECCOMAS Young Investigators Conference, A. Andrade-Campos, N. Lopes, R.A.F. Valente, H. Varum (editors), 24–27 April 2012, Aveiro, Portugal. Haremza, C., Santiago, A. and Simões da Silva, L., "Experimental behaviour of heated composite steel-concrete joints subject to variable bending moments and axial forces", ECCS-AISC, International Workshop on Connections VII, May 30-June 02, 2012, Timisoara, Romania. Haremza, C., Santiago, A. and Simões da Silva, L., "Robustness of composite steel-concrete open car park buildings subject to localised fire", 15th International Conference on Experimental Mechanics, 22-27 July 2012, Porto, Portugal. Haremza, C., Santiago, A. and Simões da Silva, L., "Behaviour of heated composite steel-concrete joints subject to variable bending moments and axial forces", Nordic Steel Construction Conference 2012, 5-7 September 2012, Hotel Bristol, Oslo, Norway. Demonceau J.-F., Comeliau L., Huvelle C. and Jaspart J.-P.. Robustness of steel buildings structures further to a column loss. The Eleventh International Conference on Computational Structures Technology. CST2012, Dubrovnik, Croatia. Fang, C., Izzuddin, B.A., Elghazouli, A.Y., Nethercot, D.A. Simplified Energy-Based Robustness Assessment for Multi-Storey Car Parks under Vehicle Fire. Fang, C., Izzuddin, B.A., Elghazouli, A.Y., Nethercot, D.A. Parametric Studies on Robustness of Multi-Storey Car Parks under Vehicle Fire – Towards Practical Design Recommendations. *Possible:* Comeliau L., Demonceau J.-F. and Jaspart J.-P. Resistance of beam-to-column joints at elevated temperature under combined bending moment and axial load. Fire Safety Journal. Joint paper(s) with partners including our comparisons against experiments and application of proposed simplified approaches. Haremza, C., Santiago, A. and Simões da Silva, L., University of Coimbra "Experimental behaviour of heated composite steel-concrete joints subject to variable bending moments and axial forces" (Journal to be defined) Haremza, C., Santiago, A. and Simões da Silva, L., "Design of steel and composite open car parks under fire" (Journal to be defined)

BUDGET INFORMATION PER BENEFICIARY		
BENEFICIARY	TOTAL AMOUNT SPENT TO DATE (€)	TOTAL ALLOWABLE COST AS FORESEEN IN GRANT AGREEMENT (€)
University of Liège (Belgium)	277.369,15	289.766
Imperial College of science, technology and medicine (United Kingdom)	202.157,28	249.902
Faculdade de Ciencias e Tecnologia da Universidade de Coimbra (Portugal)	250.884,13	247.517
Arcelormittal Balval & Differdange (Luxembourg)	225.919,82	199.395
Centre Scientifique et Techinique du Bâtiment (France)	119.360,79	116.695
Greisch Ingenierie (Belgium)	33.234,36	90.232
Centre Technique Industriel de la Construction Métallique (France)	65.444,64	60.388

V. Final summary

V.1. Objectives of the project

This project aimed at developing an assessment approach and design guidelines for the robustness of steel-concrete composite car parks under a localised fire resulting from the burning of one or few cars.The following objectives had been identified at the beginning of the project:

- Review current practice and state of the art in the design and assessment of car parks subject to localised fire, and propose potentially robust structural schemes for subsequent investigation.
- Develop and validate detailed numerical models as well as simplified analytical models of the fire response of critical structural components, including columns, connections and beams.
- Propose a system level approach for simplified analytical modelling of steel composite car parks under localised fire, and verify against validated numerical modelling.
- Develop a robustness assessment approach for steel composite car parks under fire, to be event independent as far as possible, and propose relevant and practical design guidance.
- Demonstrate using a real case study the accuracy and practicality of the developed analytical models, robustness assessment approach and corresponding design guidance.

In the next sections, it will be demonstrated how these objectives have been achieved. Obviously, only a summary of the achieved works is reported herein. More info is available in § VII and all details may be found in the six deliverables of the project (see § VI).

V.2. WP1 – Definition of the problem and selection of appropriate investigation ways

WP1 objectives were identified in the project description as follows:

- Definition of the car park structures (constitutive elements, connection types, loading, bracing systems …), of the specific design requirements and of the risks to be possibly encountered in terms of localised fire (destruction of one column or more than one column according to the position of the column in the structure, intensity and duration of the fire …).
- Identification of the distribution of temperatures within the affected part of the structure all along the event on the basis of previous research works performed, in particular within past RFCS projects.
- Selection of the philosophy to be followed so as to derive robustness requirements and related design recommendations (indirect methods, direct methods – alternate load path method or specific load resistance methods – …).
- Identification of the appropriate scenario(s) to be considered later on in the studies and of the related situations.

To achieve these goals, a full literature review was first made (Deliverable I), reflecting the state of the art on different topics:

- Fire aspects: investigations about open car parks subjected to a local fire (fire scenarios, structural behaviour) as well as experimental, numerical and analytical research works on beam-to-column joints and steel columns in fire;
- Robustness aspects: mechanism of progressive collapse, simplified models, design standards;
- Design aspects, fabrication and erection aspects and design requirements: current practices for car parks in different European countries.

Based on all the collected information, a structural typology for the reference car park to be investigated in the project was identified, as detailed in Deliverable I. The exceptional event to be considered was defined as a localised fire leading to the progressive loss of column resistance, though no particular scenario on how the fire develops in the structure was defined.

According to these main decisions, the global philosophy to be followed in the project was defined as summarised below:

- Design of a reference building based on current knowledge (contribution to WP5);

- Investigations on the response of individual structural elements (contribution to WP2);
- Investigations on the global structural response (contribution to WP3);
- Derivation of design recommendations and simplified procedures (contribution to WP4);
- Application of the previously defined rules to a study case, i.e. the reference building designed at the first step (contribution to WP5).

V.3. WP2 – Structural individual response of the affected structural elements

The WP aimed at acquiring the required knowledge on:

- the behavioural response of individual frame structural elements directly affected by the localised fire;
- the resultant reduction of carrying capacity of: i) the heated column in compression and bending; ii) the heated beam subject to bending and axial force (membrane effects); and iii) the heated beam-to-column joints subject to bending and axial force (membrane effects).

To reach this goal, experimental, numerical and analytical developments were carried out, with the aim, at the end, to derive two types of behavioural models: "sophisticated" ones (FEM models) and "simplified" ones (models for designers).

Seven experimental tests, most of them at high temperature, have been performed at the University of Coimbra on a substructure including composite steel-concrete beam-to-column joints. This 2D has been selected so as to reflect as closely as possible the actual response (in terms of loading, load sequence, variation of temperature …) of the beam-to-column joints in the reference structure defined in WP1. More particularly, the tests were aimed at observing the response of joints subjected to combined bending moment and axial load, at elevated temperature, when the column loses its resistance further to a localised fire. Different temperature conditions and axial restraints at beam extremities were considered:

- Test 1: ambient conditions and realistic axial restraint (reference test)
- Test 2: 500°C, no axial restraint
- Test 3: 700°C, no axial restraint
- Test 4: 500°C, full axial restraint
- Test 5: 700°C, full axial restraint
- Test 6: 700°C, realistic axial restraint
- Test 7: temperature increasing up to failure, realistic axial restraint (demonstration test)

The six first tests represent rather "theoretical" situations while the seventh one is reflecting "the reality". The six first tests are anyway quite important to perform, as they constitute extreme situations or reference situations to which the reality has to be compared so as to understand the influence of the various factors affecting the actual frame response.

The above-reported temperatures are those reached in the bottom flange of the beams, 20cm away from the column face. They were kept constant during the loss of the column loss, for the six first tests. The temperature distribution is obviously not uniform in the joint area; local temperatures have therefore been measured in the joints, during the tests. Details about the experimental tests can be found in Deliverable II, section II.

In order to validate the utilisation of the finite element programs used by each partner for the simulation of steel and composite steel-concrete structures subject to fire, three benchmark studies have been performed on three main structural elements: column, composite beam and beam-to-column joint. The influence of various parameters on the response of these elements (acting forces, distribution of temperatures and level of temperatures) has been investigated through the use of rather sophisticated numerical models.

The column benchmark was based on the simulation of a column extracted from the so-called "Cardington building" and for which test results were available (Franssen et al., 1995). Three FE programs were used: the Liège homemade program for the analyses of structures subjected to fire SAFIR, the commercially available program Abaqus and the Imperial College homemade finite element program ADAPTIC.

First, a thermal analysis was performed with Safir and Abaqus (Adaptic does not allow) so as to obtain the temperature distributions in the beam and the column. The results obtained by Safir and Abaqus showed very good correlation as well as good agreement with the experimental results. Then, structural analyses were performed with the three programs, first for the benchmark itself and then for some variations, so to evaluate the influence of the model definition, the axial restraint to beam, the frame continuity, the thermal expansion and non-uniform temperature. The comparison of the three programs results showed good correlation and quite reasonable agreement with the test results. Through this work, FE models with beam elements were so validated. The detailed results of the study are available in Deliverable II, section III.1.

The behaviour of other steel columns subject to a localised fire was also numerically studied, as detailed in Deliverable II, section III.2. These investigations showed that the column totally loses its resistance once the localised fire has developed around it (no residual bearing capacity is to be contemplated). This observation justifies the assumption of complete column removal made in the robustness studies, in the present project.

The benchmark for composite beams refer to tests on simply-supported composite beams found in *(Huang et al., 1999*) where the experiments are compared to results obtained by means of the VULCAN software. Both ambient and fire conditions have been considered in the structural analyses made by using Abaqus and Adaptic. Good correlation was observed between these two programs and Vulcan. Moreover, three other situations were also compared, according to the selected level of steel-concrete interaction: no, partial and full interactions. Finally, composite beams with additional axial restraints were studied and good comparisons were again achieved between Abaqus and Adaptic results. All details are provided in Deliverable II, section IV.

For the benchmark on joints, three representative tests undertaken in this project (tests 2, 3, and 6) were selected for a comparison with the component-based spring joint models implemented in Adaptic. Various temperatures were applied to the different joint components in the model as the temperature was not uniform in the whole joint zone during the tests. The bending moment versus rotation relationships predicted from the component-based spring models were compared to the experimental results. Good correlations were observed for test 2; but the initial stiffness was overestimated for tests 3 and 6. The bending capacities are well predicted for all the three tests. As far as ductility supplies / maximum rotations of the joints in the three tests are concerned, an underestimation, by the component-based model, is observed. More details of the joint modelling technique, including joint failure criteria and joint response under fire, are given in Deliverable II, section V.1.

Finally, the thermal and mechanical behaviours of a composite beam-to-column joint were investigated. First, a thermal finite element model of a composite beam-to-column joint submitted to the standard temperature-time curve (ISO 834) was developed using SAFIR. Thanks to this model, the evolution of the temperature distribution was observed and discussed. The detailed description of the model as well as the results of the numerical thermal analysis can be found in Deliverable II, section V.2.

As far as the mechanical response of a joint at elevated temperature is concerned, an analytical model predicting the resistance of steel or composite joints submitted to both an axial force and a bending moment was developed based on the component method. This model was validated by comparison to the ROBUSTFIRE experimental results (using the temperature distributions measured during the tests). It was also applied to another example, on the basis of temperature distributions determined through the previously mentioned thermal finite element simulation, to illustrate its application in a practical design situation. Details about the analytical procedure, its validation against the experimental tests and its application to a practical example are given in Deliverable III, section II.

V.4. WP3 – Study of the structural response under selected scenario(s)

The main task within WP3 is to integrate the knowledge acquired on elements in WP2 into a structural model enabling the prediction of the integrated structural response under localised fire. Two main objectives of WP3 were so defined:

- FEM simulations of the whole structure subjected to localised fire;
- Design practice--oriented behavioural models for the whole structure.

A comprehensive study on 3D slab behaviour has first been undertaken, including numerical and analytical approaches. Regarding the numerical approach, a benchmark study was conducted to investigate the composite slab response predicted by two finite element software packages, ADAPTIC and SAFIR. Both ambient and elevated temperature conditions were studied. The slab profile, material nonlinearity, boundary conditions and the contribution from secondary beams were considered. The studied structures are 16m×10m isolated composite slabs (both uniform slab and ribbed slab). The slab is simply supported, though the planar displacements at the supports may either be restrained or unrestrained. For the study of the ambient cases, a uniformly increasing distributed load is applied on the slab until very large deformations appear. With regard to the fire situation, a constant uniform distributed load of $5kN/m^2$ is applied on the slab, and a linear temperature gradient is assumed over the depth. The temperature of the bottom face of the slab linearly increases from the ambient temperature (0^oC) to 900^oC, while the temperature of the top face of the slab remains under the ambient condition. The following conclusions could be drawn from the different studied cases:

- In some cases, employing uniform slabs with appropriate depths can predict the response of ribbed slabs with sufficient accuracy.
- Employing a linear concrete model that ignores the compressive softening, cracking, and tensile softening leads to inaccurate predictions; hence such models should be avoided (nonlinear concrete material properties should be considered).
- The influences of the continuity of composite slabs and the stiffness of the supporting beams along the edges are significant.
- The benefit from the secondary beams is maintained until the temperature exceeds 200°C. After this temperature, the deflection of the slab with the secondary beams starts to converge to that without the secondary beams.

Besides, the slab benchmark showed good correlation between the results from the two numerical tools Adaptic and Safir.

Following the FEM simulations, an analytical model based on the work of Omer *et al.*, 2010 was employed to predict the slab behaviour. This model considers a rectangular uniform slab at ambient temperature, simply supported along its four edges (no horizontal nor rotational restraint) and subjected to a uniformly distributed load. It is a kinematic model based on the formation of a yield line mechanism followed by the development of membrane forces and the occurrence of full-depth cracks in the slab. Once the plastic mechanism has formed, the parts of the slab delimited by the yield lines are assumed to rigidly rotate around their support and the yield lines. These rigid parts are linked to each other by the reinforcement that stretches out according to a rigid-strain hardening material law. The failure occurs when the stress in the reinforcement reaches the ultimate strength of steel.

Subsequently, a detailed finite element model was developed to study the behaviour of a composite steel-concrete sub-frame under localised fire, where the commercial finite element package ABAQUS was used. The considered beam-to-column 2D sub-frame was extracted from the designed reference car park building; it is the one which was experimentally tested in Coimbra as part of WP2. The main objective of this numerical investigation was to study the detailed behaviour of the composite sub-frame suffering the loss of the column at ambient temperature. The numerical results were also compared to the experimental test (reference test 1) based on the moment-rotation curve: good agreement was observed.

A global FEM model for the reference car park was also established, where the robustness of the structure was comprehensively assessed. First, a thermal analysis was conducted with the FE program Safir, for the selected fire scenario assuming four V3 cars parked around an internal column. The temperature distributions along the primary and secondary beams as well as in the composite slab were observed and discussed. The thermal output data were extracted and input into the finite element model established in Adaptic for structural analysis. Three structural modelling levels were proposed. At Level A, consideration is given to a whole system of an influenced sub-structure with appropriate boundary conditions to represent the surrounding cool structures. The interactions among the heated column, the fire affected floor and the upper ambient floors are fully considered. Provided that the upper ambient floor systems have identical structural type and applied loading, the assessment model can be simplified to Level B, where a reduced model consisting of a fire affected floor-column system and a spring representing the upper ambient floor systems are considered. At this level, the two systems (i.e. fire and

ambient) are investigated separately. The derived characteristics of the ambient floors can be applied into the nonlinear spring. At Level C, planar effects within the floor slab are ignored, and grillage models with composite beams are considered instead. The modelling Levels B and C were employed in this project to simulate the reference car park. The considered system model was thus comprised of the fire affected column, the fire affected floor, and the non-linear spring that represents the performances of the upper ambient floors. Analysis was undertaken on the fire affected system model with the gravity load and the subsequent thermal load. Three failure types were generally observed for the reference building subject to the selected fire scenarios, namely, 'single-span failure' type, 'double-span failure' type and 'shear failure' type. The comparison of the two slab modelling approaches (grillage approximation and shell element model) showed that the full slab models predict better structural robustness than the grillage models. This indicates that although grillage approximations are usually sufficient for conventional structural designs which are based on ultimate/service limit state assessment of structures under normal loadings, they may be too conservative for structural robustness assessment that is associated with extreme loading. It was also observed that dynamic effects arise for the floor system following column buckling due to fire. This suggests that in order to predict a reliable ductility demand of a car park subsequent to column loss due to vehicle fire, dynamic analysis that accurately models the column buckling process may be necessary.

Finally, a practical analytical model aimed at predicting the response of a structure further to a column loss, and so at checking the robustness of the car park, has been proposed. This model initially developed in the RFCS Robustness project for 2D frames, has been refined and extended to 3D frames. For sake of simplicity, the floors are modelled as a grillage of composite beams (the beneficial planar effect of the slabs is neglected). The model is based on a static approach (dynamic effects, which anyway remain limited, are neglected) and does not explicitly (but for sure implicitly) include elevated temperature conditions. The aim of the model is to determine the displacements and internal forces in the structure when an internal column is completely lost. Knowing these forces and displacements, it is possible to verify whether the structure is robust or not by checking ductility conditions (joint rotation capacity vs. demand,…) and resistance conditions for key-elements (stability of the adjacent columns under additional compression and bending,…). Although the developed model is an ambient-temperature one, it could be adapted in order to cover the case of the scenario considered in this project, i.e. the loss of a column in a car park structure due to a localised fire. Basically, the fire-affected floor was neglected since its contribution is much smaller than the one of the upper cool floors. Obviously, this is only possible if the lost column is not part of the building highest storey. When it is this case, the response of the slab has to be accounted for. Other assumptions were also discussed, what lead to the simplification of the global model for the particular case of the structure investigated within this project.

Two Deliverables (DIV and DV) are provided where the reader will find all detailed information about the various developed models.

V.5. WP4 – Derivation of design recommendations adapted to the industrial request for design efficiency as well as for easy fabrication, erection and control

The objective of WP4 was the derivation of practical design recommendations useful for practitioners. The activities of this WP were divided in two tasks:

- derivation of practical recommendations and;
- critical appraisal of the practical recommendations.

For such a complex problem than the one considered in the present project, different design approaches may be contemplated, ranging from the very sophisticated thermal and mechanical simulations through FEM techniques to basic hand design procedures. The sense to give to "practical recommendations" is strongly dependent on the selected level of design sophistication. This being, and recognising the difficulty to approach the problem whatever is this level, it has been decided, in WP4, to gather all recommendations which seemed to be of practical interest for the designer.

In Deliverable DVI, different questions, corresponding to different sophistication levels, are therefore addressed:

- How to perform experimental tests on substructures so as to simulate the actual response of joints subjected to fire action, (and in which combined bending moment and axial loads are in constant evolution during the column heating).
- How to simulate numerically, through FEM techniques, the behaviour of such joints.
- How to predict analytically the M-N resistance interaction curves of such joints.
- How to predict in a simplified way the actual distribution of temperatures along the beam axis.
- How to predict analytically the response of a slab located just above the lost column.
- How to numerically simulate the global frame response according to one of the three following potential approaches: temperature-Dependent Approach, simplified Temperature-Dependent Approach and Temperature-Independent Approach.
- How to analytically check the robustness of the car park through simplified "hand" analytical procedures.

The higher is the level of sophistication, the greater is the accuracy of the design. But also the greater are the design efforts and the complexity of the approach for the designer. The powerful or more basic character of the calculation tools to be used is also a factor to be accounted for in design offices.

The most practical one is for sure the simplified analytical approach as the latter may be applied using tools available in any design office. It is the reason why the "practice-oriented" partners have mainly focused their work on the applicability of this approach.

The critical appraisal of this event-independent implicit approach may be summarised as follows. The assumptions on which the simplified analytical model for robustness check is based lead to a safe prediction of the structural response for the considered scenario, i.e. the loss of a column further to a localised fire. The conservative character of the procedure can obviously be seen as a source of inefficiency, as soon as the economy of the project is concerned. In reality, it is presently "the price to pay" to keep "easy-to-apply" analytical procedures. The designer who would like to predict more "accurately" the response of the structures would have then to use the more "sophisticated" numerical approaches.

V.6. WP5 – Case study

The objectives in WP5 were, for the "practice-oriented" partners":

- To design an "actual" reference building and to consider it further as a case study. This has been done under "normal" loading conditions, in accordance with the Eurocodes.
- Then to apply the different design recommendations proposed within WP4 to this building, in close collaborations with the "scientific" partners.

The "actual" reference building has been designed by carefully respecting the structural requirements identified in WP1. Except for the columns, all the structural elements are composite ones: the slab is made of a steel sheet filled with concrete and the steel beam profiles are connected to the slab. The whole structure is supposed to be braced thanks to concrete ramps. Internal columns are located every 10 m, the beams have a span of 16 m and are spaced of 3,333 m, which corresponds to the span of the composite slab. The height of the 8 stories is fixed at 3 m, which makes a total height of the building equal to 24 m. Moreover, no roof is considered on the last storey, this one also being used as a parking level; the selected beam and column steel sections are the same in the whole structure.

The proposed design procedures have been then applied to the "actual" reference building.

It has been demonstrated that the proposed approaches can be applied to the reference building. Through the application of the simplified analytical approach, it is demonstrated that the robustness of the reference building is not sufficient for the considered scenarios. Accordingly, the designer would have to select one of the following possibilities: (i) improvement of the resistance of the joints (in bending and/or under axial loads) and of the slab at the top level or (ii) to use a more sophisticated approach using FEM, to take into account, for instance, the membrane effects developing in the slabs (effects neglected within the analytical approach).

V.7. Conclusions

The possible progressive collapse of steel-concrete composite car parks under a localised fire resulting from the burning of cars is one of the key aspects to deal with nowadays. The absence of appropriate reply to this request is likely to limit the market for such very well appreciated structural solutions.

The project so aimed to investigate these aspects and derive design procedures and recommendations for the mitigation of the risk of progressive collapse.

The problem is rather complex as it implies to address the numerous following aspects:

- The scenarios to be considered (one car, more cars, located where, …)
- The distribution of temperatures in the air and the evaluation of the temperatures in the affected columns and the surrounding beams, slab and connections.
- The reduction of bearing resistance of the column.
- The local response of the beams, slab and joints when the bearing resistance of the column decreases and the progressive development of membrane forces in the floors.
- The global stability of the whole frame further to a local destruction of a part of the structure.

In order to achieve the goals of the project and to structure the work amongst the partnership, the following strategy has been set up further to an initial state-of-the art of the available knowledge:

- Derivation of all structural requirements for car park structures (dimensions, layout, loads, fabrication/construction/ erection constraints, realistic fire scenarios, …)
- Design of a reference structure under normal loading and in accordance with Eurocodes.
- Evaluation of the distribution of temperatures in the structure and in the constitutive structural elements during the exceptional event.
- Individual study of the main structural elements at room and elevated temperatures (columns, beams, connections, floor) through experimental and/or numerical investigations.
- Derivation of analytical approaches for the prediction of the individual response of the above-mentioned structural elements.
- Development of various numerical procedures for the evaluation of the stability and the resistance of the structure further to the event (sophisticated models with different levels of sophistication).
- Derivation of a simplified event-independent and Eurocode compatible approach for the evaluation of the robustness of the structure (simplified model).
- Application of the simplified model to the reference structure by the “practice-oriented” partners and feed back to the “scientific partners”.
- Drafting of design guidelines.

All these steps have been successively crossed along the three years of the project and practical recommendations are now made available.

The main conclusion of the project is certainly the fact that the simplified model is based on series of assumptions which allows, at the end, and at it was requested by the contract, to check the robustness of the car park through a “scenario-independent” approach, but with a non-excessive but actual level of conservatism that could be criticised. In fact, this conservatism has to be seen as the “price-to-pay” to limit the investment of a design office in terms of calculation costs.

Should the conservative character of the simplified model be considered as excessive, then more sophisticated models should be preferred. In the project, much information is made available to practitioners who would prefer to follow a numerical approach: choice of the model, distribution of temperatures, substructure to be studied, loads and boundary conditions to apply …

As a conclusion, to ensure that all questions have been answered and that all necessary tools and guidelines for practitioners have been made available would, as it is often the case in such research projects, overcome the reality. But for sure, through the present project, significant progress has been made, the initial objectives have been reached and the practitioners have nowadays at their disposal design approaches, at different levels of sophistication, allowing checking the robustness of composite car parks under localised fire.

VI. List of deliverables

Deliverables	Planned delivery date	Actual delivery date	Location of the report	Name of the file
WP1: DI	December 2008	March 2009	On CIRCA server	Deliverable I
WP2: DII & DIII	June 2010	30/03/2012 (delivered with the final report)	On CIRCA server	Deliverable II & Deliverable III
WP3: DIV & DV	December 2010	30/03/2012 (delivered with the final report)	On CIRCA server	Deliverable IV & Deliverable V
WP4 & WP5: DVI	June 2011	30/03/2012 (delivered with the final report)	On CIRCA server	Deliverable VI

VII. Scientific description of the results

VII.1. Objectives of the project

This project aimed at developing an assessment approach and design guidelines for the robustness of steel-concrete composite car parks under a localised fire resulting from the burning of one or few cars. The following objectives had been identified at the beginning of the project:

- Review current practice and state of the art in the design and assessment of car parks subject to localised fire, and propose potentially robust structural schemes for subsequent investigation.
- Develop and validate detailed numerical models as well as simplified analytical models of the fire response of critical structural components, including columns, connections and beams.
- Propose a system level approach for simplified analytical modelling of steel composite car parks under localised fire, and verify against validated numerical modelling.
- Develop a robustness assessment approach for steel composite car parks under fire, to be event independent as far as possible, and propose relevant and practical design guidance.
- Demonstrate using a real case study the accuracy and practicality of the developed analytical models, robustness assessment approach and corresponding design guidance.

In the next sections, it will be demonstrated how these objectives have been achieved. Obviously, only a summary of the achieved works is reported herein. All details may be found in the six deliverables of the project (see § VI).

VII.2. Comparison of initially planned activities and work accomplished

Globally, and despite some delay in the realisation of the “more than expected” complex character of the experimental campaign, the activities developed in accordance with the initially planned schedule.

In fact, the delay in testing has finally resulted in the postponement to the end of the project of the delivery of Deliverables II to V. By way of consequence, this postponement affected some of the other activities in which the experimental results had to be exploited, but without affecting the publication of the corresponding Deliverables.

In the end, thanks to the flexibility of the partnership, the whole work has been completed and all the project objectives have been achieved.

VII.3. WP1 – Definition of the problem and selection of appropriate investigation ways

The work package 1 objectives were fully contemplated within the project; these objectives were identified within the project description as follows:

- Definition of the car park structures (constitutive elements, connection types, loading, bracing systems …), of the specific design requirements and of the risks to be possibly encountered in terms of localised fire (destruction of one column or more than one column according to the position of the column in the structure, intensity and duration of the fire …).
- Identification of the distribution of temperatures within the affected part of the structure all along the event on the basis of previous research works performed, in particular within past RFCS projects.
- Selection of the philosophy to be followed so as to derive robustness requirements and related design recommendations (indirect methods, direct methods – alternate load path method or specific load resistance methods - …).
- Identification of the appropriate scenario(s) to be considered later on in the studies and of the related situations.

Each contractor contributed more to some items according to their expertise:

- Fire aspects: FCTUCOIMBRA, ULGG, ARCELORPROFIL, CTICM
- Robustness aspects: ICSTST, ULGG
- Design aspects: GREISCH
- Fabrication and erection aspects: ARCELORPROFIL
- Design requirements: CSTB, CTICM

State-of-the-arts were prepared for the different topics; all the details are reported in Deliverable I. In particular, information was collected on current practices for car parks in Europe. Founded on the collected information, a typology of structure to be investigated within the project was identified; accordingly:

- Only open car park have been considered within the project;
- Two types of slabs have been contemplated: composite slabs (steel sheet + concrete) and concrete slabs;
- Simple steel connections have been considered for the beam-to-column joints although a semi-rigid behaviour of the latter should be observed as a result of the composite action;
- I profiles have been considered for the beams (the cellular beams will not be considered as their behaviour when subjected to fire still be under investigation in other research projects);
- Steel H profiles for the columns have been considered (composite columns have not been investigated as this configuration of columns is less sensitive to a localised fire);
- Only braced buildings have been studied, what reflects the most usual configuration.

Concerning the scenario associated to the exceptional event to be considered, it was decided to study localised fires leading to the progressive loss of column resistance; however, no particular scenario on how fire develops within the structure has been contemplated. It has also been assumed that the beam-to-column joints at the top of the loss column are subjected to fire action too, what will affect their mechanical properties.

According to these main decisions, the following philosophy to be followed within the project was adopted:

- First, a reference building have been designed (based on the actual knowledge);

- Then, from this reference building, structural elements have been extracted in order to investigate the response of these individual elements numerically, analytically and experimentally (main objective of WP2);
- Founded on the knowledge gained from WP2, investigations on the global structural response have been conducted numerically and analytically (main objective of WP3);
- From the investigations made within WP2 and WP3, it has been then possible to derive design recommendations and simplified analytical procedures, what is the objective of WP4;
- Finally, the so-obtained design recommendations have been applied to an "actual" study case in WP5. For the latter, the reference building designed at the beginning of the project was considered as the study case to be investigated.

For the design of the reference building, the following decisions were taken (founded on the knowledge gained from the present work package):

- General layout and arrangement of beams and columns:
    - It has been decided to investigate structures with internal columns and what has been investigated is the loss of an internal column.
    - It has been proposed to place steel columns each 10m. The proposed layout for the reference frame is given here below. The primary composite beams are represented in green. The secondary composite beams are represented in blue. The steel columns are represented in red. The slab can be composite or made of prefabricated elements. For the first slab solution, more secondary beams are requested because the maximum span for a composite slab is 3,33m. However, it is possible to go up to 5m span with special deck systems (with a thicker slab); this solution has not been considered herein. Within the project, for the definition of the tested specimens, the composite solution has been chosen.

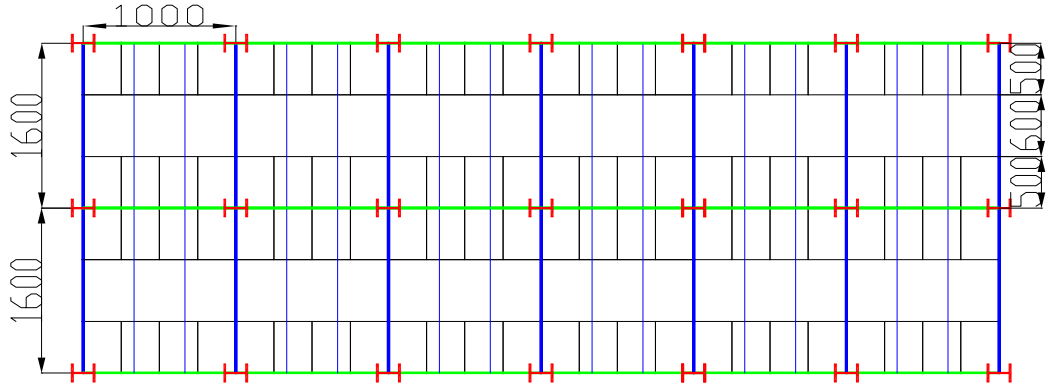

Figure 6. Chosen layout (dimensions in cm)

    - The height of a storey is taken as equal to 3,0 m. It has been assumed that the building has 8 floors.
    - It has been assumed that all the columns are the same at a same level of the building (i.e. one profile for the columns). Also, one profile for the secondary beams and one profile for the primary beams has been designed.
    - For the bracing system, it is assumed that concrete ramps are each side of the building and are connected to the small façades. Accordingly, the horizontal displacements of the columns in the small façades can be assumed as blocked.
- Configuration of the joints
    - For the beam-to-beam joints (between the primary and secondary beams) and the minor axis beam-to-column joints, double web cleats have been chosen.
    - For the major axis beam-to-column joints, flush end plate solutions have been chosen.
    - For the column bases, hinges have been assumed.
- Slabs

- A composite solution with a span of 3,33m has been used.
- The beam-to-slab connection has been designed as a full strength one.

- Materials
  - S355 steel grade for beams
  - S355 and S460 steel grades for columns have been contemplated. Two solutions have been proposed and the solution for the tested specimens has been chosen according to the availability of the proposed profiles (see WP 2).

- Load cases and combinations (SLS and ULS)
  - The distributed load to be considered for the vehicles weight is 2,5 kN/m².
  - An estimated weight of safety barrier has also been put around the building.
  - For the combination of loads, the recommendations from the Eurocodes have been followed.

As mentioned previously, the WP1 objectives were fully reached at the end of the first six months, what was in line with the original planning of the project.
According to this philosophy, it was decided to anticipate the launching of WP5 compared to the initial planning and, in particular, the launching of Task 5.1. Indeed, according to the initial planning, WP5 should have only started at the beginning of the third year while we decided to start this work package at the beginning of the second period (i.e. in January 2009) with the design of the reference structure (which has been later on used as case study).

All the details about the reference structure are available in Deliverable VI, Section II. The conducted investigations on the latter are reported in Section 0.

VII.4. WP2 – Structural individual response of the affected structural elements

VII.4.1. Introduction

The objectives of WP2 were to acquire the required knowledge on the behavioural response of the individual frame structural elements directly affected by the localised fire, and on the resultant reduction of carrying capacity of: i) the heated column in compression and bending; ii) the heated beam subject to bending and axial force (membrane effects); and iii) the heated beam-to-column joints subject to bending and axial force (membrane effects). To reach this goal, experimental, numerical and analytical developments were carried out, with the aim, at the end, to derive behavioural models for elements at two different levels: a “sophisticated level” (FEM models) and a “simplified” level (models for designers).

Seven experimental tests were performed at the University of Coimbra on a composite steel-concrete beam-to-column frame at elevated temperatures. This two dimension frame was extracted from a real composite open car park building specially designed in this project (see WP5 in § VII.7.2), keeping the real cross-section dimensions of the beams (IPE 550) and the columns (HEB 300), and using bolts M30, cl 10.9 in the composite connection. The tested composite frame was subjected to mechanical (bending and axial forces) and thermal loadings (constant temperature equal to 20ºC, 500ºC or 700ºC; or linear increase up to 800ºC). The objective of these tests was to observe the combined bending moment and axial loads in the heated joint after the loss of the column due to a localised fire. In order to reach this goal, the effect of the axial restraint to beam was simulated. The tests specimens were fabricated in the shop of APLR in Luxembourg, and additionally, tensile coupon tests were performed at ambient and elevated temperatures to define the real steel properties.

Three benchmark examples were defined in order to validate the utilisation of the finite element programs used by each partner for steel and composite steel-concrete structures subject to fire: i) the column benchmark: a steel sub-frame subject to a natural fire *(Franssen et al., 1995)*, ii) the composite beam benchmark: composite beams loaded at ambient temperature and under fire *(Huang et al., 1999*), and iii) the joint benchmark, validated by the experimental tests performed within this project. The influence of various parameters on the response of the elements (acting forces, distribution of temperatures and level of temperatures) was investigated in these numerical sophisticated models. In addition, the behavioural response of the columns was also studied under localised fire in order to show

that the column completely loses any resistance once the localised fire develops around it, so that for the ROBUSTFIRE project studies, the column loss could be assumed by the total removal of the column.

The behavioural response of a composite beam-to-column joint under standard temperature-time curve (ISO 834) was also studied: a thermal finite element model was defined, and the evolution of the temperature distribution was obtained. Finally, an analytical method predicting the resistance of steel or composite joints submitted to both an axial force and a bending moment at elevated temperature was developed. This model was validated by comparison with the experimental tests at elevated temperature (using the temperature distributions measured during the tests); after, it was applied to an example, based on temperature distributions determined through a thermal finite element simulation, to illustrate its application in a design situation.

VII.4.2. Experimental tests results

VII.4.2.1. Introduction

The main objective of the experimental tests was to observe the combined bending moment and axial loads in the heated joint when catenary action develops in the frame after the loss of the column. The composite joint zone was subjected to elevated temperatures in order to simulate the effect of the localised fire that leads to the column loss. Figure 1 presents the seven beam-to-column frames tested in Coimbra. According to previous experimental works performed in real composite steel-concrete open car park structures subjected to fire, a majority of the temperatures measured in the beam bottom flanges were lower than 500ºC; however temperatures of 700ºC were observed in recent tests performed in France (Deliverable I). Based on these previous observations, five tests were heated up to 500ºC or 700ºC; one reference test (test 1) was carried out at ambient temperature, and finally a demonstration test (test 7) was performed, for which the frame was subjected to an increase of the temperature up to the failure of the column, see Figure 1. The effect of the axial restraint to beam coming from the unaffected part of the building was also studied: tests 2 and 3 - no axial restraint to the beam; tests 4 and 5 - total axial restraint to the beam; and tests 1, 6 and 7 - realistic axial restraint to the beam.

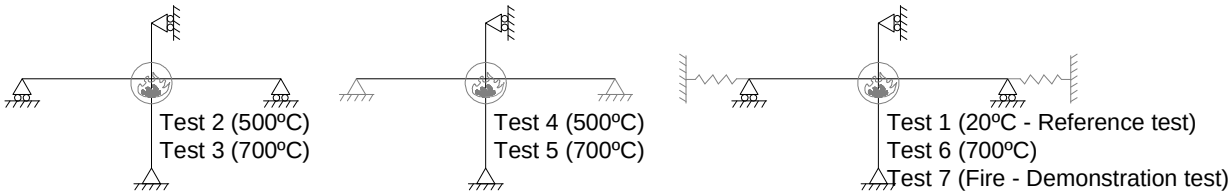

Figure 1. Seven experimental tests

VII.4.2.2. Main results

Table 1 summarizes the main results of each test: the failure modes, the local deformations, the connection rotation at the end of the test and the symmetrical or unsymmetrical behaviour of the joint defined by the column rotation; in tests 3 and 7, the column rotated a lot and the joint deformation was not symmetrical. The final deformation of the sub-frame of test 6 is showed in Figure 2. The appendix XIII.1 is dedicated to the experimental tests: the testing arrangement and the thermal and mechanical loadings are described, the tensile coupon tests results are presented, and the seven sub-frame tests results are discussed in detail. Moreover, much more details of each test are described in Deliverable II, section II.

Figure 2. Final deformation of the tested structure (test 6)

Table 1. Failure modes and local deformation of each test

Test	Temp (ºC)	Restraint (kN/mm)	Connection rotation* (mrad)	Col. rotation* (mrad)	Failure modes	Local deformations
T1	20	0 in comp., 50 in tension	74.9	-6	Concrete crushing in compression; failure of 2 bolts in tension (left side); crack at the end-plate bottom (left)	End-plate bottom and centre
T2	500	0	84.8	Not measured	Concrete crushing in compression; failure of 3 bolts in tension (left side)	End-plate bottom and centre
T3	700	0	132.4	-33	Concrete crushing in compression; failure of 2 bolts in tension (left side) during the cooling phase	End-plate bottom and centre; Column web (bottom part); Beam left bottom flange
T4	500	Total	89.4	2	Concrete crushing in compression; failure of 2 bolts in tension (right side) during the cooling phase	End-plate bottom and centre; Column web (top part); Beams webs; Column left flange deformed
T5	700	Total	122.3	6	Concrete crushing in compression	End-plate bottom and centre; Column web (bottom part); Top flange of the right beam; Plastic hinge at the right beam
T6	700	50	183.5	10	Concrete crushing in compression; failure of 3 bolts in tension (2 on the right - 1 on the left)	End-plate bottom and centre; Beams bottom flanges
T7	400; 800	50	149.8	-63	Column failure; Concrete crushing in compression; failure of 3 bolts in tension (left side); crack at the end-plate bottom (left)	End-plate bottom and centre

* Rotations measured at the end of each test.

VII.4.2.3. Final comments

In tests 1 to 6, a hogging bending moment was initially reached in the joint during the first loading step, followed by a variation of this moment during the increase of temperatures (step 2). In the third loading step, the column loss was simulated (very progressive), and the sagging bending moment increased under constant temperatures. The first failure observed in all the tests was the concrete crushing in compression; some bolts from the bottom bolt rows failed later in tension in tests 1, 2 and 6, under higher joint rotations. Finally, similar localised deformations at the centre and bottom parts of the end-plate were observed in all the tests (see appendix XIII.1). In the demonstration test 7, the bottom column (HEB 140, S355) failed under 578ºC and 359 kN of axial load; then steel temperatures in the joint increased to very high values (770ºC in the beam bottom flange) and the sub-frame resistance

depended of the unheated composite slab resistance under sagging bending moment, which reached maximum of 200ºC. Finally, the concrete crushed in compression (under 180 kN of axial load), and the entire sub-frame failed a very few time later, because of the failure of three bolts in the bottom left row (around 600ºC in the bolts).

From tests performed without axial beam restraint, the joint rotation capacity, as well as the ductility, increased with the temperature, whereas the maximum reaction load, and the corresponding maximum sagging bending moment, decreased (by 20% at 500ºC and by 50% at 700ºC).

During the beam axial restraint tests, only compression loads were developed; the main reason for that was the position of the restraint: not at the gravity centre of the composite steel-concrete beam, but at the gravity centre of the steel beam. However, under total axial restraint to the beam, test 5 reached higher bending moment/axial restraint loads than test 4 at 500ºC, certainly because of the non-uniform and locally much higher concrete slab thickness on one side (due to a problem during the concreting of the sub-frames); it was observed that the concrete crushed against the column flanges for similar rotations, but under more 50% of axial compression loads. The advantage of the compression axial loads was the capacity of the joint to sustain a higher sagging bending moment without any problem of bolt failure: the compression load from the axial restraint combined with sagging bending moment, moved the neutral axis of the connection downward, allowing the development of additional compression loads in the concrete slab, and reducing tensile loads in the bottom bolt rows. The compression axial loads also increased the joint rotation capacity and the ductility of the joint.

Additionally, it was observed that the initial stiffness of the load/displacement curves (Figure 77 in appendix XIII.1) decreased with the joint temperature and increased with the axial beam restraints.

VII.4.3. Column benchmark

This benchmark example was about a natural fire test on a fully loaded, two dimensional, unprotected steel framework carried out in a purpose-built compartment in Cardington (Franssen et al., 1995). Three FE programs were used: the specialised homemade program dedicated to the analyses of structures subjected to fire, SAFIR (Franssen, 2005), the commercially available program Abaqus (2007), and the homemade finite element program ADAPTIC (2009). The influence of the model definition, axial restraint to beam, frame continuity, thermal expansion and non-uniform temperature were analysed by the three programs, and were discussed; the detailed results are available in Deliverable II, section III.1. The reference frame was modelled using the symmetry conditions, as shown in Figure 3a. First, a thermal analysis was performed with SAFIR and Abaqus (ADAPTIC only deals with structural analysis) to obtain temperature distributions in the beam and the column. The results obtained by SAFIR and Abaqus showed a very good correlation. Then, for the structural analysis, results of the three programs for the reference frame and for each study case were compared. The results obtained for the reference frame are showed in Figure 3 and Figure 4, Figure 3b shows the lateral displacement at column mid-height, and Figure 4 shows a) the beam vertical displacement and b) the axial force in the beam. Good correlations between the three FE programs Abaqus, SAFIR and ADAPTIC are showed, and FE models with beam elements were validated for analysis of steel structures subjected to fire.

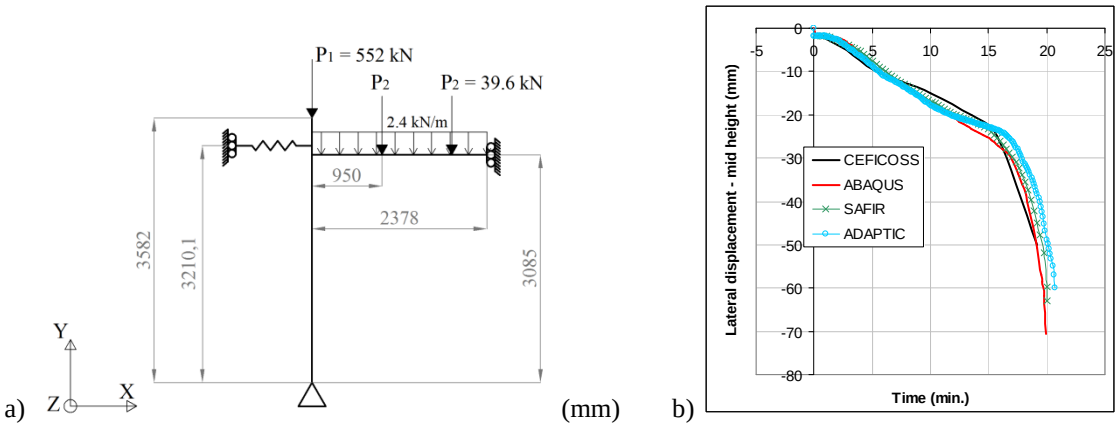

Figure 3. a) Reference frame; b) Lateral displacement at column mid-height

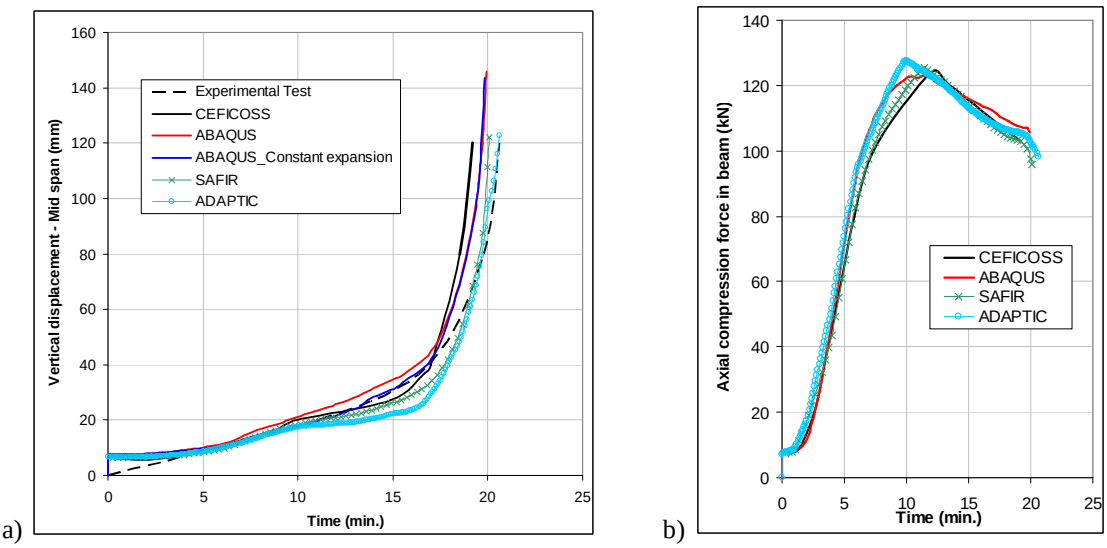

Figure 4. a) Vertical displacement of the beam; b) Calculated axial force in the beam

VII.4.4. Behaviour study of a steel column subject to a localised fire

The purpose of this study was to show that the column completely loses any resistance once the localised fire develops around it, so that for the ROBUSTFIRE project studies, the column loss could be assumed by the total removal of the column. The studied steel column is 3 m height, HEB 300 steel cross-section, class S460. Two alternative studies were developed: i) the column behaviour was analysed under constant temperatures, using the Eurocode 3 parts 1.1 and 1.2, and a numerical model (Figure 5a, b); and ii) the column behaviour was analysed under localised fire (Figure 5c), using the method described in Franssen (2000).

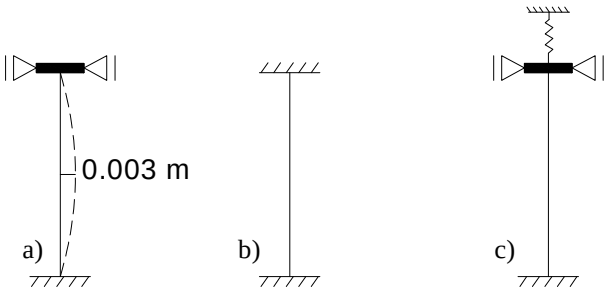

Figure 5. Numerical models of the column

According to Eurocode 3, the buckling of the column influences the maximum load capacity of the studied column. However, the numerical model showed that at ambient and elevated temperatures, the column fails by yielding of the cross-section and three plastic hinges are formed at the top, bottom and centre of the column. A mechanism is developed, and the column sustains the loads until the complete failure of the hinges. It was also showed that the maximum load capacity of the column at ambient temperature (6193 kN) was reduced up to 80% at 700ºC (1245 kN). Moreover, under constant temperature equal to 600ºC, the column load capacity was reduced by 59% according to the FE model (2541 kN), and 60% according to Eurocode 3 (2594 kN), and the column was not able anymore to support the column axial force design value for the fire situation $N_{Ed,fi,20^oC}$ (2713 kN).

The column was also analyzed under varying temperatures, defined by a fire scenario including 4 class3-cars. Steel temperatures were estimated using the Hasemi method, and the average temperature was applied to the finite element model of the column. It was observed, as in Franssen (2000), that the restraint from the unaffected part of the building has no effect on the column critical temperature. The column was not able anymore to sustain to $N_{Ed,fi,20^oC}$ (2713 kN) from 578ºC (after 26.9 min. of fire). The detailed results of this numerical study can be found in Deliverable II, section III.2.

VII.4.5. Composite beam benchmark

The considered composite beams were based on the paper published by Huang *et al.*, 1999, who selected two test programmes (one for ambient condition and one for fire condition) and compared these test results with the simulation results obtained from their in-house software VULCAN (Bailey, 1995). At ambient temperature, two simply-supported composite beam tests (Tests A3 and A5) conducted by Chapman and Balakrishnan (1964) were considered. For the elevated temperature conditions, two fire tests (Tests 15 and 16) on simply-supported composite beams conducted by Wainman and Kirby (1988) were referred to. Within this project, the structural behaviour of the tests was simulated using the commercially available program Abaqus (2007) and the homemade FE program ADAPTIC (2009). The corresponding response predicted by ADAPTIC, Abaqus, VULCAN and the test results are given in Figure 6 and Figure 7. Good correlation is observed, but small discrepancies exist between the numerical results and the test results, particularly for Test 16 at elevated temperature. These differences were due to the difficulties in building a perfect simple support condition in the furnace at elevated temperatures (Huang *et al.*, 1999). Moreover, three concrete-steel interactions were considered, namely, zero interaction, partial interaction and full interaction, respectively. The additional results are presented in Deliverable II, section IV.

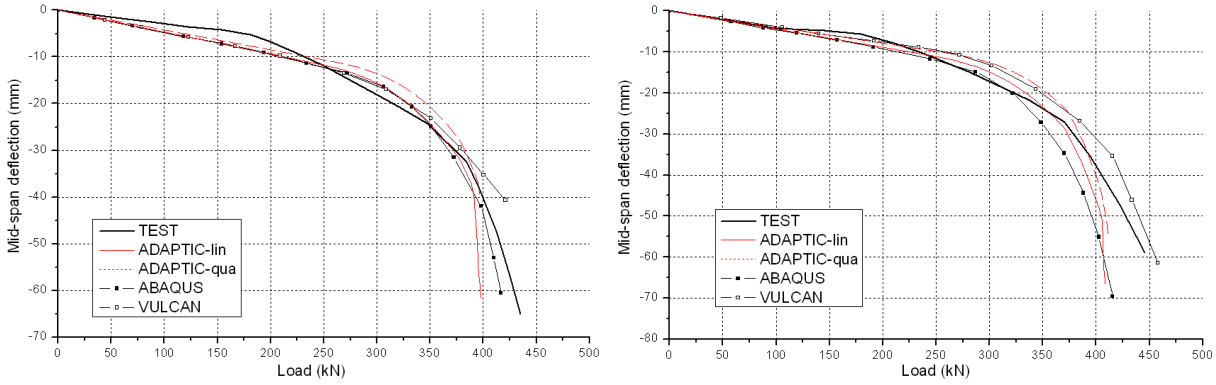

a) b)

Figure 6. a) Comparison of load-deflection response for Beam A3; b) Comparison of load-deflection response for Beam A5

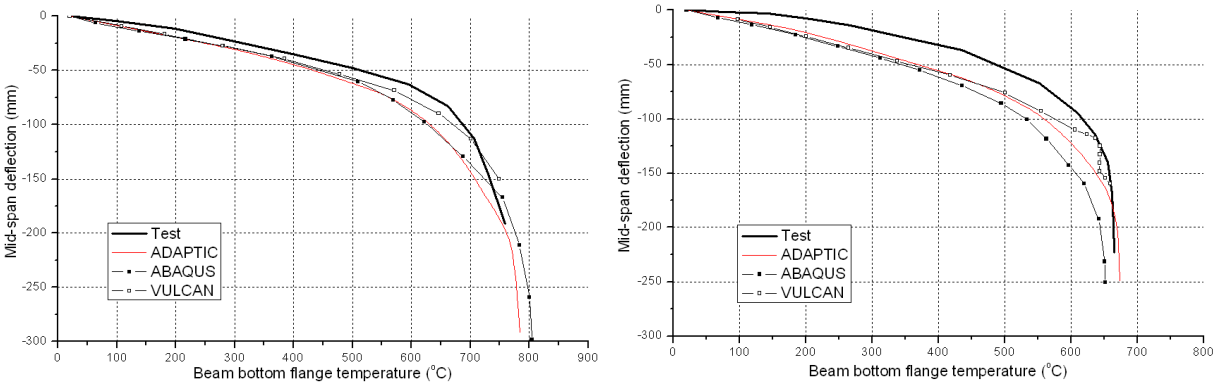

a) b)

Figure 7. a) Comparison of temperature-deflection response for Test 15; b) Comparison of deflection-temperature response for Test 16

Further to the benchmark study, composite beams with additional axial restraints were considered. For A3 and A5 (ambient cases), five levels of axial stiffness were assumed, namely, axially rigid, EA/L, 0.5EA/L, 0.2EA/L, and simply-supported, respectively, where EA/L is the axial stiffness of the bare steel beam (221.8kN/mm). With respect to Test 15 and Test 16 (elevated temperature cases), the restraining conditions of axially rigid, 0.2EA/L and simply-supported were assumed, where in these two tests EA/L was 254kN/mm. Good comparisons were achieved between the results obtained from ADPATIC and Abaqus. The results are detailed in Deliverable II, section IV.

VII.4.6. Joint benchmark

Three representative tests undertaken in this project (tests 2, 3, and 6) were selected to compare with the component-based joint models established in ADAPTIC. The joint was first heated to a stabilised peak temperature, then the column base was gradually relaxed and subsequently an increasing downward vertical point load was applied at the top of the HEB 300 column. No axial restraint was applied at the beam ends throughout the entire test for tests 2 and 3, and axial restraints with a constant axial stiffness of 50kN/mm were applied at the two ends of the beam for test 6. The maximum temperatures in the bottom flange of the steel beam were 500°C and 700°C for tests 2 and 3/6, respectively, and the temperature was kept almost unchanged during the loading procedure. The temperature distribution was not uniform in the entire joint area, and different temperatures were found in the other parts of the joints, as given in Table 2. Therefore, for the component-based joint model, various temperatures were applied to different joint components. It is worth noting that in test 6, the joint temperature during the loading procedure was not stable (see Deliverable II, section V.1), so the temperature distribution at the time of 8 hours (where the temperature is close to the mean value) was employed for the component model.

Table 2. Temperature distribution of tested joints

Positions	**Test 2**	**Test 3**	**Test 6**
Column flange	400°C	483°C	570°C
Column web	470°C	565°C	710°C
End-plate	430°C	529°C	575°C
Beam web	470°C	620°C	600°C
Beam flange	500°C	700°C	700°C
Bolt	390°C	505°C	550°C
Concrete	180°C	216°C	260°C

The component-based model developed in ADAPTIC is illustrated in Figure 8a. For the four inner bolt-row spring series, the axial property in tension is contributed from four components, namely, column web in tension (cwt), column flange in bending (cfb), bolt in tension (bt), and end-plate in bending (epb). The compressive characteristic for all the five spring series were based on the resistance of column web in compression (cwc). For the top and bottom outer spring series representing the contacting positions between the beam flanges and the column flange, the resistance of beam flange/web in compression (bfwc) was considered. The effect of column web in shear (cws) was ignored due to the symmetry of the tested frame. The spring assembly for half of the joint model is illustrated in Figure 8b. Three types of post-limit responses for each ductile component were considered, namely, no strain hardening (μ=0), bi-linear response (μ=3%), and bi-linear response (μ=5%). The concrete slab was simulated via beam-column elements neglecting the ribs and the steel deck. Rigid links were employed to connect the steel beam and the concrete to consider full shear interaction. More details of the joint modelling technique, including joint failure criteria and joint response under fire, are given in Deliverable II, section V.1.

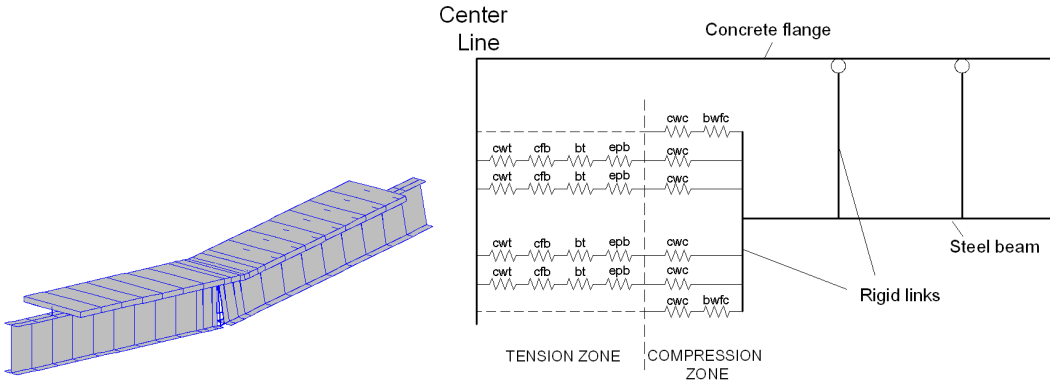

Figure 8. a) Illustration of ADAPTIC joint component model; b) Frame model with joint components

The bending moment vs. rotation relationships predicted from the component-based spring models are illustrated in Figure 9, Figure 10 and Figure 11 for tests 2, 3 and 6, respectively. Failure of the joint in the component-based model is associated with tensile failure of the lowest bolt-row, where the elongation exceeds the allowed value of 25mm which is determined as one of the joint failure criteria for this study (Deliverable II, section V.1). Good correlations are observed for test 2, but for tests 3 and 6 the initial stiffness is overestimated. The bending capacities are well predicted for all the three tests. In addition, the ductility supplies / maximum rotations of the joints in the three tests are underestimated by the component-based model. This is due to the predefined limitation of the 25mm maximum bolt-row elongation, which is shown to be conservative at elevated temperature.

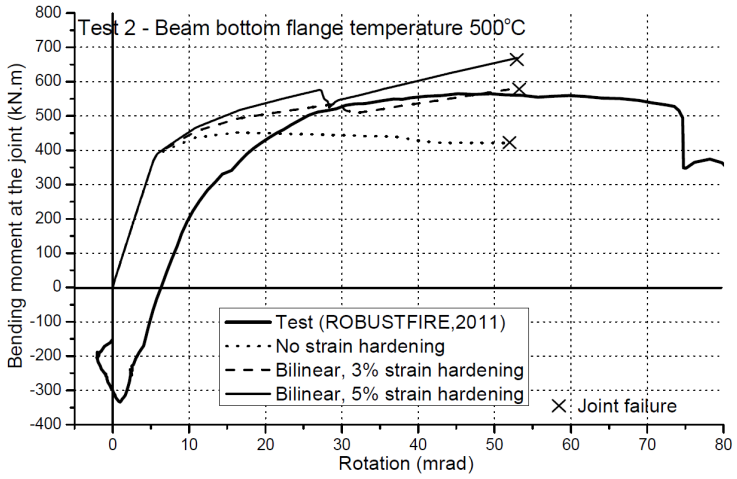

Figure 9. Moment-rotation response of joint in Test 2

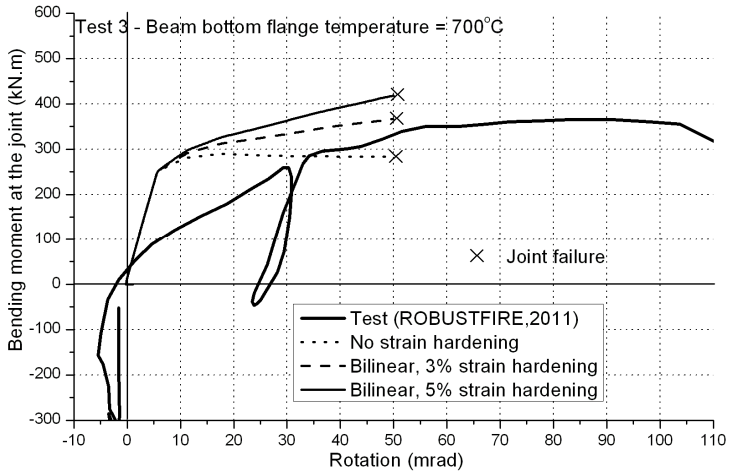

Figure 10. Moment-rotation response of joint in Test 3

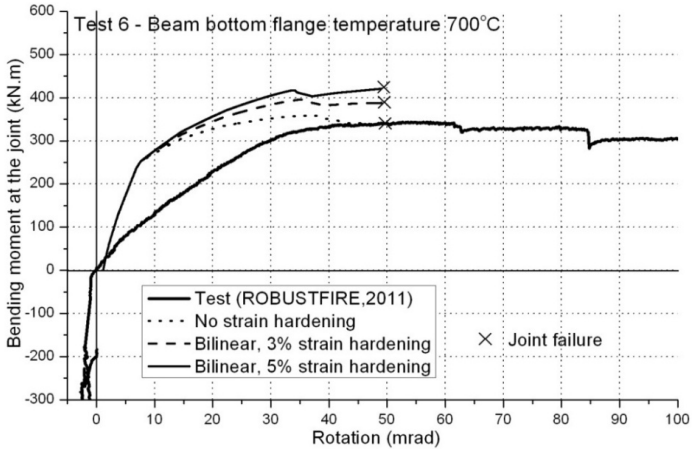

Figure 11. Moment-rotation response of joint in Test 6

VII.4.7. Joint thermal finite element model

VII.4.7.1. Introduction

This section presents a thermal finite element model of a composite beam-to-column joint submitted to the standard temperature-time curve (ISO 834), developed using the specialised homemade program SAFIR (Franssen, 2005). The studied joint links two IPE550 beams to a HEB300 column. It is the same as the one designed for the connections of the primary beams to the columns in the reference car park structure designed and investigated in the present project (the resistance of this joint is studied in VII.4.8.3), except that a 12cm thick solid concrete slab is considered here instead of a composite slab. In the following, the model is first briefly described before the evolution of the temperature distribution is presented. More details about this model can be found in Deliverable II, section V.2.

VII.4.7.2. Description of the numerical model

The developed model uses 3D elements with 8 nodes. For reasons of symmetry, only 1/4 of the column was modelled, with the associated parts of beam and joint. The bolts and slab reinforcement have not been represented in the model (Figure 12). The limit conditions are defined as follows: nominal ISO 834 fire curve on the frontiers below the slab and ambient conditions above the floor.

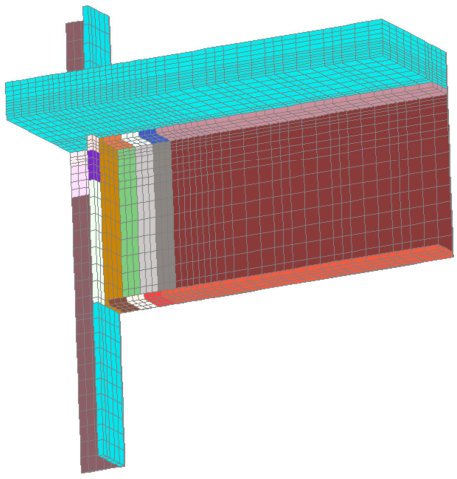

Figure 12. Joint model

Steel and concrete properties are in accordance with Eurocode 3 and 2 (EN 1993-1-2:2005 and EN 1992-1-2:2004) respectively. The convection coefficient on hot surfaces is taken equal to 25 W/m²K and the convection coefficient on cold surfaces is taken equal to 4 W/m²K. The relative emissivity of concrete surfaces is taken equal to 0.7. This parameter should also be taken equal to 0.7 for carbon steel according to Eurocode 3. However, in order to take account of the position and shadow effects in the

numerical simulation, the relative emissivity of steel surfaces is multiplied by a reduction factor k_ε ($\leq$ 1) based on the configuration factors related to the different zones as explained in detail in Deliverable II, section V.2 (the different volumes defined with proper k_ε values are represented in different colours in Figure 12).

VII.4.7.3. Temperature distribution

Figure 13 shows the temperature distribution in the joint after 10, 20, 30, 40, 50, 60, 90 and 120 minutes.

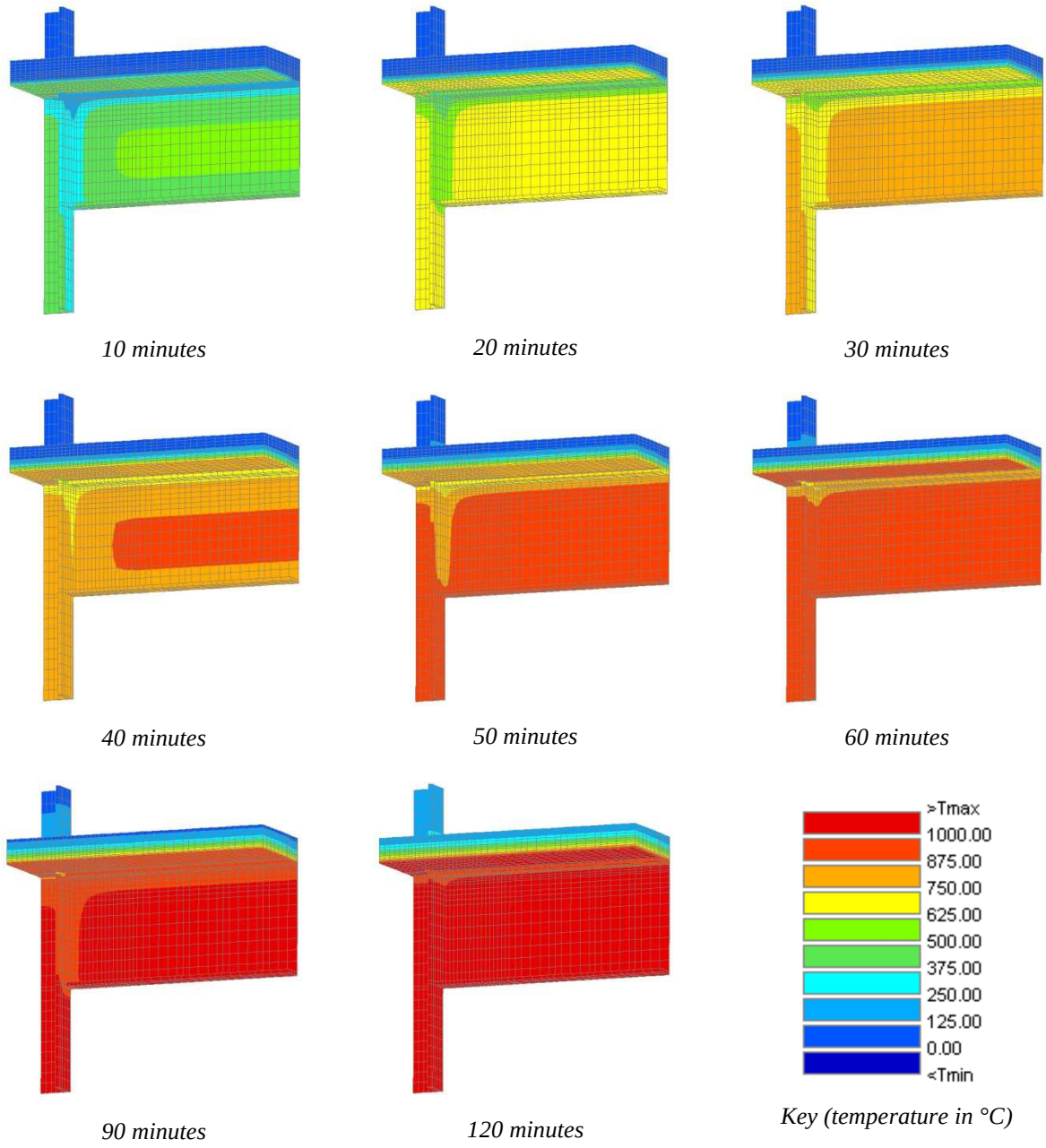

Figure 13. Temperature distribution after 10, 20, 30, 40, 50, 60, 90 and 120 minutes

Figure 14 gives the temperature of the beam bottom and top flanges in the connection section versus time and compares this evolution with the temperature of the gases corresponding to the standard iso ISO 834 fire curve.

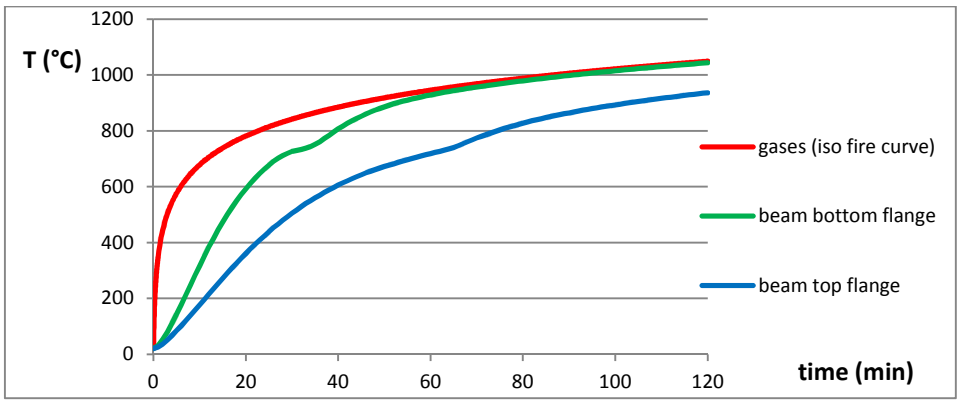

Figure 14. Temperature in the beam flanges versus time

Figure 15a shows the temperature profiles along the end-plate (vertical line at the location of the bolts) and beam web after 10, 20, 30, 60 and 120 minutes. The vertical coordinate *y* is equal to 0mm at the level of the beam bottom flange lower face and to 550mm at the level of the beam top flange upper face. Figure 15b shows the temperature profile in the concrete slab at a distance of 10cm from the column flange after 10, 20, 30, 60 and 120 minutes. The vertical coordinate *y* is equal to 550mm at the level of the beam top flange upper face (slab lower face) and to 670mm at the level of the concrete slab top face.

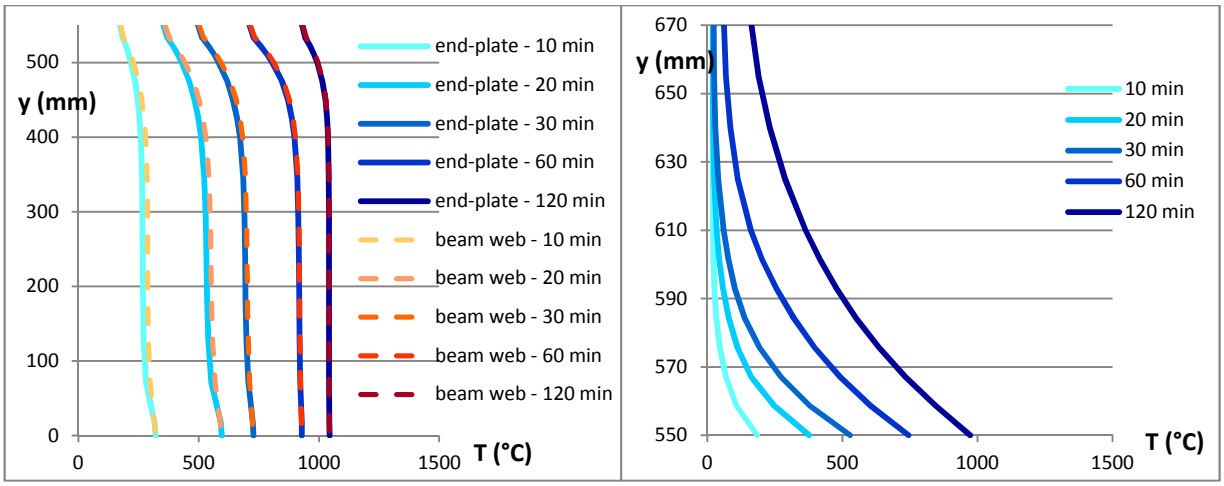

a) b)

Figure 15. Temperature profiles a) in end-plate and beam web; b) in concrete slab

VII.4.7.4. Conclusion

In this section, the evolution of the temperature distribution within a composite beam-to-column joint subjected to the standard fire curve has been investigated through a thermal finite element analysis. Such simulations could be carried out for other limit conditions corresponding to particular fire scenarios or for other joint configurations.

Based on the described thermal finite element simulation, the procedure for the prediction of joint resistance at elevated temperature, introduced in VII.4.8, could be applied to the joint considered.

VII.4.8. M-N resistance of the joint at elevated temperature

VII.4.8.1. Introduction

This section presents an analytical method predicting the resistance of steel or composite joints submitted to both an axial force and a bending moment at elevated temperature. First, the method is explained based on the particular case of the bolted joint linking the primary beams to the columns in the reference car park structure designed and investigated in the present project. Then, the model is validated by comparison to experimental tests performed on this joint at elevated temperature (using the

temperature distributions measured during the tests). Finally, the analytical method is applied to an example based on temperature distributions determined through a thermal finite element simulation (see VII.4.7) to illustrate how the developed model can be applied in a situation of design. More details about all this are given in Deliverable III, section II.

VII.4.8.2. Description of the considered joint

The studied joint links two IPE550 primary beams to a HEB300 column, as represented in Figure 16; it is the joint configuration tested in Coimbra as a contribution to the present project. It is a double-sided composite beam-to-column joint subjected to symmetrical loading. Only the solid part of the composite slab is taken into account for the joint computation (steel sheet and concrete in the ribs are neglected).

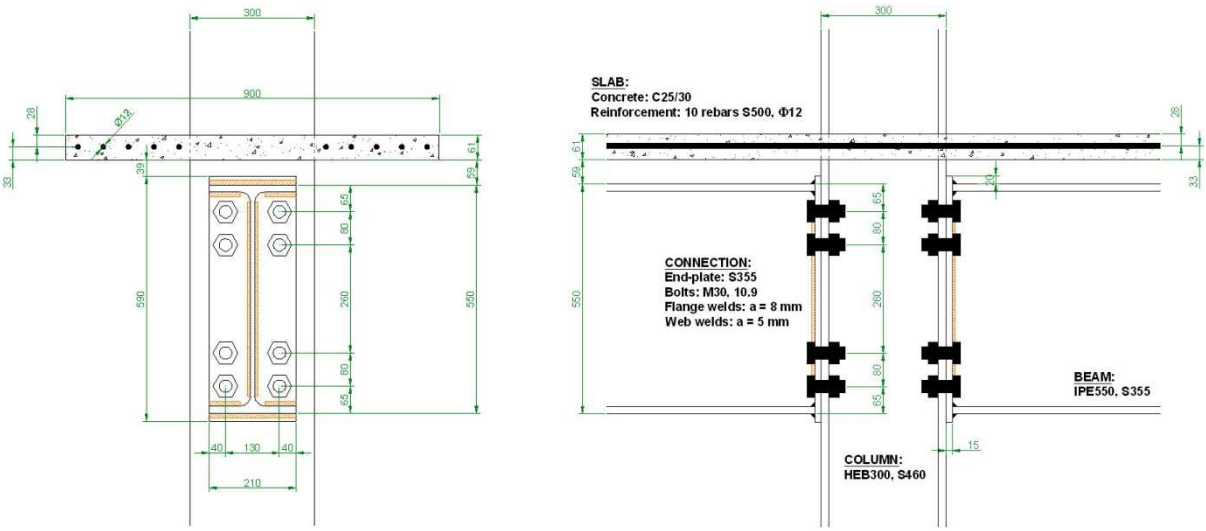

Figure 16. Considered joint

VII.4.8.3. M-N interaction curve for joint resistance

When a joint is subjected to both bending moment and axial load, its resistance is represented by an interaction curve that can be evaluated following the procedure presented in Deliverable III, section II. The proposed analytical model is based on the component method and on the assumption that all components activated at failure are fully ductile, meaning a plastic redistribution of the forces is considered within the joint without any displacement limitations.

Figure 17 shows the nominal M-N resistance curve of the considered joint at ambient temperature (the reference axis is taken at mid-height of the steel profile). The procedure can be applied at elevated temperature as well, provided the temperature distribution in the joint is known. Each component resistance is then simply evaluated based on the material resistance at its given temperature.

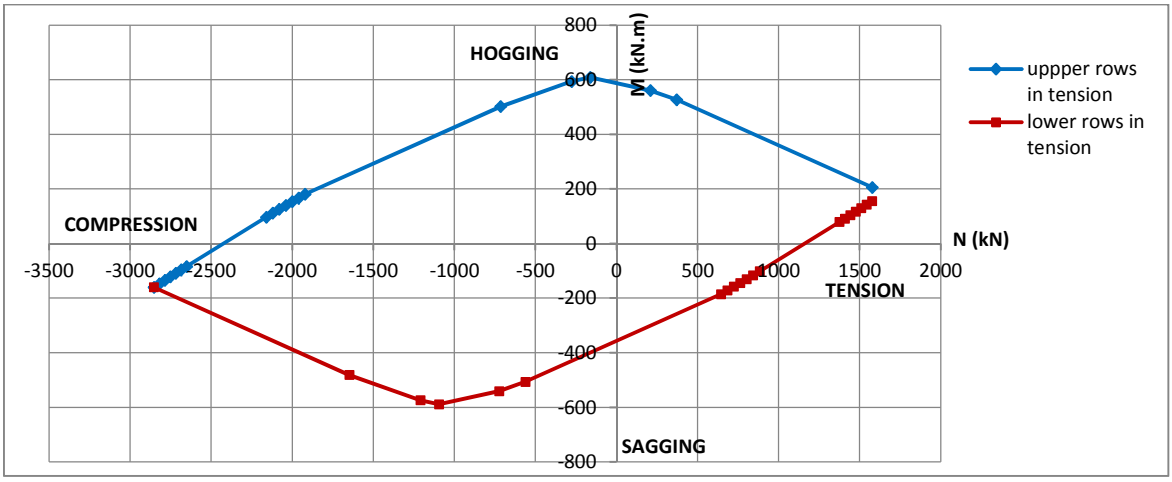

Figure 17. Nominal resistance curve at ambient temperature

VII.4.8.4. Validation of the analytical model against experimental tests

a. Assumptions for the analytical predictions

The aim of these analytical predictions is to be compared to the loading of the tested joints at failure. Consequently, the ultimate joint resistance should be predicted instead of the nominal resistance. That is why all safety factors γ_M were taken equal to 1.0 and the material ultimate resistances were considered instead of the yield resistances. The component temperatures were estimated based on the measurements made during the tests. The material resistances at elevated temperatures were evaluated based on the Eurocode rules and material tests when available. The detail of the considered rules for the decrease in resistance as a function of temperature is given in Deliverable III, section II for all elements (concrete, slab reinforcement, bolts, steel profiles and end-plate).

b. Comparison of the analytical predictions to the test results

For each test, the loading M+N of the joint at failure could be identified. This loading corresponds to one particular point on a (M,N) diagram and can be compared to the analytically predicted M-N interaction resistance (based on the temperature distribution recorded at the moment the joint fails). As the temperature distribution during the tests was not exactly the same in the right and left connections, one analytical resistance curve was computed for each side.

Figure 18 compares the experimental resistance to the analytical prediction for test 4. For this test, the temperature distribution within the joint is supposed to remain constant during the loading simulating the column loss. The reference temperature is measured at the beam bottom flange, 20cm away from the column face, and is kept at 700°C.

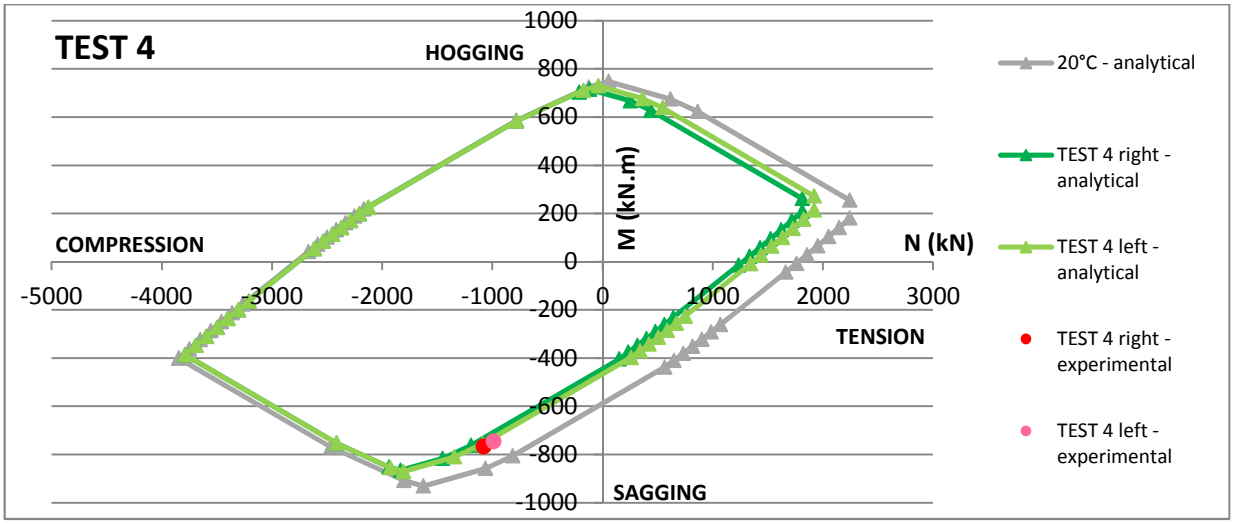

Figure 18. Comparison of the experimental resistances to the analytical curve for TEST 4

Similar results for all tests are provided in Deliverable III, section II. These comparisons proved good agreement between experimental and analytical results, which validates the model predicting the M-N resistance curve for joints at elevated temperature.

VII.4.8.5. Application of the model to a practical example

In the previous section, the analytical model has been validated by comparison to experimental tests. For this validation, the method was applied using the temperatures measured during the tests. In practical design situations, the temperature distribution has to be determined. It can be estimated using simplified models or computed with more sophisticated methods such as thermal finite element simulations. An example of such a thermal numerical model for a composite joint subjected to an ISO 834 fire curve has been presented in VII.4.7. Based on the temperature distributions determined from this analysis, the reduction of the nominal M-N resistance curve in time has been computed; it is presented in Figure 19 (more details are given in Deliverable III, section II).

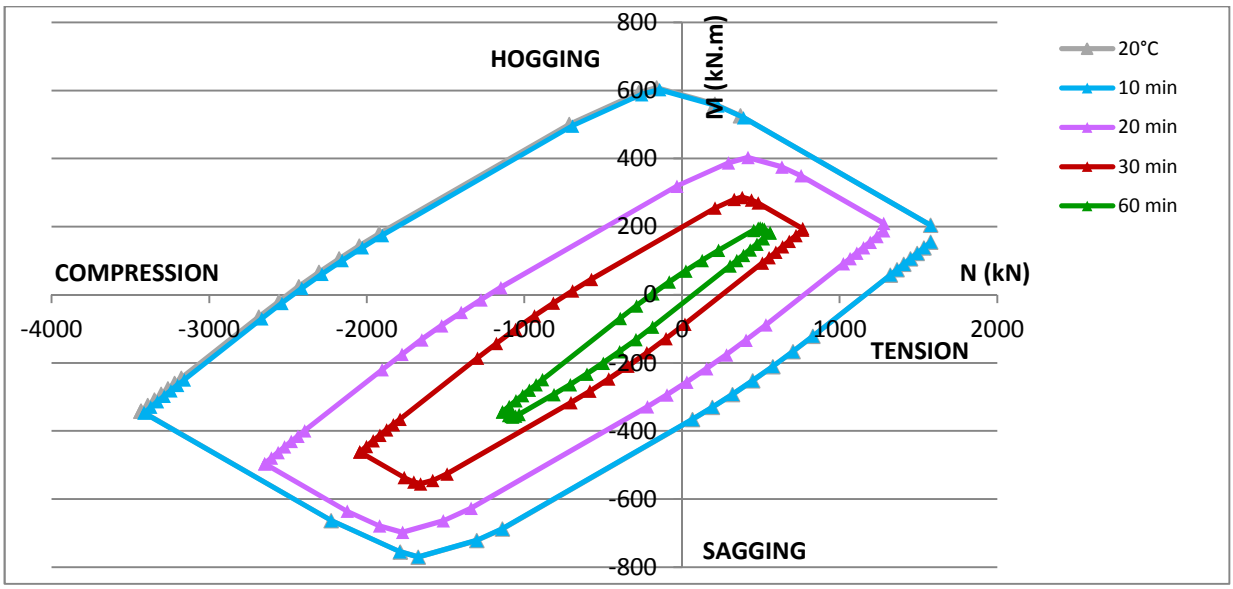

Figure 19. Shrinkage of the M-N resistance curve with the increase in temperature

VII.4.8.6. Conclusion

In this section, an analytical procedure for the prediction of the M-N interaction resistance of steel and composite joints, already developed for ambient conditions, has been extended to elevated temperature and validated against experimental results. This model can be applied provided the temperature distribution within the joint is known, which can be determined using simplified or sophisticated models.

VII.4.9. Concluding remarks

Within this work package 2, behavioural models for beams, columns and joints were derived at two different levels: the FEM models (sophisticated level) and the designer's models (simplified level).

Seven experimental tests were performed on a composite steel-concrete beam-to-column frame under mechanical (bending and axial forces) and thermal loadings (constant temperature equal to 20ºC, 500ºC or 700ºC). The tests results were analysed in detail, and even though compression axial loads were developed at the beams restraints during the tests (instead of membrane effects), they permitted the calibration of the sophisticated and simplified joint models (joint benchmark and M-N resistance of the joint at elevated temperature). Additionally to the joint benchmark, a sophisticated thermal model studied the evolution of the temperature distribution within a composite beam-to-column joint subjected to the standard fire curve.

The behavioural response of the heated beams and columns was studied: i) the column benchmark was performed by three FE programs SAFIR, ADAPTIC and Abaqus and results were compared to experimental results described in Franssen et al. (1995); ii) a simple study of the columns subject to localised fire was detailed, and it was shown that the column loss can be assumed by the total removal of the column; and finally, iii) the composite beam benchmark was developed by ADAPTIC and Abaqus, and models were calibrated against experimental results from Huang et al. (1999). Good consistency of the results obtained from the three software's SAFIR, ADAPTIC and Abaqus was showed. Moreover, the influence of various parameters on the response of the elements (acting forces, axial restraint to beam, distribution of temperatures, level of temperatures, …) was investigated in these models, and the so-validated tools for the investigation of the structural components were used in WP3 when investigation the sub-structures and the structures at the simplified and sophisticated levels.

As an outcome of WP2, two main deliverables are identified: i) experimental tests and development of sophisticated behavioural models (DII), and ii) development of simplified behavioural models (DIII). The first ones are of particular importance as they are the only ones able to follow as closer as possible the reality. This allows considering them as references in research, to use them with full confidence for parametrical studies and finally to use them as a direct design tool for complex structures for which the

use by the designer of simplified behavioural models would be questionable. The simplified models are models which can be more easily used in practice and which could possibly be later on implemented in design guides, software or codes and which allow the designer to assess the behaviour of the structure in a rather easy and direct way, i.e. in agreement with his requirements in terms of efficiency and competitiveness.

VII.5. WP3 – Study of the structural response under selected scenario(s)

VII.5.1. General

The main task of WP3 is to integrate the knowledge acquired on elements in WP2 into a structural model enabling prediction of the integrated structural response under localised fire. Two main objectives of WP3 are identified:

- the development of FEM simulations of the whole structure subjected to localised fire;
- practical behavioural models for the whole structure for design practice.

Under the framework of WP3, a comprehensive study on 3D slab behaviour was undertaken first, including numerical and analytical approaches. Regarding the numerical approach, a benchmark study was conducted to investigate the slab response predicted by two finite element software packages, ADAPTIC (Izzuddin, 1991) and SAFIR (Franssen, 2005). Following the FEM simulations, an analytical model based on the work of Omer *et al.*, 2010 was employed to predict the slab behaviour. Subsequently, a detailed finite element model was developed to study the behaviour of a composite steel-concrete sub-frame under localised fire, where the commercial finite element package ABAQUS, 2011 was used. The overall FEM model for the reference car park was established using ADAPTIC, where the robustness of the structure was comprehensively assessed. Finally, a practical analytical model which is able to predict the response of a structure following column loss was proposed. This model was then adapted to the scenario investigated within this project, i.e. the loss of a column in a car park structure subject to a localised fire. In particular, the main assumptions leading to simplification of the global model were discussed.

VII.5.2. Slab benchmark

In order to study both the ambient and elevated temperature properties of composite slabs, and to validate the numerical tools, a benchmark study was proposed, where the slab profile, material nonlinearity, boundary conditions and the contribution from secondary beams were considered. Two finite element software packages, ADAPTIC and SAFIR, were employed in this study. In ADAPTIC, the new shell element for realistic modelling of composite and reinforced concrete floor slabs (considering the geometric orthotropy of ribbed slab) subject to extreme loading conditions developed by Izzuddin *et al.*, 2004 was employed. Extensive validation of this slab model against experimental results on flat or ribbed reinforced concrete/composite floor slabs had already been undertaken (Elghazouli and Izzuddin, 2004). Further verification of this model was conducted in this benchmark study by comparing the ADAPTIC results with SAFIR predictions.

The studied structures are 16m×10m isolated composite slabs. The basic outlines of the slab models (both uniform slab and ribbed slab) are illustrated in Figure 20, and the corresponding dimensions are listed in Table 3, where a is the slab length, b is the slab width, t is the thickness of steel deck, d is the depth for uniform slab, s is the distance from the top of the slab to the location of reinforcement. In addition, for the slab with ribbed profile, d_1 is the thickness of the cover, d_2 is the thickness of the rib, w_1 is the width of the rib bottom, and w_2 is the width of the rib top. For both of the uniform thickness slab (reference case) and the ribbed slab, the location of reinforcement mesh is 50mm below the top face of the slab. It is assumed that the slab is simply supported, though the planar displacements at the supports may either be restrained or unrestrained. The steel deck is assumed to be unidirectional, acting only along the rib direction while no action is considered along the transverse direction. Therefore, the equivalent area for steel deck can be modelled as 900mm^2/m and 982mm^2/m for uniform and ribbed slabs respectively, and 0mm^2/m along the transverse direction for both cases.

Table 3. Values of slab dimensions

Dimensions(mm)	a	b	d	d_1	d_2	w_1	w_2	w_3	t	s
Value	16000	10000	100	70	60	272	376	224	0.9	50

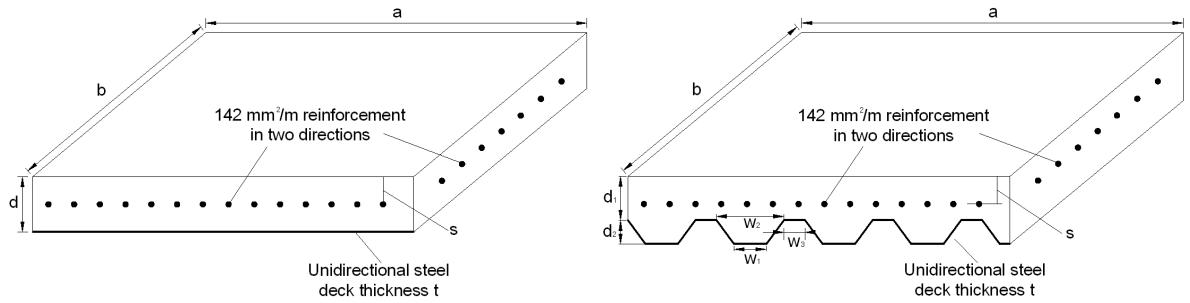

Figure 20. Geometric properties of slab

For the study of the ambient cases, an increasing uniformly distributed load is applied on the slab until very large deformation. With regard to the fire situation, a constant uniform distributed load of 5kN/m^2 is applied on the slab, and a linear temperature gradient is assumed over the depth. The temperature of the bottom face of the slab linearly increases from the ambient temperature (0ºC) to 900ºC, while the temperature of the top face of the slab remains under the ambient condition. The temperature distribution along the length/width of the slab is assumed to be uniform. The thermal characteristics for steel and concrete are based on EN1993-1-2, 2005 and EN1994-1-2, 2005, respectively.

Five cases/models were considered in this study, namely, the reference model, the ribbed slab model, the linear concrete model, the laterally unrestrained model, and the model with secondary beams. The ambient and fire analysis were applied on all the models. The reference case (case 1) was considered as the slab with the following parameters:

- The slab is modelled as a uniform slab without the ribs, and the value of $d=d_1+d_2/2=100$mm is assumed for the thickness of the reference slab.
- The slab is laterally restrained and vertically supported along the four edges, while it is free to rotate at its boundaries.
- A full non-linear behaviour law for concrete is assumed.
- The secondary beams are not included.

Figure 21 and Figure 22 provide respectively the load-deflection and the deflection-temperature response for the uniform thickness slab (reference case) from ADAPTIC and SAFIR. Good correlation is found between the ADAPTIC and SAFIR results. It is worth noting that both of the ambient response curves show a sudden increase in deflection at about 100mm, which is due to concrete cracking.

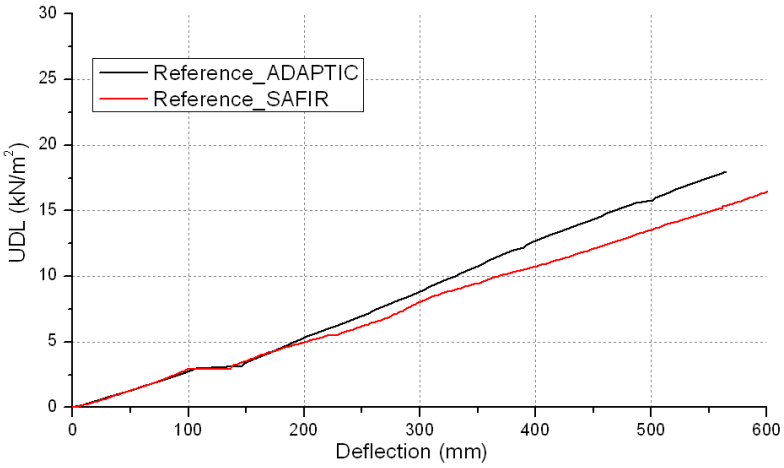

Figure 21. Ambient response of reference (uniform) slab

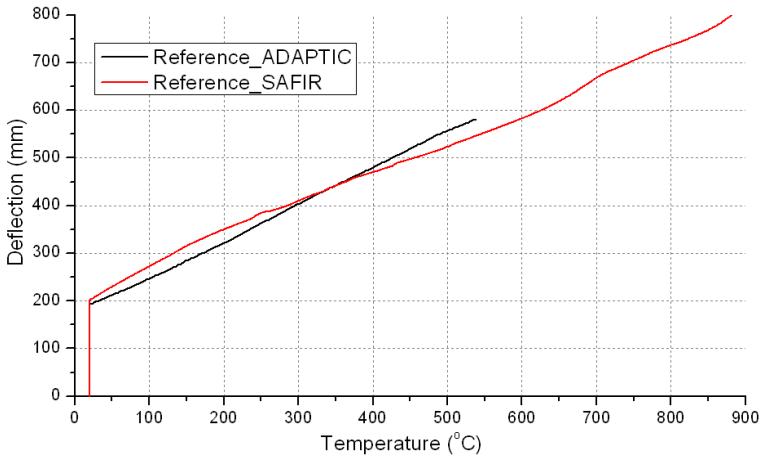

Figure 22. Elevated temperature response of reference (uniform) slab

For the ribbed case (case 2), Figure 23 andFigure 24 provide respectively the load-deflection and the deflection-temperature response for the uniform thickness slab (reference case) and the ribbed slab from ADAPTIC and SAFIR. Good comparisons are found between the ADAPTIC and SAFIR predictions. A small discrepancy is observed in the elevated temperature response, which is attributed to the different modelling approaches employed in the two programs for simulating the ribbed slab profile. It is also found that the ribbed slab has a similar response to the uniform thickness slab with a depth of $d_1+d_2/2$, which indicates that in some cases, employing uniform slabs with appropriate depths can predict the response of ribbed slabs with sufficient accuracy.

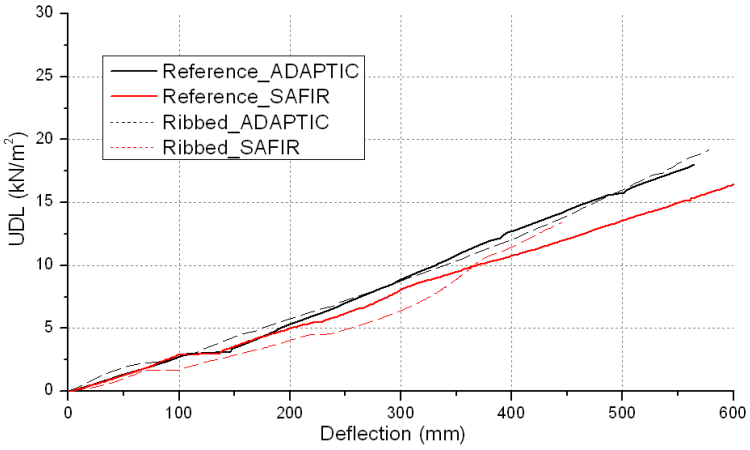

Figure 23. Ambient response of uniform and ribbed slabs

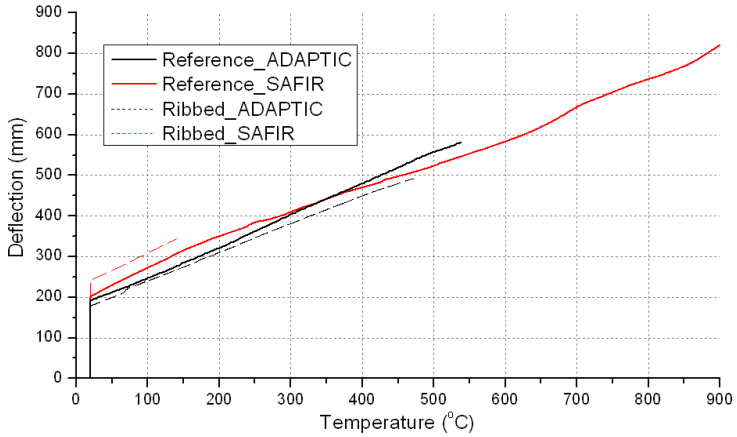

Figure 24. Elevated temperature response of uniform and ribbed slabs

In the linear concrete case (case 3), the slab with a linear law of concrete was employed to compare with the reference slab. The model was the same as the reference case except that the full nonlinear

concrete material properties are replaced by a linear law. The goal of adopting the linear material model was to highlight the importance of concrete nonlinearity on predicting the response of concrete/composite slabs. The variation of material properties (e.g. young's modulus, Poisson's ratio and the thermal expansion coefficient) with the changing of temperature was the same as those considered in the reference model. Through the outcome of this study, it was concluded that employing a linear concrete model that ignores the compressive softening, cracking, and tensile softening leads to inaccurate predictions; hence such models should be avoided.

In case 4, two slabs with two different planar restraint conditions − restrained and unrestrained, were compared. For the restrained slab (reference model), full planar restraints and vertical restraints were applied, hence no planar displacement is permitted for the edge nodes. With regard to the unrestrained slab, the four edges of slab are free to move inwards but are restrained vertically. The edges are free to rotate for both conditions. The aim of considering different boundary conditions was to check if the planar restraint has a significant effect on the load resistance of concrete slabs. Through the outcome of this study, the influences of the continuity of composite slabs and the stiffness of the supporting beams along the edges were shown to be significant.

In case 5, the effect of secondary beams was considered. The locations of secondary beams (IPE500) are consistent with the reference building. Vertical and horizontal restraints are applied along four edges of slab as well as the ends of the secondary beams (the beams at the edges of the slab are not considered). Under the elevated-temperature condition, a uniform temperature was assumed over the depth of secondary beams that have the same material properties of the steel deck, and the temperature was assumed to increase linearly from 0°C to 900°C over the depth of the slab. Full shear interaction was assumed between the slab and the secondary beams. From the results, it was found that the benefit from the secondary beams is maintained until the temperature exceeds 200°C. After this temperature, the deflection of the slab with the secondary beams starts to converge to that without the secondary beams. This phenomenon implies that at certain stages during a fire, the contribution from the secondary beams may be ignored.

As a general remark of the slab benchmark, the results from the two numerical tools compared generally well, but slight discrepancies were observed at larger deflections, which is likely due to differences in the modelling technique adopted in the two models.

VII.5.3. 3D slab behaviour – analytical approach

VII.5.3.1. Introduction

In this part, it will be assumed that a localised fire occurring near a supporting column just above a composite slab will lead to the total loss of this supporting column as well as a reduction in the resistance of of the beams (primary and secondary) and the steel profile of the composite slab. Also, it is assumed that the unidirectional concrete ribs of the composite slabs are not significantly influencing the behaviour of the slab when significant membrane effects are developing i.e. it is assumed that only the upper part of the slab is contributing to the slab resistance.

Accordingly, the behaviour of the composite slab can be investigated through the study of a 3D uniform slab, subjected to the loss of one of its supporting columns, assuming that this slab remains at ambient temperature. The objective here was to investigate if the response of the slab following the loss of a column support can be predicted through analytical methods, taking into account the membrane effects.

In the first step, a parametric numerical study has been conducted to investigate the influence of the boundary conditions on the slab behaviour. Then, in the second step, the applicability of existing analytical methods to predict the behaviour of the slab under the considered scenario has been investigated.

VII.5.3.2. Influence of boundary conditions

In Lemaire, 2010, a preliminary study has been conducted to investigate the effect of the boundary conditions of a slab on the development of membrane forces in case of a column loss (see Figure 25). In total, four slab configurations have been investigated in Table 4:

Table 4. Slab information

	Horizontally unrestrained edges	**Horizontally restrained edges**
No rotational restraints	CASE 1	CASE 2
Rotational restraints	CASE 3	CASE 4

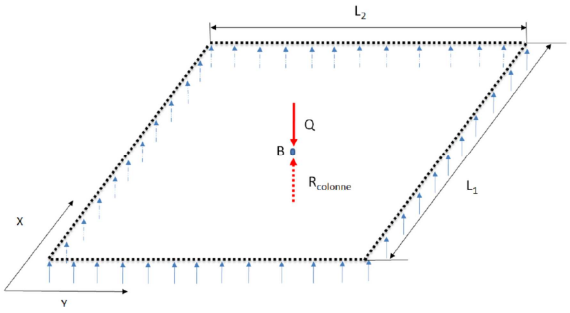

Figure 25. Investigated slab further to a column loss

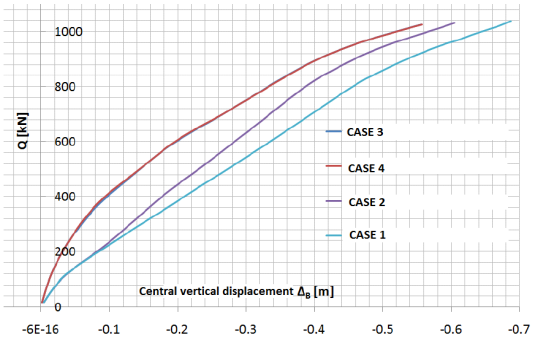

Figure 26. Results for different boundary conditions

For the 4 cases, it has been observed that significant tension forces developed in the center of the slab, while a compression ring forms on the slab borders, to equilibrate the central membrane forces (more details on each case can be found in Deliverable V). As can be seen in Figure 26, the most critical case is case 1, which is the case for which the slab is less restrained.

So, the case that has been studied analytically is case 1. The analytical models which will be used come from the article “Failure of unrestrained lightly reinforced concrete slabs under fire, Part 1: Analytical Models”, by Omer *et al*., 2010.

VII.5.3.3. Presentation of existing models for totally unrestrained slabs

The simplified ambient temperature models developed by Omer *et al*., 2010 are presented within the present section.

The studied slab is assumed to be loaded by a uniformly distributed load. The models are kinematic models. They are based on the assumption of the development of a yield line mechanism, followed by the development of membrane forces and the occurrence of full depth cracks in the slab. It is also assumed that the yield line mechanism occurring in slabs submitted to uniformly distributed load is as shown in Figure 27, η being a function of the slab dimensions, a and b.

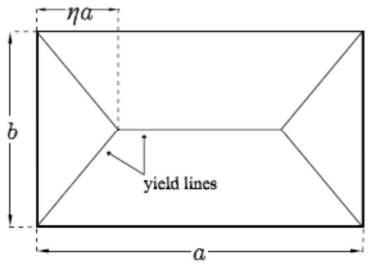

Figure 27. Yield line plastic mechanism in uniformly loaded slabs

When the plastic mechanism is formed, the stress in the reinforcement crossing the yield lines is equal to f_y. It is assumed that the elastic deformation of the slab can be neglected towards the deformation occurring after the development of this plastic mechanism.

Once the plastic mechanism is formed, the parts of the slab, delimited by the yield lines, are assumed to rotate rigidly around their support and the yield lines. These rigid parts are linked to each other by the reinforcement that stretches out, according to a rigid-strain hardening law material. The failure occurs when the stress in the reinforcement reaches the ultimate strength of the steel.

The kinematic models take into account the strain concentration in the reinforcement that links the rigid parts of the slab. This strain concentration is influenced by the bond-slip strength σ_b: if the latter is large, then the bond length l_b will be short and the strain concentration will be important.

As the models are kinematics models, crack patterns have to be defined. It is assumed that two configurations are possible for the position of the full depth cracks for the case of unrestrained slabs, parallel to the shorter span of the slab (Figure 28).

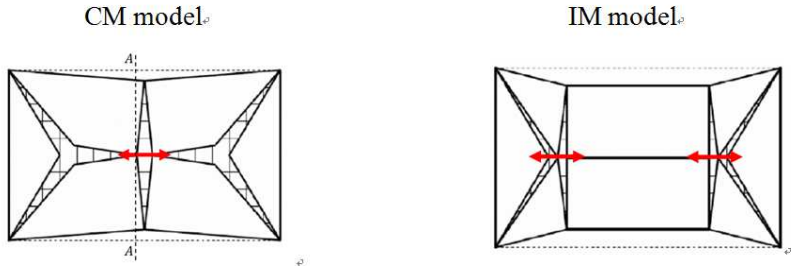

Figure 28. Crack mechanisms for horizontally unrestrained slabs (Omer et al., 2010)

Summary of the assumptions and of the solving procedure

- Main assumptions:

– No horizontal and rotational restraints at the slab edges (= simply supported edges)
– Slab subjected to uniformly distributed load (q)
– Uniform slab (constant thickness, no ribs)
– Single layer of reinforcement
– Orthotropic reinforcement (layers in the two directions assumed at the same level)
– Rigid-strain hardening material model for steel
– Negligible concrete tensile strength
– Concrete fully rigid in compression
– Bond-slip response described by a rigid-plastic law

- Solving procedure to obtain the $q - U_c$:

– choose a value of U_C, the central deflection of the slab
– by compatibility of displacements (assuming one of the two crack patterns in Figure 28), find the elongations Δ_s of reinforcement in the different cracks
– knowing these elongations, determine the rebar forces T_s, according to the rigid-strain hardening law material
– knowing the elongations and the rebar forces, compute the internal dissipated energy $\dot{D}$ which is a function of U_c(through Δ_s and T_s) (all the energy is dissipated in the steel reinforcement and through bond-slip because concrete is assumed to be fully rigid)
– compute the external dissipated energy $\dot{E}$, which is a function of q, the uniformly distributed load acting on the slab
– find the q corresponding to the chosen U_c by writing $\dot{D} = \dot{E}$ ($\dot{D} = f(U_c)$ and $\dot{E} = f(q)$)

Rupture occurs when the reinforcement across the full depth crack (in the centre or at the intersection of the yield lines) reaches the ultimate strength of steel T_u. Writing that the rebar force in the full depth crack reaches T_u, the corresponding elongation can be found, and finally, the $U_{c,limit.}$

Accordingly, with this procedure, it is possible to predict the maximum deformation capacity of the slab ($U_{c,limit.}$) and its associated load (q_{limit}). Knowing that, it is finally possible to check if the slab is sufficiently resistant by checking if the uniformly applied load q is smaller than q_{limit}.

VII.5.4. Sub-frame FEM model

VII.5.4.1. Introduction

A finite element model was developed to study the behaviour of a composite steel-concrete sub-frame. The commercial general finite element package Abaqus (2011) is used to model the composite steel-concrete beam-to-column frame extracted from the real open car park building. The symmetry of the joint is taken into account, and the structural elements are modelled combining C3D8R solid elements and contact pairs. The main objective is to study the detailed behaviour of the composite sub-frame when it is subjected to the loss of a column in the car park building. Materials for steel members and connection components are established by the steel tensile coupon tests, whereas the concrete behaviour is defined according to Eurocode 2 part 1.1 (EN 1992-1-1:2004). The behaviour of the joint under bending moments is discussed: first, numerical results for the steel frame under hogging and sagging bending moments are shown (the "steel model"); then, preliminary results for the composite steel-concrete frame under sagging bending moment (the "composite model") are presented and compared with the results of the experimental test that was performed at the University of Coimbra at ambient temperature (reference test 1); good agreement is observed.

VII.5.4.2. Numerical model

In order to save computational time, the symmetry of the joint is taken into account in the model; only one fourth of the column, half of the end-plate, four bolts and one fourth of the concrete slab are modelled (Figure 29). The main joint members are modelled with C3D8R solid elements, and the upper part of the steel column away from the joint zone is modelled using general B31 beam elements (the Abaqus "Coupling" function joins these two finite elements). The initial deformation of the end-plate measured in the laboratory (space of 0.6 mm between the end-plate centre and the column flange) is reproduced in Abaqus using a sinusoidal shape between bolt rows 2 and 3. Bolts M30 are modelled with a reduced diameter size d_s equal to 26.73 mm, equivalent to the resistant section A_s (561 mm^2), and the hole around the bolt shank (diameter of 26.83 mm) is only slightly higher than the bolt diameter. For the composite model, the composite slab is simplified by a concrete slab, with an equivalent rectangular section of thickness 94 mm and width 450 mm (it is assumed that the concrete from the ribs is uniformly allocated to the entire slab). The five steel rebars of 12 mm diameter, as well as the constructional longitudinal (8 mm diameter) and transversal rebars (6 mm diameter), are modelled with solid elements and are embedded in the concrete slab. In order to prevent sliding, the full connection between the concrete slab and the steel beam is modelled using the TIE option.

The general static analysis is used. Several steps are defined: step 1 - pre-loading of bolts; step 2 - application of the self-weight; step 3 - hogging bending moment; steps 4 and 5 - sagging bending moment. Mechanical properties of the steel from the beam, the column, the end-plate and the bolts are defined by the tensile coupon tests (see WP2). The true stress-strain values are used in Abaqus. Concrete properties are defined according to Eurocode 2 part 1.1 (EN 1992-1-1:2004) for the stress-strain behaviour of the concrete C25/30 in compression. The behaviour of the reinforced concrete in tension is defined by the maximum tensile stress (2.6 MPa), and by its fracture energy G_F (93.4 N/m), defined in CEB, 1990. Contact interactions (surface-to-surface contact) are defined between the end-plate and the column flange, and between each bolt and the column flange and the end-plate. The y-direction at the beam extremity is restrained during steps 1 to 3; during the application of the sagging bending moment (steps 4 and 5), the support is modelled by a rigid cylinder in contact with the beam, no friction is applied (Figure 29). The x-direction beam extremity is free; the top of the column is free in the y-direction, the x and z directions are restrained all along the column and the concrete slab, and the column and beam webs are restrained in the z-direction. The application of the hogging and sagging bending moments in the joint are simulated by displacement control at the top of the column.

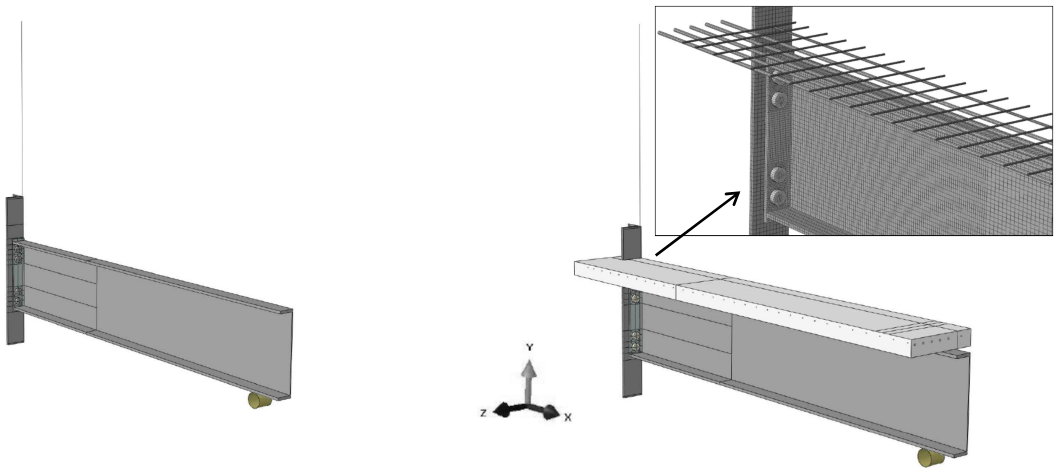

a) b)

Figure 29. 3D FE model of the steel (a) and composite steel-concrete (b) sub-frame in Abaqus

VII.5.4.3. Numerical results

The comparison between the results from the experimental test and FE models is made based on the Moment-Rotation curves (Figure 30a), calculated as for the experimental test (see WP2). The FE steel model reached a hogging bending moment equal to -244 kNm and a maximum sagging bending moment equal to 507 kNm, which corresponds to a maximum rotation of 33 mrad. Plastic deformations of the end-plate are evidenced in the compression zone, and the ultimate stress-strain is reached in the bottom bolt (row 4). Once this bolt failed, the bending moment begin to decrease and the FE model ended because of non-convergence. The comparison between the experimental test and the steel model shows that the main advantages of the concrete slab are the increase of: i) the initial stiffness, more 70% and 95% under sagging and hogging bending moments respectively; and ii) the resistance, the first failure of the bolt happens latter, and the maximum sagging bending moment is increased of 40%.

The initial stiffness of the FE composite model is 23% higher than the stiffness obtained from the experimental test. The behaviour of both under sagging bending moment (experimental test and FE model) is very similar and close. Under the last increment (bending moment equal to 584 kNm, and rotation equal to 13.3 mrad), the bolt has not yet reached the ultimate stress-strain; Figure 30b shows that the equivalent plastic strains in the bottom bolt (row 4) are localised near the bolt head, just like the bolt failure during the experimental test. At this point (13.3 mrad), the concrete is not yet crushed against the column flange. However, in the experimental test, the concrete was crushed against the column flanges for 13/14 mrad of rotation.

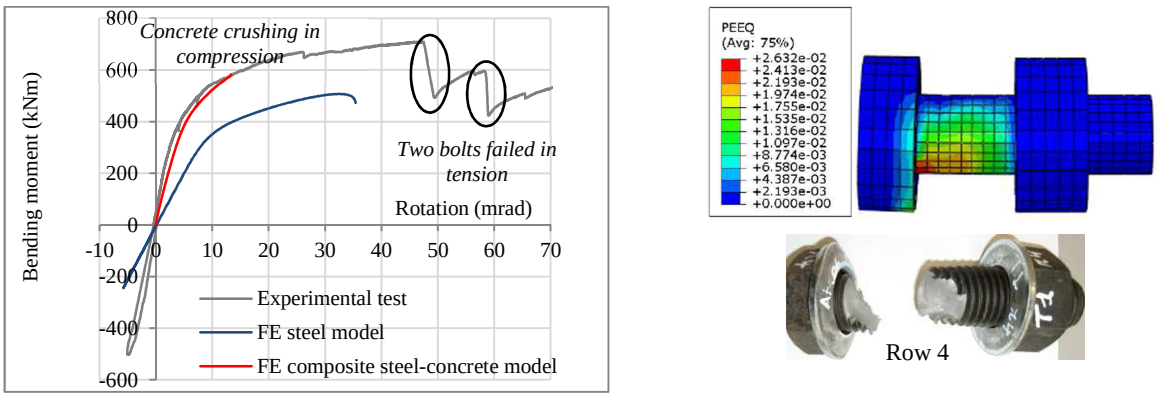

a) b)

Figure 30. a) Bending moment vs rotation at the joint left side – Comparisons between experimental and FE results; b) Location of the bolt failure and equivalent plastic strains

The deformation mode under sagging bending moment for the FE steel and composite models are compared in Figure 31 to the experimental deformations obtained at the end of the test, which do not correspond to the same level of loading; deformation modes are similar. The deformation at the end-plate centre do not appear as high as the experimental test, but it is not quantitative comparable for now because: i) the maximum deformation of the frame in the experimental test is higher than for the FE models, and ii) the hole in the end-plate and column flange for the shank of the bolt is not modelled as in reality, with more 3 mm for the diameter defined in EN 1990-2:2008 for bolts M30. The convergence of the composite model could be improved, notably by an appropriate definition of the damping energy, but also by modelling: i) the shear connectors between the concrete slab and the steel beam; ii) a higher bolt hole in the end-plate and in the column flange (in order to observe if the 3 mm space would influence the centre deformation of the end-plate under sagging bending moment).

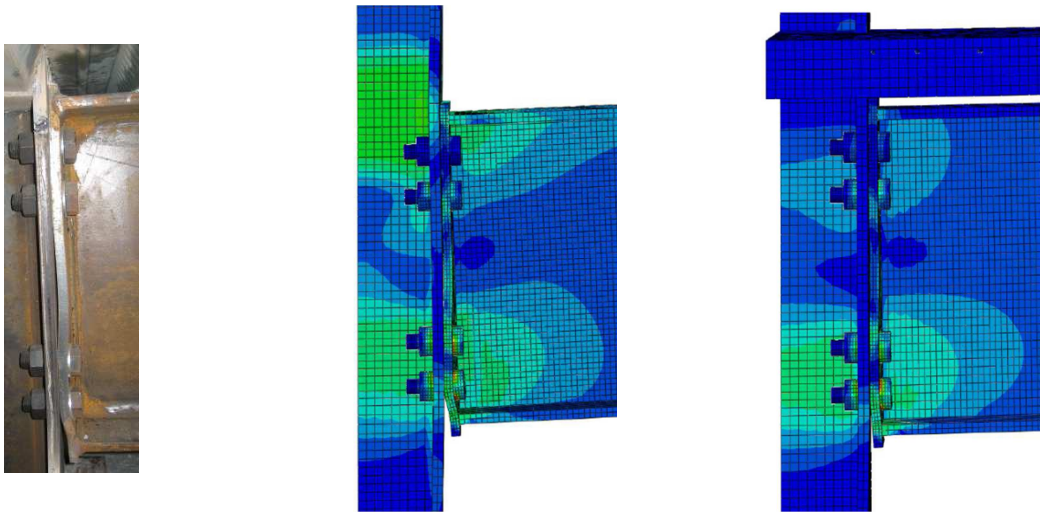

a) b) c)

Figure 31. End-plate deformation at: a) the end of the experimental test (vertical displacement of 220 mm); b) the steel model (vertical displacement of 104 mm); c) the composite model (vertical displacement of 39 mm)

VII.5.5. Global FEM model

VII.5.5.1. Multi-level structural modelling approach

Three modelling levels were proposed, as shown in Figure 32. At Level A, consideration is given to a whole system of an influenced sub-structure with appropriate boundary conditions to represent the surrounding cool structures. The interactions among the heated column, the fire affected floor and the upper ambient floors are fully considered. Provided that the upper ambient floor systems have identical structural type and applied loading, the assessment model can be simplified to Level B, where a reduced model consisting of a fire affected floor-column system and a spring representing the upper ambient floor systems are considered. At this level, the two systems (i.e. fire and ambient) are investigated separately. The derived characteristics of the ambient floors can be applied into the nonlinear spring. At Level C, planar effects within the floor slab are ignored, and grillage models with composite beams are considered instead.

The modelling Levels B and C were employed in this project to simulate the reference car park designed in accordance with WP5. Cubic elasto-plastic beam-column elements were employed to model the steel beams and columns (Izzuddin and Elnashai, 1993). Full shear connection between the steel beams and concrete slab was assumed and was realised by interconnecting the steel beams and the slab with rigid links. Linear elastic boundary springs were applied at the ends of the beams to represent the restraints from adjacent members. The shell element (Izzuddin *et al.*, 2004), which considers the geometric orthotropy, compressive nonlinearity, crack opening and closure as well as temperature effects, were employed for the Level B model. With respect to the level C model where a composite grillage is established, the slab was represented by elasto-plastic beam-column elements (Izzuddin and Elnashai, 1993). The effective width for the concrete slab was obtained from EN1994-1-1, 2004 to consider the shear lag effects.

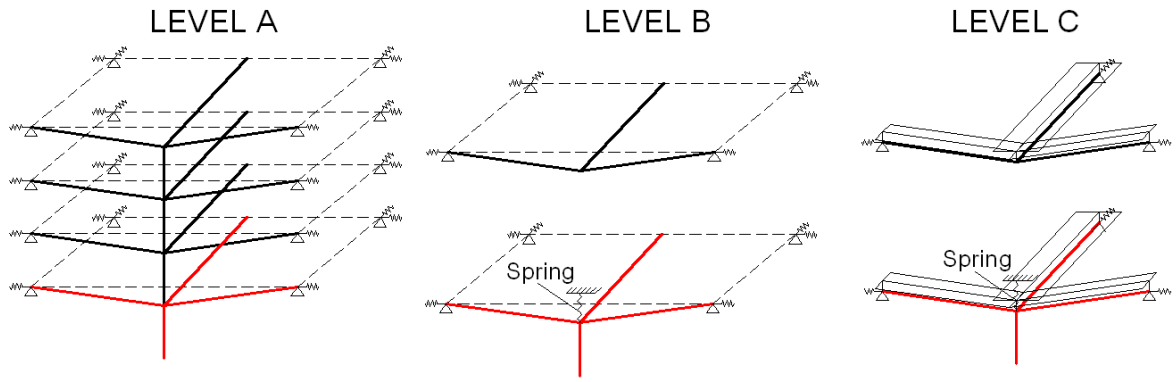

Figure 32. Illustrative descriptions of the three proposed modelling levels

VII.5.5.2. Thermal analysis

The selected fire scenario assumed that four V3 class cars are parked around an internal column, and the fires are triggered in the sequence as shown in Figure 33. The maximum heat release rate of each car is 8.3MW. The interval of the fire spreading from one car to another/other car/s is 12 minutes, and the history of temperature distribution within structural members (e.g. steel beams and composite slab) were captured at 3 minute intervals. The vertical distance between the fire origins and the ceiling is 2.4m. The finite element programme SAFIR was employed to conduct the thermal analysis for the car park under the selected fire scenario. The thermal output data were extracted and input into the finite element model established in ADAPTIC for structural analysis.

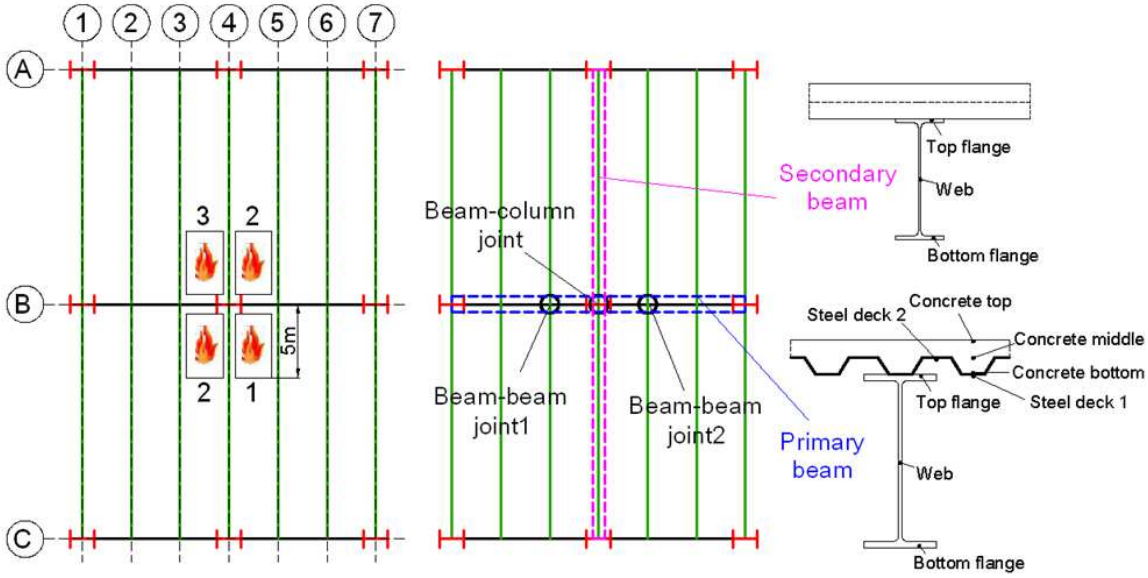

Figure 33. Selected fire scenario

Figure 34 shows the obtained temperature distributions along the primary beam, secondary beam, and the concrete flange of the primary beam (beam positions are identified in Figure 33) at a time of 30 minutes obtained by SAFIR. It is observed that for both primary and secondary beams, high temperatures are only observed within parts of the beam length in the vicinity of the fire origins, whereas for adjacent beam parts which are not immediately above the fire origins, the temperature decreases rapidly to room temperature. This indicates that the fire affected area is rather localised, and the surrounding structural members may be seen at ambient temperature. For the slab, it is observed that at a time of 30 minutes, the temperature in the steel deck is much higher than that in the concrete, even for the concrete immediately above the steel deck. The temperature decreases further towards the top of the slab which is almost under room temperature. Also, high temperatures are only observed within the slab near the fire origins, while the surrounding part of the slab remains under a much lower temperature.

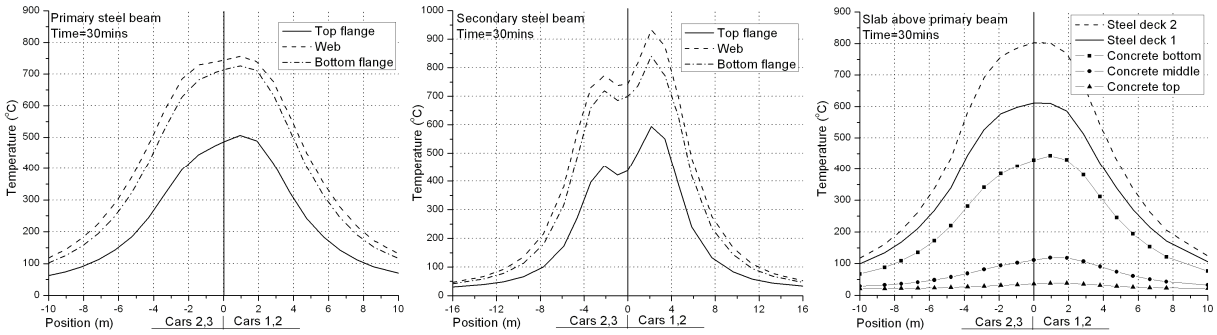

Figure 34. Temperature distribution within steel beams and slab

VII.5.5.3. Failure assessment procedure

Based on the defined joint failure criteria (Fang *et al.*, 2010), a structural robustness assessment procedure was proposed. Recent research (Izzuddin *et al.*, 2008) indicated that even the collapse of one floor can cause severe damage in the floor below for typical steel-framed composite constructions, thus triggering progressive collapse. Therefore, the definition of safe structure in this study is based on the avoidance of collapse in any of the affected floors, In other words, structural failure/progressive collapse occurs when the deformation of either the fire affected floor or the upper ambient floors exceeds their respective ductility capacity. In this respect, the failure of any floor system is attributed to the ductility failure of any surrounding ambient joint on that floor, thus failure criteria are defined in terms of whether the ductility limits of the joint are exceeded. If the surrounding ambient joints have sufficient resistance, but the joints directly exposed to fire fails first, the structure is still deemed safe. The proposed failure assessment procedure is given in Figure 35. It should be noted that it is possible for a structure to survive after failure of the surrounding ambient joints, provided that sufficient resisting mechanism (e.g. membrane action) is maintained by the slab. However, residual load resistance beyond failure of surrounding ambient joints has not been fully studied and thus needs further investigation.

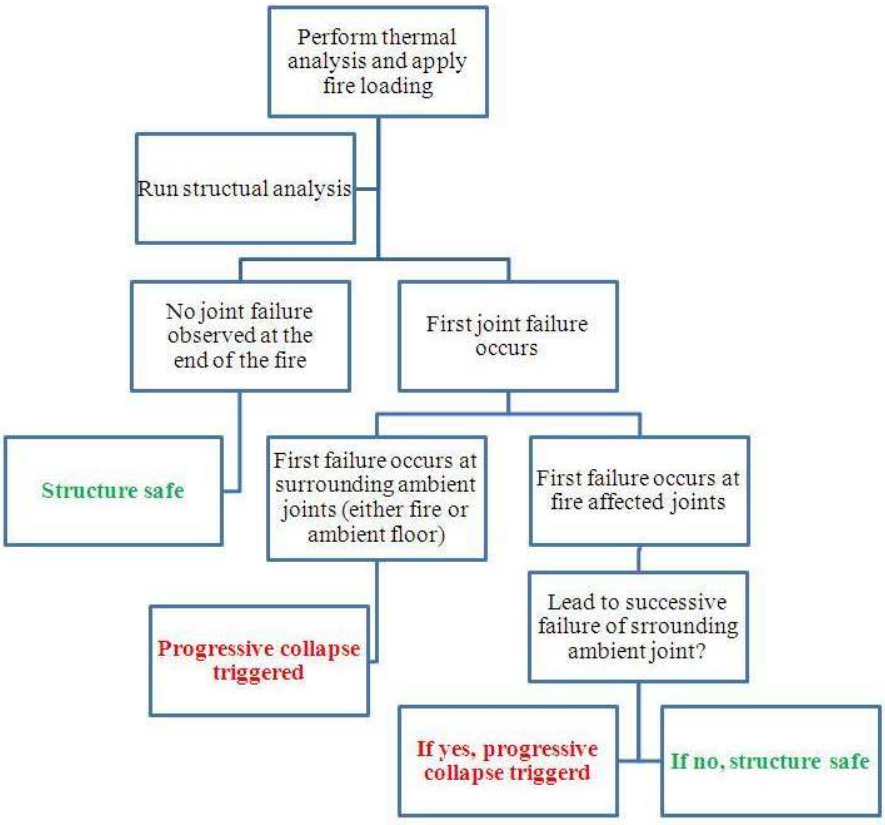

Figure 35. Robustness assessment procedure of car parks subject to vehicle fire

VII.5.5.4. Structural analysis

The considered system model was comprised of the fire affected column, the fire affected floor, and the non-linear spring that represents the performances of the upper ambient floors. Each individual ambient floor has to be investigated first to assess its stiffness and resistance. Accordingly, the characteristics of the spring can be obtained from the superposition of the responses of all the above floors. Afterwards, analysis was undertaken on the fire affected system model with the gravity load and the subsequent thermal load. The selected fire scenarios at three selected floors levels were considered in this project, which are floor level 1, level 5, and level 8. Two slab modelling approaches (grillage approximation and shell element model) were used and compared. The analysis was performed over a time domain, where the temperature-time response of the entire system model is extracted from the thermal analysis conducted in SAFIR. Employing the structural model, dynamic analysis was performed to capture potential dynamic effects, where equivalent lumped masses are applied at each node of the slab.

Based on the results of structural analysis, three failure types were generally observed for the reference building subject to the selected fire scenarios, namely, 'single-span failure' type, 'double-span failure' type and 'shear failure' type, as illustrated in Figure 36.

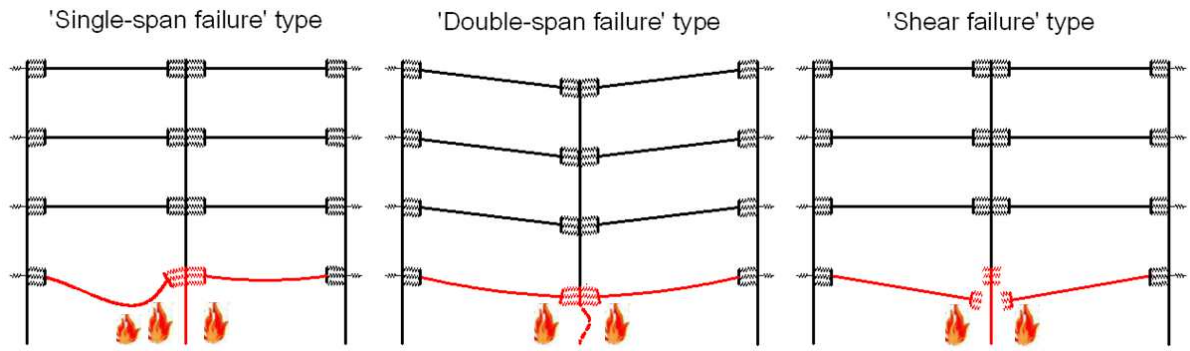

Figure 36. Typical fire-induced failure types

The single-span failure type usually occurs in the cases when the fire affected column maintains its strength during a fire, or the upper ambient floors can offer sufficient resistance for the fire affected floor system with an acceptably small deflection after the buckling of the column, while the single-span beams are unable to survive due to the failure of the supporting joints. This failure type is only found in the grillage model established in this study.

The 'double-span failure' type is associated with the case where the fire affected floor and the upper ambient floors do not have sufficient ductility to redistribute gravity load after the fire affected column is buckled. This failure type is typical for 'column loss' scenarios, and is found in both full slab and grillage models considered in this study.

The 'shear failure' type is associated with the shear failure of steel connections, and it is normally triggered by the shear failure of the fire affected joint. This failure type can either happen before or after the buckling of the fire affected column, as long as significant shear force is transferred between the column and the connected steel beams. When shear failure occurs, the fire affected floor can be completely detached from the middle supporting and subsequently deflects in a double-span cantilever manner. This failure type may be avoided through employing appropriate design strategies, e.g. making the rebars go through the column web/flange openings.

Table 5 provides key results of the reference car park subject to the considered fire scenarios. It can be concluded that the full slab models predict better structural robustness than the grillage models. This indicates that although grillage approximations are usually sufficient for conventional structural designs which are based on ultimate/service limit state assessment of structures under normal loadings, they may be too conservative for structural robustness assessment that is associated with extreme loading.

Table 5. Structural responses under fire

Structural response	Fire floor levels	Full slab model	Grillage model
Column buckling time	1	24m56s	25m27s
	5	25m25s	26m00s
	8	27m10s	No buckling
First joint failure time	1	30m00s	25m27s
	5	No first joint failure	25m20s
	8	27m10s	25m20s
First joint failure position	1	Fire affected beam-to-column steel connections in shear	Fire affected major axis beam-to-column joint under sagging moment
	5	No first joint failure	Fire affected minor axis beam-to-column joint under hogging moment
	8	Fire affected major axis beam-to-column joints under sagging moment	Fire affected minor axis beam-to-column joint under hogging moment
First joint failure type	1	Shear failure	Double-span
	5	No first joint failure	Single-span
	8	Double-span	Single-span
Progressive collapse triggered after first joint failure?	1	No	Yes
	5	-	Yes
	8	No	Yes
Successive joint failure position triggering progressive collapse	1	Structure safe	Ambient major axis beam-to-column joint under hogging moment
	5	Structure safe	Ambient major axis beam-to-column joint under hogging moment
	8	Structure safe	Ambient minor axis beam-to-column joint under hogging moment

Finally, dynamic effects arise for the floor system following column buckling due to fire. The corresponding final floor deflection was found to fall between two idealised extreme cases, which are ‘static column loss’ and ‘dynamic sudden column loss’. It was also observed that more significant dynamic effects arise when the vehicle fire occurs at the top floor. This suggests that in order to predict a reliable ductility demand of a car park subsequent to column loss due to vehicle fire, dynamic analysis that accurately models the column buckling process may be necessary.

Based on the detailed numerical analysis, a multi-sophistication robustness assessment framework was proposed for WP4, attempting to bridge the gap between the current codified treatments of fire hazards and progressive collapse. The robustness assessment framework is comprised of three basic components, namely, detailed Temperature-Dependent Approach (TDA), simplified Temperature-Dependent Approach (TDA), and Temperature-Independent Approach (TIA). Details of the applications of these approaches can be found in the deliverables for WP4.

VII.5.6. Global analytical model

VII.5.6.1. Introduction

Within the present section, a global analytical model able to predict the response of a structure following column loss will be first introduced. Then, this model will be adapted to the scenario investigated within this project, i.e. the loss of a column in a parking structure further to a localised fire. In particular, the main assumptions leading to a simplification of the global model will be considered. The global concept will be first introduced on a 2D frame, and then generalised to a 3D frame.

The aim of the global model is to determine the displacements and internal forces in the whole structure when the column is completely lost. Knowing these forces and displacements in the structure, it is possible to verify if the structure is robust or not, by checking, on one hand, ductility conditions (can the joints sustain such rotations?,...) and on the other hand, resistance conditions for key-elements (can the columns next to the lost one sustain the additional compression?,...).

To achieve this goal, a substructure is extracted from the entire structure; the influence of the rest of the structure is considered by inserting horizontal springs in the simplified substructure.

VII.5.6.2. 2D-frame

In this part, the beneficial effects of the slab are not considered. The study is focusing on frames only composed of columns and beams. No dynamics effects are considered and the method is for ambient temperature.

When a 2D frame still has its column, the frame is normally loaded (phase n°1); the column which will be lost is supporting a compression load N_0. Then, to simulate the loss of the column, a concentrated load Q, going downwards, (Figure 37) is introduced. This force Q increases as the column disappears, and the column is totally removed when $Q = N_0$.

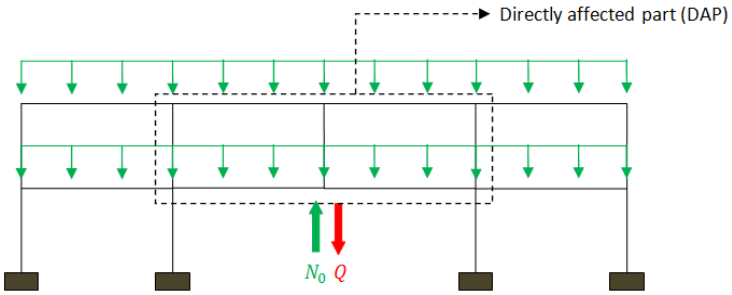

Figure 37. Force Q simulating the column loss

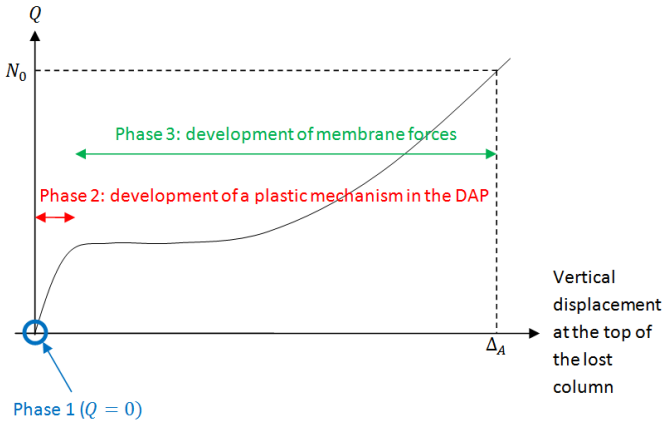

Figure 38. $Q - \Delta_A$ curve

When the column is progressively removed (i.e. Q increases), the directly affected part begins to deform. During the column removal, two phases are identified:

- Phase 2, which is developing from $Q = 0$ to $Q = Q_{pl}$, which corresponds to the formation of a plastic mechanism in the directly affected part
- Phase 3, which starts at $Q = Q_{pl}$ and ends at $Q = N_0$, i.e. when the column is fully removed

During Phase 3, as a plastic mechanism has formed in the directly affected part, the first order stiffness of the structure is equal to zero and so, large displacements occur. Due to these large displacements, significant membrane forces develop in the beams of the directly affected part.

To predict the behaviour of the structure during phase 1 and 2 is easy as usual methods of analysis can be used. However, during phase 3, the analysis of the frame and the prediction of its response become difficult as significant second order effects are developing.

The objective with the developed analytical procedure is to be able to predict the response of the frame during phase 3. In particular, the object is to determine the displacement Δ_A (the vertical displacement at the top of the lost column) when Q reaches the value of N_0, i.e. when the column has totally disappeared (Figure 38). Knowing this value of Δ_A, it is possible to determine:

- the requests in terms of deformation capacity for the structural elements
- the load distribution within the structure and so, to check the structural member resistance

a. Development of a frame behavioural model

- Extraction of the substructure

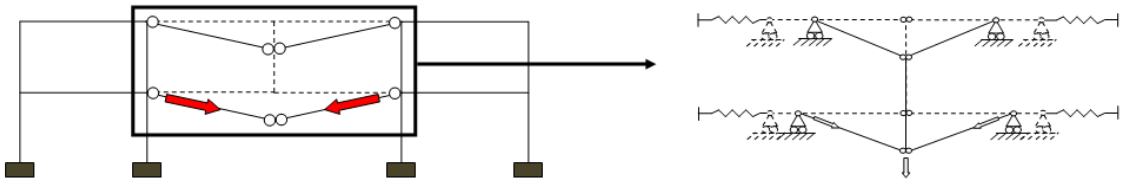

Figure 39. Extraction of the substructure

As can be seen in Figure 39, the studied substructure is composed with all the stories of the directly affected part. The indirectly affected part is replaced by horizontal springs, representing the lateral anchorage provided by the rest of the structure, leading to the development of membrane forces. As the developed method is used to predict the structural response during phase 3, i.e. when a plastic mechanism is formed in the directly affected part, this substructure is studied through a rigid-plastic analysis.

- Equations of the analytical model

The equations used in the analytical model come from two distinct parts of the frame: the directly affected part (above the lost column) and the indirectly affected part (beside the directly affected part) (Figure 40).

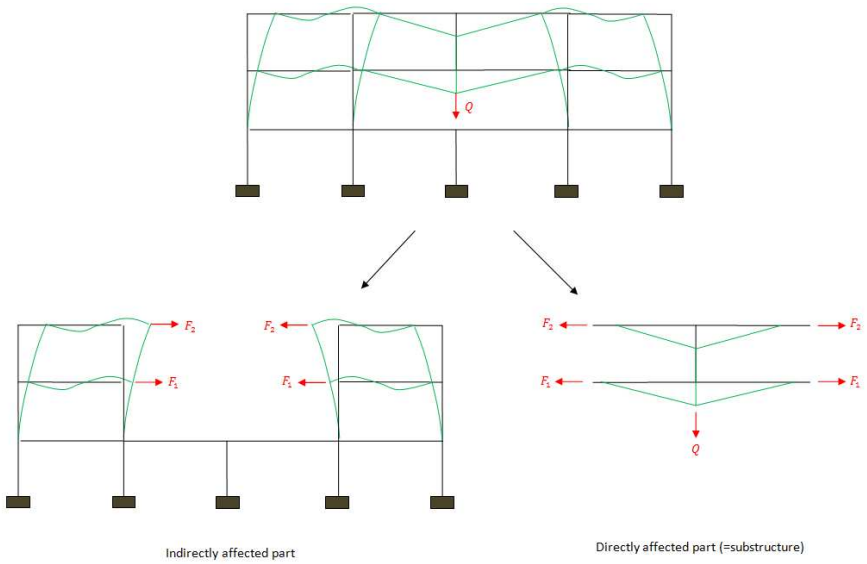

Figure 40. Directly and indirectly affected parts

For these two parts of the structures, equations can be written (compatibility of displacement, elongations, forces equilibrium...). These equations are coupled, representing the coupling between the directly and indirectly affected parts.

b. Derivation of robustness requirements

The system of equations allows finding the forces and displacements in the entire structure when the column has completely disappeared (i.e. when $Q = N_0$). Knowing these forces and displacements, ductility and resistance conditions have to be checked to ensure the frame's robustness.

VII.5.6.3. 3D-frame

For the analytical study of a 3D-frame (still considered with no slab), the idea is the same as for the 2D-case: write equations for a substructure containing all the directly affected part, in which the indirectly affected one is replaced by horizontal springs. The substructure is now a 2×2D-substructure (Figure 41). Indeed, it is assumed here that the two main perpendicular plans are not coupled to each other. Moreover, the frames are assumed to be uncoupled to the other frames parallel to them (Figure 41). Accordingly, it is possible to study a 3D-frame through the study of two 2D-substructures.

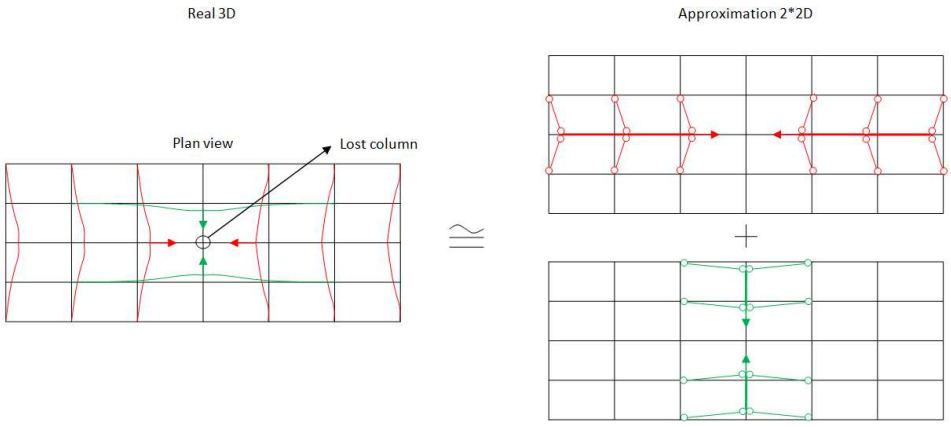

Figure 41. 2×2D approximation for 3D frames

VII.5.6.4. Application of the global model to the investigated car park

Now that the general method has been presented, for 2D and 3D case, the study case of the ROBUSTFIRE project (designed within WP5) is examined. Its specificities are as follows:

- The beams are composite beams
- There is a reinforced concrete slab “linking” these composite beams
- The exceptional event is a fire occurring next to a supporting column
- There is a bracing system in the two main directions

To apply the global model, the following assumptions are made:

- The first assumption is to consider that, due to the fire, the column is completely lost and there is no remaining strength in the column.
- The second assumption is to neglect the beneficial effect of the slab. Only a mesh of composite beams will be considered.
- The third assumption consists in considering that the extremities of the substructure are totally fixed. Indeed, we can assume that, thanks to the bracing systems in both directions and the slabs acting as diaphragms and ensuring the formation of a compression ring, the rigidity of the indirectly affected part is very high against membrane forces.
- The fourth assumption is to neglect the heated beams, just above the lost column. Indeed, its rigidity will be very small compared to the other stories, so the contribution of the first storey to the structural resistance is considered as negligible.

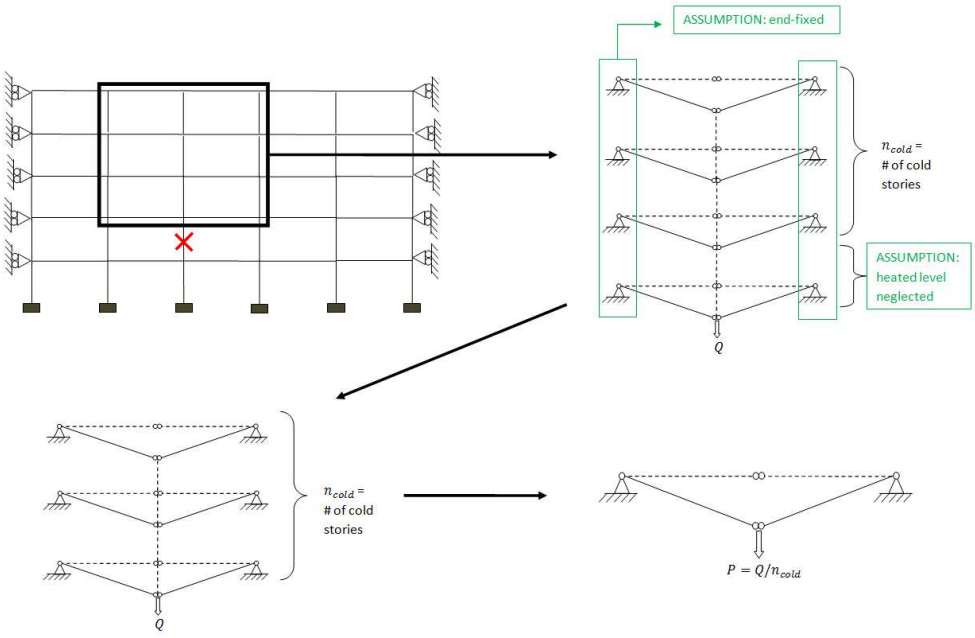

Figure 42. Simplifications for the case study

All these assumptions are summarized in Figure 42. The substructure to be studied at the end is only composed with a single double-beam, at ambient temperature, submitted to a force P equal to the total load Q acting on the structure, divided by the number of cold stories, n_{cold}. In Figure 42, a 2D-frame is represented. In the case study, it is a 3D-frame, so the substructure to study will be composed with two double-beams, one in each plan.

Remark: if the lost column is at the last storey, $n_{cold} = 0$. In this case, only the slab will be considered, and the heated beams will be neglected. Accordingly, the analytical model presented for slabs (as discussed previously) will have to be used.

The complete equations and solving procedure can be found in Deliverable V.

VII.6. WP4 – Derivation of design recommendations adapted to the industrial request for design efficiency as well as for easy fabrication, erection and control

VII.6.1. Introduction

The objective of WP4 was the derivation of practical design recommendations useful for practitioners. The activities of this WP were divided in two tasks:

- derivation of practical recommendations and;
- critical appraisal of the practical recommendations.

For such a complex problem than the one considered in the present project, different design approaches may be contemplated, ranging from the very sophisticated thermal and mechanical simulations through FEM techniques to basic hand design procedures. The sense to give to "practical recommendations" is strongly dependent on the selected level of design sophistication. This being, and recognising the difficulty to approach the problem whatever is this level, it has been decided, in WP4, to gather all recommendations which seemed to be of practical interest for the designer.

All the details of the recommendations are given in Deliverable VI, representing the outcome of WP4 and WP5. A summary of the latter is reported here after.

In Deliverable DVI, different questions, corresponding to different sophistication levels, are therefore addressed:

- How to perform experimental tests on substructures so as to simulate the actual response of joints subjected to fire action, (and in which combined bending moment and axial loads are in constant evolution during the column heating) - § VII.6.3.
- How to simulate numerically, through FEM techniques, the behaviour of such joints - § VII.6.2.2.
- How to predict analytically the M-N resistance interaction curves of such joints - § VII.6.4.1.
- How to predict in a simplified way the actual distribution of temperatures along the beam axis - § VII.6.2.1.
- How to predict analytically the response of a slab located just above the lost column - § VII.6.4.2.b.
- How to numerically simulate the global frame response according to one of the three following potential approaches: temperature-Dependent Approach, simplified Temperature-Dependent Approach and Temperature-Independent Approach - § VII.6.2.1.
- How to analytically check the robustness of the car park through simplified "hand" analytical procedures - § VII.6.4.2.

The higher is the level of sophistication, the greater is the accuracy of the design. But also the greater are the design efforts and the complexity of the approach for the designer. The powerful or more basic character of the calculation tools to be used is also a factor to be accounted for in design offices.

The most practical one is for sure the simplified analytical approach as the latter may be applied using tools available in any design office. It is the reason why the "practice-oriented" partners have mainly focused their work on the applicability of this approach.

VII.6.2. Practical design recommendations – Numerical approaches

VII.6.2.1. Robustness assessment framework

A robustness assessment framework of different levels of sophistication was proposed for WP4, attempting to bridge the gap between the current codified treatments of fire hazards and progressive collapse assessment. The robustness assessment framework is comprised of three basic components, namely, detailed Temperature-Dependent Approach (TDA), simplified Temperature-Dependent Approach (TDA), and Temperature-Independent Approach (TIA). These approaches have been developed and verified extensively using sophisticated numerical simulations of the car park structure under localised fire, making use of high performance computing equipment purchased for this purpose.

The detailed TDA should be the most sophisticated yet computationally expensive approach under the current robustness assessment framework, so it is more suitable for research purposes and assessment of safety-critical structures. In this approach, details of the fire scenario, e.g. the position and the heat release rate of the fire origins, need to be considered. Thermal analysis is required in order to obtain the actual temperature distribution within the structural model, which is then used for the structural analysis model. In this approach, structural analysis is usually performed over the time domain, so the fire resistance time (evacuation time) can be estimated accordingly. The application of the detailed TDA was illustrated in an internal report (Fang *et al.*, 2010) by considering the reference car park model, where the floor slab was modelled using either 2D shell elements or beam-column elements in a grillage approximation.

Considering the fact that some thermal characteristics during a localised fire can have insignificant influence on overall structural robustness, the detailed TDA can be simplified. The simplified TDA only considers the position, the range, and the maximum temperature of the localised fire; therefore, it should be more close to typical robustness provisions, which are intended to limit the progression of local damage under unforeseen events. The main methodology of the simplified TDA is to propose a monotonic 'block' temperature model that can be directly applied into the structural model so as to avoid complex heat transfer analysis, thus the structural analysis can be performed over a more event-insensitive temperature domain (instead of the time domain). In this project, a simplified temperature distribution (i.e. uniform temperature along the member length, and linear temperature distribution over the cross-section) was proposed within a rectangular fire-affected zone, as elaborated in an internal report (Fang *et al.*, 2011). Through comparisons with the predictions from the detailed TDA, the simplified TDA was found to provide reliable predictions. The discrepancies in the key predictions, e.g. column buckling temperature, first joint failure temperature, first failure mode and deflection, were typically within 5%.

As a further simplification, a TIA has been developed towards a fully event-independent strategy for design-oriented robustness assessment, in the sense that the maximum temperature is assumed to be unknown. Based on the fact that certain parts of structural members under high temperatures can lose their strength considerably, thus offering negligible contribution to progressive collapse resistance, these structural members are considered as completely removed within the TIA framework. Therefore, the TIA model does not require thermal analysis, and can provide a simplified robustness assessment procedure regardless of temperature. This strategy is inspired by the idea of the event-independent 'sudden column loss' scenarios currently adopted in some of the commonly used guidelines for progressive collapse assessment (GSA, 2003; DoD, 2009). For this project, the fire affected joint, column and parts of the beams were considered as removed, although it was found that the length of the beam removed has a relatively small influence on the overall structural robustness.

VII.6.2.2. 3D sophisticated model of a composite joint

In this section, advices are given to perform three-dimensional sophisticated models of heated composite beam-to-column bolted joints subject to variable bending moments and axial forces. The studied joint corresponds to the main beam-to-column joint, internal column, which is lost due to a localised fire. It is assumed that the loss of the column can be modelled by statically removing it, and that the column stays perfectly straight at the joint zone (no column rotation). The composite steel-concrete joint should be modelled combining 3D solid and contact elements, thereby taking into account the effect of the local failure modes. Material properties, thermal and mechanical loadings, boundary conditions, failure criteria … to be considered in a finite element model are explained in details in Deliverables VI, section IV.

VII.6.3. Practical design recommendations – Experimental approaches

In this section, practical recommendations to perform experimental studies of composite beam-to-column joints subject to axial and bending loadings under elevated temperatures are provided to the researchers, based on the feedback from the seven experimental tests performed within the present project. Sub-frames with the real cross-section dimensions (beams IPE 550, column HEB 300 and bolts M30) were tested in the laboratory for the first time under complex loadings (elevated temperature, variable bending moments and axial forces). The fact that dimensions cross-sections were not scaled permitted to observe the behaviour of the joint as in reality, with bolts M30 cl. 10.9 failures, and new

deformations of the steel end-plate between the bolts, not usually seen in smaller tested joints (the space between the two bolt rows 2 and 3 was 260 mm). However, the loads and displacements reached very high values and the equipment from the laboratory needed to be adapted to be able to measure them, and to apply the thermal and mechanical loadings. Open fire testing facilities (electrical Flexible Ceramic Pad heating elements) were chosen to heat the joint because of their capacities of adaptation to the heated zone dimension (in this case: an internal beam-to-column joint of large dimensions) and to maintain constant temperatures during many time. However, at the heated zone of the sub-frame, loads, displacements and strains cannot be directly measured (loads cells, displacement transducers and strain gauges are limited to 60ºC/80ºC); the instrumentation, and therefore the results, are limited to the temperatures. More details about the fire testing facilities, mechanical loadings, realistic axial restraints to the beams, sub-frame restraints, instrumentation, control tests (to define the real material properties), are given in Deliverables VI, section V.

VII.6.4. Practical design recommendations – Analytical approaches

VII.6.4.1. Prediction of the M-N joint resistance at elevated temperatures

Within WP 2, an analytical procedure aiming at predicting the resistance M-N interaction curves of joints was developed and validated through comparisons to the experimental results obtained in Coimbra. The analytical procedure is presented in § VII.4.8 (with an example of application) and detailed in Deliverable III, Section II.

VII.6.4.2. Global frame behaviour

In this section, simplified analytical models are provided to predict the response of the frame when submitted to the loss of one of its supporting column further to a localised fire. In these simplified analytical approaches, the affected column is supposed to be an internal one (the loss of a perimeter column is not studied herein). Moreover, the column is admitted to be completely and statically removed (no residual bearing capacity – no dynamic effects).

If the lost column is part of the structure upper storey, section b of this document should be referred to. In the opposite case, the method suggested in section a should be followed.

a. Internal column – upper storey excepted

In order to study the structural response of the frame when submitted to a column loss, an elementary substructure is isolated for sake of simplicity. First, the part made up of the 3D vertical slice above the lost column, called “directly affected part” is extracted. The rest of the structure is called “indirectly affected part”.

When the column is removed, a beam plastic mechanism forms in the directly affected part (Figure 40) and, due to the large displacements induced, tension loads develop in the beams of the directly affected part (Figure 40). These loads are applied to the indirectly affected part which provides a sort of lateral “support” to these tension forces. The stiffness of the indirectly affected part against these forces is very high thanks to the bracing systems in both planes and the slabs acting as diaphragms and ensuring the formation of a compression ring. The indirectly affected part can thus reasonably be assumed as fully restrained at its extremities when isolated (as far as the horizontal displacement is concerned) (Figure 43). In this approach, the directly affected part is studied as a mesh of composite beams: only a given effective width of slab is considered in both directions (collaborating with the steel profile) and the rest of the slab is neglected. For sake of simplicity, the development of membrane forces in the slabs further to the column loss is thus not taken into account in this part.

The beams of the directly affected part lower level are at elevated temperature because they are subjected to fire. Their stiffness is much decreased and thus much lower than the stiffness of the ambient temperature upper beams. Consequently, the contribution of the lower “hot” beams to sustain the column removal will be much smaller than the contribution of the other storeys. That is why the fire-affected level is neglected in the simplified approach: only the “cold” floors of the directly affected part are taken into account (Figure 43). As all these floors are the same and have the same infinite restraint at their extremities (fixed supports), they will all contribute identically to sustain the column loss.

Finally, an elementary substructure such as represented in 2D in Figure 43 is studied: it is made up of the beams of only one floor with the joints at their extremities – two double-beams perpendicular to each other define the 3D substructure. If the initial compression load in the column (before it fails) is N_0 the structure will be considered as robust if the above-defined 3D substructure is able to sustain a force $P = N_0/n_{cold}$, where n_{cold} is the number of cold floors in the directly affected part (i.e. the number of floors in the directly affected part minus one).

Besides, in the considered case, the partial-strength joints at the beam ends are such that their *M-N* resistance curve is entirely included within the beam *M-N* plastic resistance curve. So no yielding will appear in the beams; the joint resistance and deformability will be crucial and will determine the development of a plastic mechanism in the so-defined substructure.

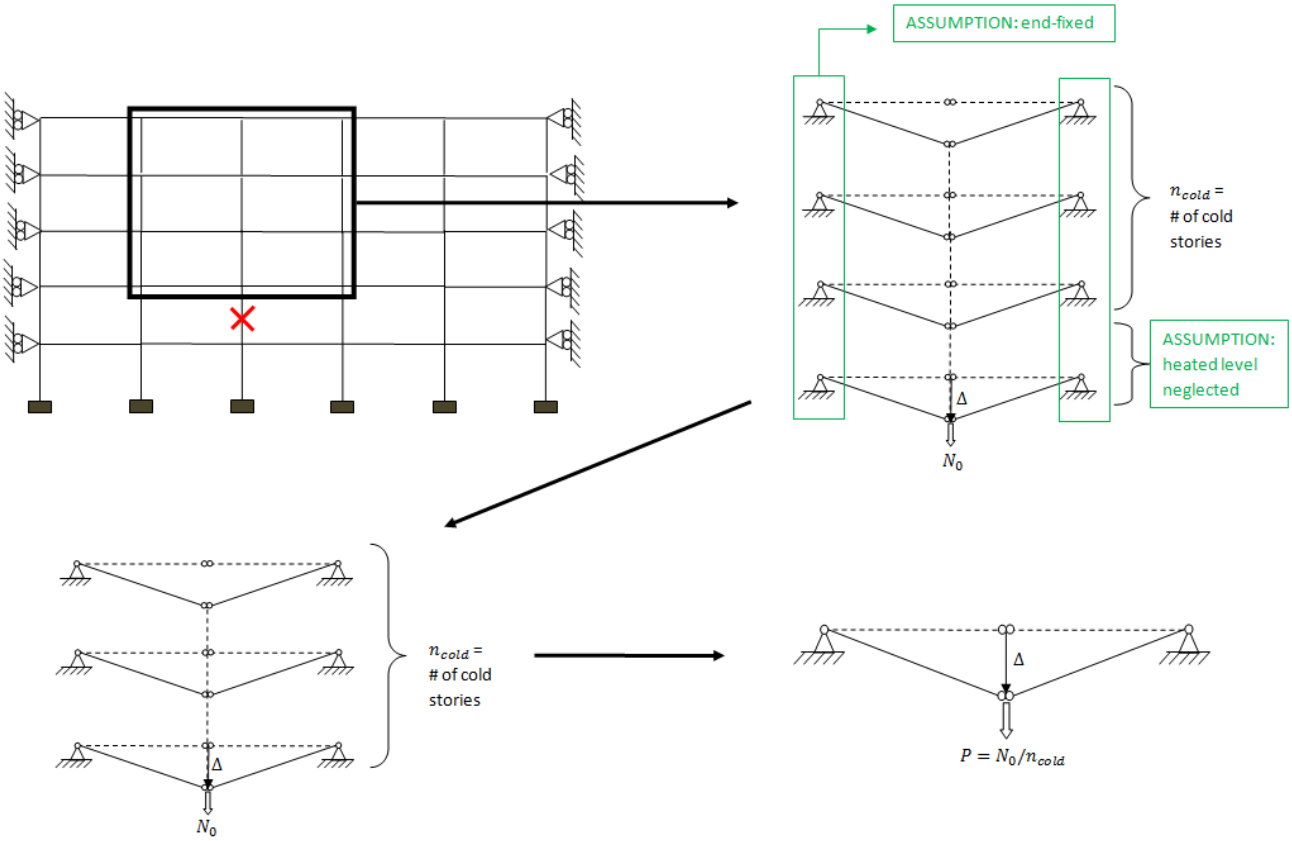

Figure 43. Simplifications for the case study

For the considered 3D-substructure, a system of equations can be written. These equations can be found in Deliverable V, section IV. Solving this system of equations, it is possible to find the efforts and displacements in the structure when the column is completely removed. Once these efforts and displacements are known, ductility and resistance conditions must be checked. All the solving procedure is described in details in Deliverable V, section IV.

If the resistance and/or ductility would not be sufficient, two solutions can be contemplated:

- to upgrade the structure to satisfy the ductility and/or resistance criteria or;
- to use a more sophisticated procedure (i.e. numerical approaches) allowing taking into account positive effects (such as the development of membrane forces in the slab) which have been neglected in the proposed simplified procedure.

b. Internal column – upper storey

In this part, it will be assumed that a localised fire occurring near a supporting column just above a composite slab will lead to the inefficiency of the heated beams (primary and secondary) supporting the slab and to the inefficiency of the heated steel profile of the composite slab.

Also, it is assumed that the unidirectional concrete ribs of the composite slabs are not significantly influencing the behaviour of the slab when significant membrane effects are developing i.e. it is assumed that only the upper part of the slab is contributing to the slab resistance (as demonstrated through the performed Benchmark study on floor slabs – see Deliverable IV).

Accordingly, the behaviour of the composite slab can be investigated through the study of a 3D uniform slab, uniformly loaded and submitted to the loss of one of its supporting column, assuming that this slab remains at ambient temperature.

To study the behaviour of a 3D uniform slab submitted to membrane forces, analytical models are available (Izzudin B.A., 2010) and the applicability of the latter were investigated within WP3. The equations related to this model can be found in Deliverable V, section IV.

VII.6.5. Critical appraisal from the "practice-oriented" partners

Most of the presented design recommendations result in the proposal of design procedures of different natures (numerical, experimental or analytical), for different part of the structure (structural members, joints or the structure as a all) and with different level of sophistications.

The most practical ones are for sure the simplified analytical approaches as the latter may be applied using tools available in any design offices. It is the reason why the "practice-oriented" partners have mainly focused their work on the applicability of the approach allowing predicting the global frame response, in particular by applying the latter to the reference building as presented in WP5 (§ 0).

This approach is funded on two main assumptions:

- the development of membrane forces in the slab is neglected for a column loss which does not occur at the top level;
- the fire effects are not explicitly taken into account (indeed, the elements directly affected by the fire are neglected).

The assumptions on which the simplified analytical model for robustness check is based lead to a safe prediction of the structural response for the considered scenario, i.e. the loss of a column further to a localised fire. The conservative character of the procedure can obviously be seen as a source of inefficiency, as soon as the economy of the project is concerned. In reality, it is presently "the price to pay" to keep "easy-to-apply" analytical procedures. The designer who would like to predict more "accurately" the response of the structures would have then to use the more "sophisticated" numerical approaches.

VII.6.6. Conclusions

Within the present WP, practical design recommendations derived within the ROBUSTFIRE project were presented, reflecting three types of approaches (numerical approach, experimental approach and analytical approach) and different levels of sophistication.

A critical appraisal of the latter from the "practice-oriented" partners was made, highlighting the advantages/disadvantages of the proposed design recommendations, in particular for the simplified analytical approach allowing predicting the global frame response, which constitutes the more "practice-oriented" approach.

VII.7. WP5 – Case study

VII.7.1. Introduction

The objective of WP5 was, first, to design an "actual" reference building as case study and then, to apply, the different design recommendations proposed within WP4 to this building and that, with interactions between the "scientific" and the "practice-oriented" partners.

The designed reference building is first presented in § VII.7.2; the latter has been designed respecting the structural configuration described in WP1 (see § VII.3).

Then, the application of the design procedures is addressed in § VII.7.3.

VII.7.2. Case study description

VII.7.2.1. Design of a reference structure

a. Introduction

In order to realise tests and studies of this research on the basis of a common structure used in our countries, a standard structure of an open car-park has been designed. This structure will be called in all documents “the reference structure”.

The geometry of the designed car-park must be the most general possible in order to cover the greatest number of existing structures. After discussions between the partners of the research (as a result of WP1 – see § VII.3), the structure selected is described on Figure 44. Except for the columns, all the structural elements have a composite resistance. Thus, the slab is composite and the steel beam profiles are connected to this one, but are not coated with concrete. The whole structure is supposed to be braced and this is made with the help of the concrete ramps which are not drawn in the field of this project.

It is thus about a car-park having internal columns laid out every 10 m, the beams have a span of 16 m and are spaced of 3,333 m, which is the span of the slab.

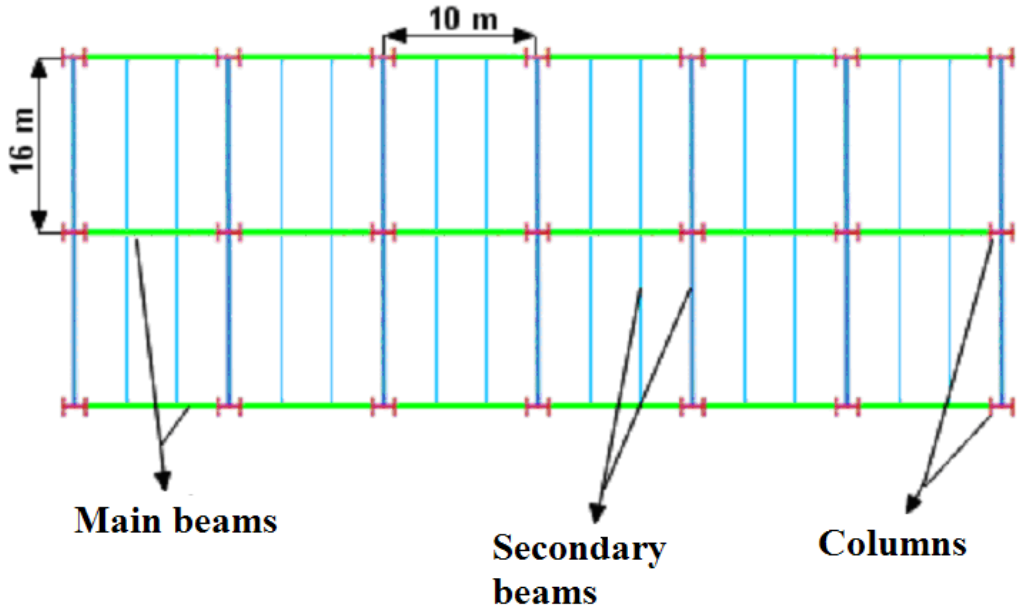

Figure 44. Structure description (plan view)

The height of the 8 stories is fixed at 3 m, which makes a total height of the building equal to 24 m. Moreover, no roof is considered on the last stage, this one also being used as level of parking and the selected steel sections will be the same ones on the whole structure.

All plans of this reference structure and the details of the design can be found in the Deliverable VI.

b. Properties of the designed cross-sections

1. Composite slab

The composite slab is of type COFRAPLUS 60, made up of a ribbed metal sheet of 1 mm of thickness which represents the lower reinforcement in the longitudinal direction of the slab, but also the formwork of this one during the casting of the concrete; this sheet thus has a double function. The thickness of this slab is of 120 mm which is relatively weak.

A basic mesh of Φ8 mm spaced by 200 mm is placed all over in the slab and some reinforcement have to be placed in the joint zone of the main beams.

2. Main beams

The static schemes for those beams consider a semi-rigid joint for the connection with the column. The rigidity is different for the self-weight loads and for the variable loads because of the behaviour of concrete

Finally, the dimensioning lead to consider for those main beams an IPE 550 profile (S355). The joint is described on Figure 45.

3. Secondary beams

The static schemes for those beams consider a pinned connection with the column and with the main beam. This is valid for the self-weight when the steel structure acts alone and also for the variable load because the composite sections are not able to carry loads in case of dissymmetrical loading.

Finally, the dimensioning lead to consider for those secondary beams an IPE 450 profile (S355). The joint is described on Figure 45

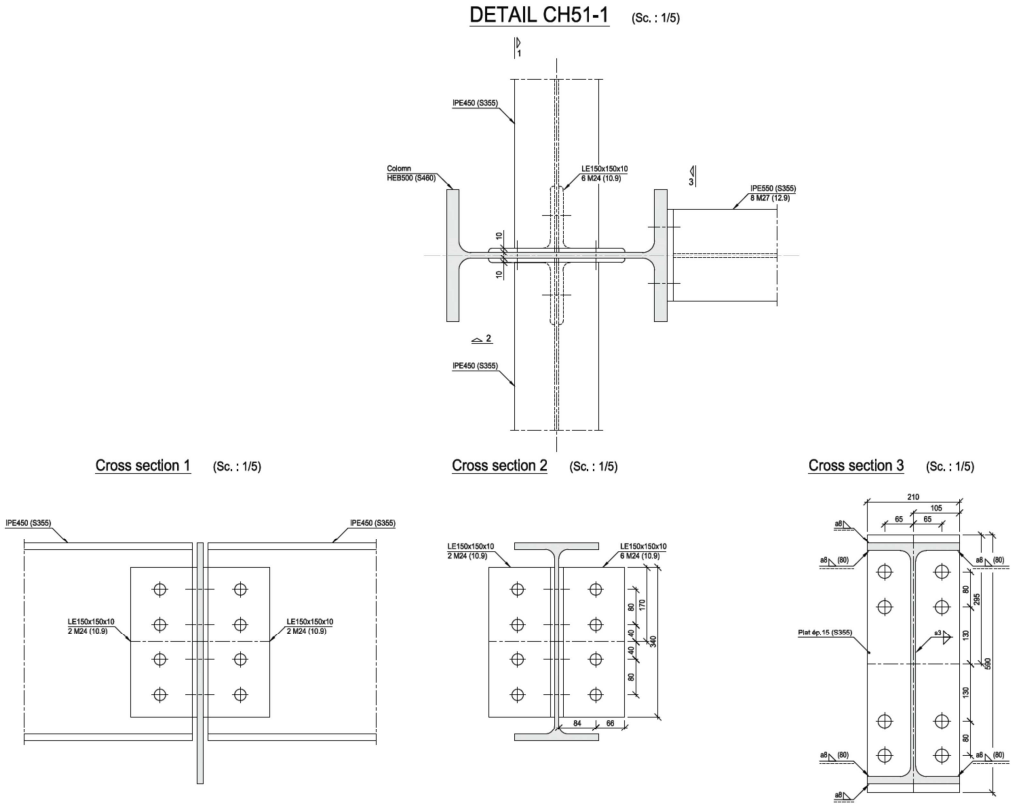

Figure 45. Main beam and secondary beam to column joint

4. Columns

The columns have a buckling length of 3 meters and are considered in S460 grade in order to minimise their width. It is possible to change the sections of the column on the height of the structure from HEB 550 to HEB 220. The calculation of the rigidity of the joints between column and main beams are made with a HEB 300 column which is the section used for the test and for floors 4 and 5 from the reference car-park.

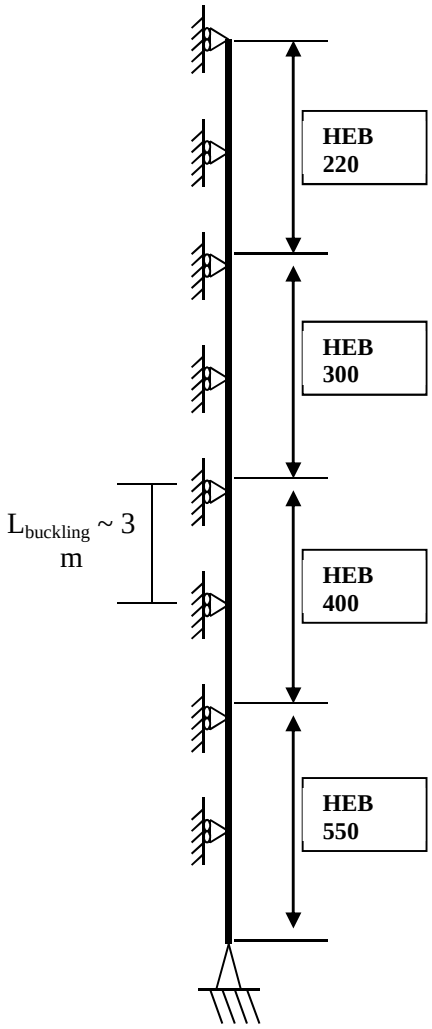

Figure 46. Column description

VII.7.3. Fire scenarios for robustness

Basic idea consists in defining a fire potentially impacting a column in the car park structure. Under fire conditions, this column is deeply affected, and could even fail. According to car park regulation and fire safety engineering practices, worst scenario for column is as follows: four cars are burning around the column and the fire spreading from one car to the others after a short time (12 minutes). An alternative scenario for edge column could include only two cars. In this report, only internal columns of the structures are considered for robustness scenario. Location of the fire could potentially be anywhere at any floor, provided that there are 4 car places around a column (see Figure 47).

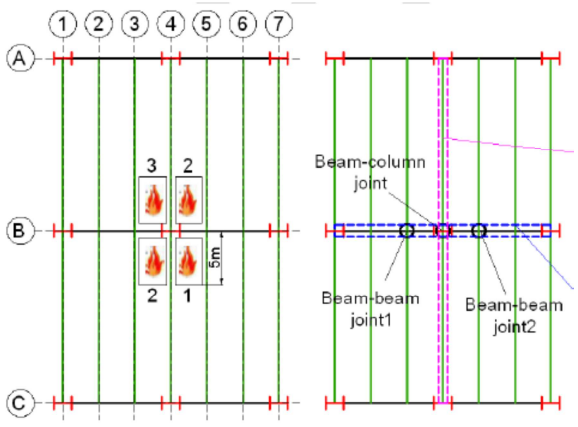

Figure 47. Initial position of fire cars.

VII.7.3.1. Application of the Robustfire methodology - "Sophisticated" FEM approaches

The applicability of the "sophisticated" FEM approaches (developed within WP3) to the reference building have been investigated but these investigations have already been reported in WP 3 (see § VII.5.5.4), as demonstrative example for the presented developments, and are detailed in Deliverable V, Section III. Accordingly, this contribution will not be repeated herein and in Deliverable 6.

VII.7.3.2. Application of the Robustfire methodology - Simplified analytical approach

Here, for demonstration purpose, only two column locations are studied, one at ground floor and the other under roof floor. First location corresponds to the most loaded column. The second one corresponds to the minimized alternative loading paths from the upper structure, limiting the possibility of structural adaptation to a local failure.

Under each of above fire scenarios, the fire affected column is considered to fail fully and in consequence their resistance disappears totally.

The fire stability of slab and beams is supposed to be verified with FSE method. This part focuses on robustness issues related to the stability of structures.

VII.7.3.3. Methodology aspects

Basically, two levels of analysis can be applied. One is called "sophisticated model", based on FEM analysis, with several levels of refinement. The other is called "simplified method" and relies on analytical analysis. The details for this model are given in Deliverable VI. Following paragraphs illustrate an application on the basis of simple approach which is considered to be more practical for ordinary design engineers.

Directly impacted zone and indirectly impacted zones are analysed separately. This approach uses a simple grillage model for the directly impacted zone, the surrounding elements at ambient temperature are considered as boundary condition (supports) of the grillage. Like in the complex model, it is necessary to calculate properties of the springs that represent the indirectly impacted zone.

In theory, the impacted zone can be studied with analytical formulas. Two levels of refinement are proposed:

1. To consider the remaining load bearing capacity of elements exposed to fire, by reducing their capacity according to their level of heating. It requires assessing properly the behaviour of joints in high temperatures conditions.
2. To simply ignore the elements exposed to fire, considering that they failed. This leads to temperature independent analyses.

The following illustrates the application of simplified method for the case study. This method could be applied without difficulties by common design offices.

VII.7.3.4. Substructure

As analytical models to predict the temperature distributions in joints are not yet available, a 3D model where a column and the heated beams and floor are removed is studied, according to Deliverable V, section IV. This temperature independent analysis is supposed to be solved mainly analytically, with the help of simple simulations to determine rigidity.

Main steps are:

1. extract sub structure (beams) and calculate tension force due to the loss of the down column,
2. indirectly affected zone supposed infinitely stiff due to the ring of compression,
3. define the join MN curves,
4. calculate the structural response of the affected part, modeled with beams and springs and verify the joint capacity.

Due to the fact that, in the transverse direction, the structures have only two bays, it seems that the anchorage of the sub structure in the indirectly affected part is only efficient in the longitudinal direction. In the transverse direction, anchorage is neglected. It comes that 2D model could be a satisfactory modelling (see Figure 48). More precise approach requires more insight in the membrane

effect of the slab, which probably contributes to stiffness of supports of the substructure in the transverse direction.

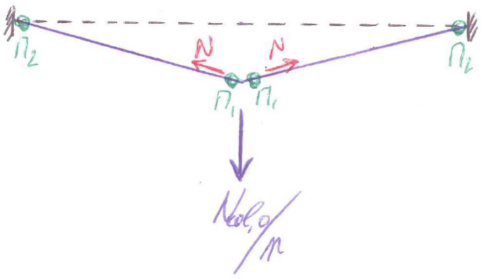

Figure 48. Elementary substructure – 2D view

VII.7.3.5. Subsystem global behaviour

a. Description of simplified method – Loss of a column other than a column at the top floor

In this section, it has been considered that the fire takes place in ground floor and for this reason this floor is not taken into account. We have verified the robustness of the non-affected structure by the fire.

For a vertical displacement *u* (see Figure 49) at the head of a column, at the connection level, the rotation could be expressed in function of this displacement as follow:

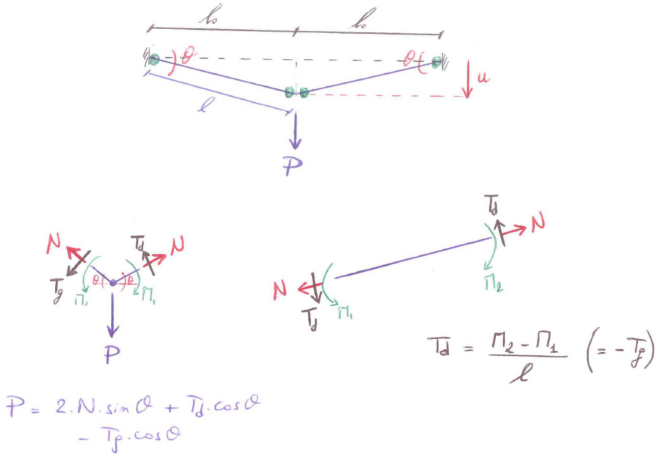

Figure 49. Deformed structure.

$$\theta_x = \arctan\left(\frac{u}{l_{0,x}}\right) \quad (2.3.1) \qquad \text{and} \qquad \theta_y = \arctan\left(\frac{u}{l_{0,y}}\right) \quad (2.3.2)$$

$$l_x \cdot \cos\theta_x = l_{0,x} \quad (2.3.3) \qquad \text{and} \qquad l_y \cdot \cos\theta_y = l_{0,y} \quad (2.3.4)$$

$$l_x = l_{0,x} + \delta_{Nx,1}\left(N_x\right) + \delta_{Nx,2}\left(N_x\right) \quad (2.3.5) \qquad \text{and} \qquad l_y = l_{0,y} + \delta_{Ny,1}\left(N_y\right) + \delta_{Ny,2}\left(N_y\right) \quad (2.3.6)$$

The equilibrium equation in head connection point (in 3D) leads to the following relation:

$$P = 2 \cdot N_x \cdot \sin\theta_x + 2 \cdot \frac{M_{x,2} - M_{x,1}}{l_x} \cdot \cos\theta_x + 2 \cdot N_y \cdot \sin\theta_y + 2 \cdot \frac{M_{y,2} - M_{y,1}}{l_y} \cdot \cos\theta_y \quad (2.3.7)$$

In this last relation the indices *x* and *y* refer to the two main vertical planes of the structure.

b. Data for case study

For our case study the following parameters are known:

- $l_{0,x1} = l_{0,x2} = l_{0,x} = 10$ m and $l_{0,y1} = l_{0,y2} = l_{0,y} = 16$ m,
- Principal beam is IPE 550 with a steel grade of S355,

- Secondary beam is IPE 450 with a steel grade of S355,
- Column HEB 550, HEB 400, HEB 300 and HEB 220 with a steel grade of S460 (see Figure 46).

The sizes and the properties of bolts and end plates are designed by GREISCH and ULg in pre-dimensioning of the reference's car park report. The entire design of the reference's car park can be found in Deliverable VI, section II.

Furthermore it is necessary to know the following parameters:

- N_x, N_y, M_x and M_y are defined by MN rsistant diagrams for the joints,
- For primary beams joints: $K_{Nx,1} = K_{Nx,2} = 20000$ kN/m,
- For secondary beams joints: $K_{Ny,1} = K_{Ny,2} = 15000$ kN/m,

The $N-\delta_N$ laws cannot be, at this stage of the developments, determined analytically. They are assumed to be linear (as highlighted through numerical simulations), so that $K_N * \delta_N = N$. The development of an analytical procedure for the prediction of this law are still under progress, what constitutes a perspective to the present project. The values of K_N given here above are realistic values of the parameters, inspired from (Demonceau, 2008).

As stated above, it is considered that the fire takes place in ground floor and for this reason this floor directly affected by fire (first level) is not taken into account. The check of the robustness considers only the non-affected structure by the fire that is from second floor to eighth floor.

c. MN diagrams for studied car park

The MN diagrams of main beam joints are defined according to the method explained in in Deliverable III, section II. Figure 50 to Figure 53 give the resultant MN diagram of 4 main beam-to-column joints of studied structure.

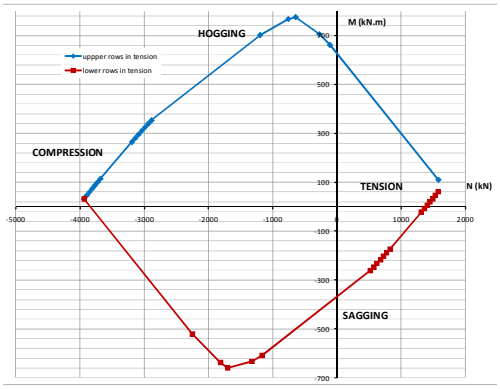

Figure 50. MN diagram for HEB500 column.

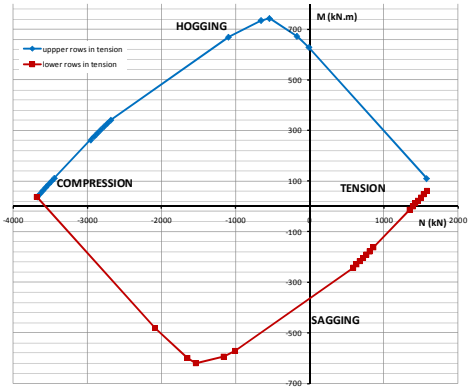

Figure 51. MN diagram for HEB400 column.

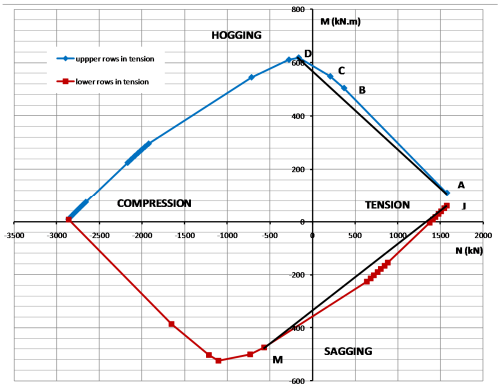

Figure 52. MN diagram for HEB300 column

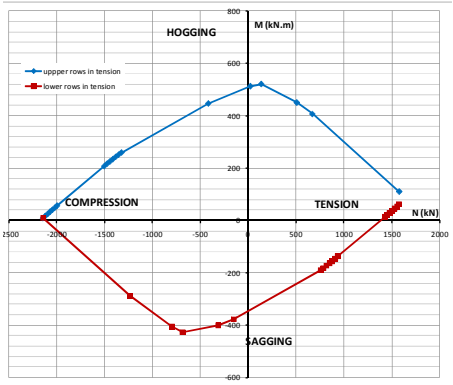

Figure 53. MN diagram for HEB220 column.

These diagrams allows to know that the maximum tensile resistance of all main beam joints for the studied case is $N_{x,max}$ =1577 kN.

With respect to secondary beam to column joints, as they are designed as pined ones, they will not have any moment resistance. But the maximum tensile resistance of these joints is limited to 468 kN.

d. Determination of maximal vertical displacement of connection point of each floor

In the case where $l_{o,x1}=l_{o,x2} = l_{o,x}$ and $l_{o,y1}=l_{o,y2} = l_{o,y}$ the Equations 2.3.5 and 2.3.6 could be written as:

$$l_x = l_{o,x} + 2\ \delta_{Nx} = l_{o,x} + 2\ \frac{N_x}{K_{Nx}} \text{ and } \quad l_y = l_{o,y} + 2\ \delta_{Ny} = l_{o,y} + 2\ \frac{N_y}{K_{Ny}}.$$

Using these two last equations and the equations 2.3.1 to 2.3.4, the maximal vertical displacement of the connection point (column head) could be defined in function of $N_{y,max}$ =468 kN, $N_{x,max}$ =1577 kN, K_{Nx} = 20000 kN/m and K_{Ny} =15000 kN/m given previously.

The maximum vertical displacement will be limited by the tensile force developed in two perpendicular beam to column joints (main and secondary beams respectively), which cannot exceed the maximum tensile resistance of these joints.

e. Determination of bearing capacity of the connection of each level and robustness verification

The applied load taken into account for the design of the car park structure is defined by following relation: $A = G + 0.7 * 0.8 * Q$.

G takes into account the dead load of concrete slab (2145 N/m^2) and steel structure (400 N/m^2) and Q=2500 N/m^2 is the variable load.

The two coefficients affecting the term Q correspond to the coefficient Ψ_2 (EN1990, Annex A1) coming from the accidental combination load case, and to a coefficient α_n (EN 1991-1-1, §6.3.1.2 (11)), which is a reduction factor for a column supporting a large surface.

The bearing capacity of all steel beams connected to the lost column can be obtained using the formula 2.3.7. In this formula: if the vertical displacement at column point is defined, N_x, l_x, l_y, θ_x, θ_y are known and, M_y equals to zero because the secondary beams are supposed to have hinged connection. Concerning $M_{x,1}$ and $M_{x,2}$, it is necessary to define them. In order to simplify the calculation, it is suggested to use linear relations derived from accurate MN diagram (see Figure 52) in order to get their values directly.

If one observes the four MN diagrams given in figures from Figure 50 to Figure 53, it can be easily concluded that MN curves are nearly linear. Consequently it is proposed to consider that from the point A to C or from the point J to M (see Figure 52) the MN curves are perfectly straight.

In fact, for robustness calculations, only the points located at the tension side will be used. In consequence, the second point over the MN curves in our case for the hogging moment could be B, C or D. The result will be more precise if the accurate values based on all points between lines AB (C.) and JM are used. However, the advantage of actual approach resides on its efficiency.

With this assumption, it is possible to define the $M_{x,1}$ (sagging moment) and $M_{x,2}$ (hogging moment) with the following relations:

$$M_{x,1} = (\frac{M_J - M_M}{N_J - N_M}).(N_x - N_M) + M_M \text{ and } \quad M_{x,2} = (\frac{M_A - M_D}{N_A - N_D}).(N_x - N_D) + M_D$$

Finally, the bearing capacity is defined by the simplified relation:

$$P = 2 \cdot N_x \cdot \sin\theta_x + 2 \cdot \frac{M_{x,2} - M_{x,1}}{l_x} \cdot \cos\theta_x + 2 \cdot N_y \cdot \sin\theta_y$$

For all levels over the whole height of the structure with four different column sections, the MN diagrams are given respectively in figures from Figure 50 to Figure 53, the maximum load-bearing capacities obtained from above calculation procedure are:

- floor with column in HEB550: P = 469.8 kN,
- floor with column in HEB400: P = 469.7 kN,
- floor with column in HEB300: P = 462.9 kN,
- floor with column in HEB220: P = 456.0 kN,

The total applied load to the bottom of the column of the structure is:

$P_{applied}$(tot)=619.2 x 8=4953.6 kN.

The total bearing capacity of the structure once the column fails at ground level is:

P_{res}(tot)= 469.8+469.7x2+462.9x2+456x2=3247 kN

$P_{res}/P_{applied}$=0.655

Consequently it is necessary to modify the connection parameters proposed by the pre-dimensioning report of the car park structure in order to increase the axial resistance of the connections.

f. Verification of robustness – Fire in upper storey – Loss of a column at the top floor

As explained in simplified approach report provided by this project, in case of a fire in the upper storey, the column of this storey fails. The robustness of the top floor has to be provided by the rectangular slab given in Figure 54.

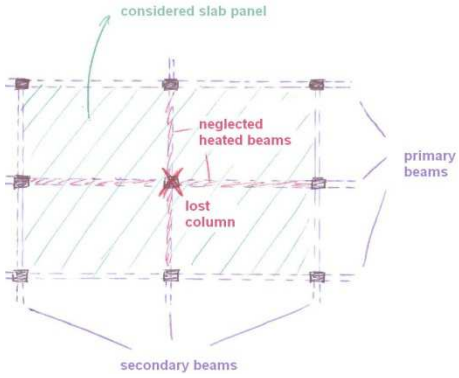

Figure 54. Slab considered for robustness of th top floor.

The mechancial load taken into account is calculated as shown in §VII.7.3.5.e. The robustness of this floor is ensured if following two criteria (defined in Deliverable V, section IV) are met:

- 1st or CM criterion: not full depth crack in the centre of the slab,
- 2nd or IM criterion: not full depth crack at the intersections of diagonal yield-lines.

For CM and IM criteria (see § VII.5.3.3 for more details), the failure happens when the reinforcement crossing the cracks reaches its ultimate strength f_u. At this moment the deflection at failure is U_{fc}.

In order to have a robust floor, its load bearing capacity must be higher than applied load. This point is defined by the interaction point of the limit deflection line and the bearing capacity curve (see Figure 55 and Figure 56).

For the car park structure dealt with in this study, the basic mesh of the top slab is:

- reinforcement spacing 200 mm,
- reinforcement diameter 8 mm

With these dimensions, none of the two criteria given above is met. In order to satisfy these criteria, the following mesh must be employed:

- reinforcement spacing 100 mm,
- reinforcement diameter 15 mm (this values is used just as an example for the optimization of CM and IM criteria).

Figure 55 and Figure 56 represent the results for the CM and IM criterion.

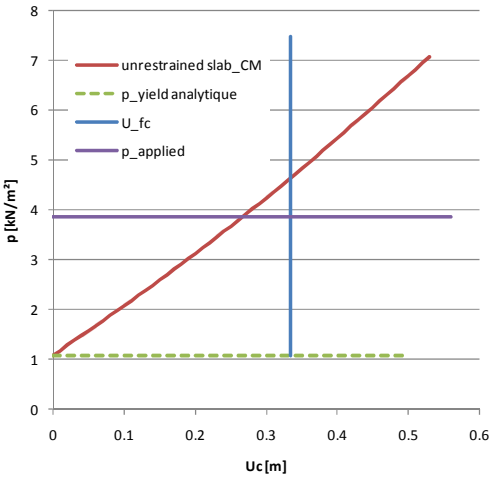

Figure 55. Result of CM criterion for a reinforcement mesh Ø15 by 100.

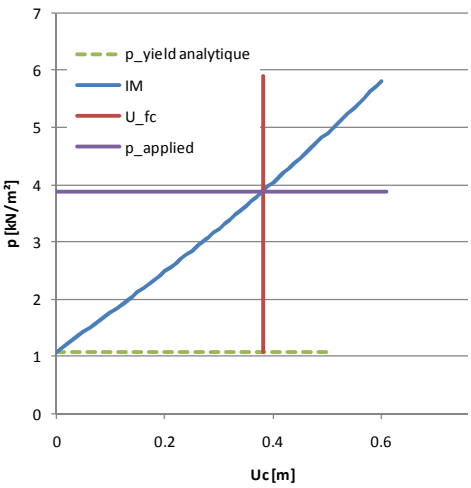

Figure 56. Result of IM criterion for a reinforcement mesh Ø15 by 100

VII.7.4. Conclusions

The proposed design procedures have been applied to the "actual" reference building designed within the present WP.

For the "sophisticated" numerical procedures, the application of the latter has been reported in WP3.

Concerning the application of the simplified analytical approach, it has been demonstrated within the present WP that this approach can be applied to the reference building. Only one parameter, the axial stiffness of a yielded joint, cannot yet be computed through an analytical procedure, what constitutes a perspective of development for the future (investigations already in progress).

Through the application of the simplified analytical approach, it is demonstrated that the robustness of the reference building is not sufficient for the considered scenarios. Accordingly, the designer would have to select one of the following possibilities: (i) improvement of the resistance of the joints (in bending and/or under axial loads) and of the slab at the top level or (ii) to use a more sophisticated approach using FEM, to take into account, for instance, the membrane effects developing in the slabs (effects neglected within the analytical approach).

VII.8. Conclusions

The possible progressive collapse of steel-concrete composite car parks under a localised fire resulting from the burning of cars is one of the key aspects to deal with nowadays. The absence of appropriate reply to this request is likely to limit the market for such very well appreciated structural solutions.

The project so aimed to investigate these aspects and derive design procedures and recommendations for the mitigation of the risk of progressive collapse.

The problem is rather complex as it implies to address the numerous following aspects:

- The scenarios to be considered (one car, more cars, located where, …)
- The distribution of temperatures in the air and the evaluation of the temperatures in the affected columns and the surrounding beams, slab and connections.
- The reduction of bearing resistance of the column.
- The local response of the beams, slab and joints when the bearing resistance of the column decreases and the progressive development of membrane forces in the floors.
- The global stability of the whole frame further to a local destruction of a part of the structure.

In order to achieve the goals of the project and to structure the work amongst the partnership, the following strategy has been set up further to an initial state-of-the art of the available knowledge:

- Derivation of all structural requirements for car park structures (dimensions, layout, loads, fabrication/construction/ erection constraints, realistic fire scenarios, …)
- Design of a reference structure under normal loading and in accordance with Eurocodes.
- Evaluation of the distribution of temperatures in the structure and in the constitutive structural elements during the exceptional event.
- Individual study of the main structural elements at room and elevated temperatures (columns, beams, connections, floor) through experimental and/or numerical investigations.
- Derivation of analytical approaches for the prediction of the individual response of the above-mentioned structural elements.
- Development of various numerical procedures for the evaluation of the stability and the resistance of the structure further to the event (sophisticated models with different levels of sophistication).
- Derivation of a simplified event-independent and Eurocode compatible approach for the evaluation of the robustness of the structure (simplified model).
- Application of the simplified model to the reference structure by the “practice-oriented” partners and feed back to the “scientific partners”.
- Drafting of design guidelines.

All these steps have been successively crossed along the three years of the project and practical recommendations are now made available.

The main conclusion of the project is certainly the fact that the simplified model is based on series of assumptions which allows, at the end, and at it was requested by the contract, to check the robustness of the car park through a “scenario-independent” approach, but with a non-excessive but actual level of conservatism that could be criticised. In fact, this conservatism has to be seen as the “price-to-pay” to limit the investment of a design office in terms of calculation costs.

Should the conservative character of the simplified model be considered as excessive, then more sophisticated models should be preferred. In the project, much information is made available to practitioners who would prefer to follow a numerical approach: choice of the model, distribution of temperatures, substructure to be studied, loads and boundary conditions to apply …

VII.9. Exploitation and impact of the research results

As mentioned in the previous section, practical recommendations and guidelines for practitioners are now made available for car park structures affected by a localised fire, what perfectly fit with the main objective of the project.

To ensure that all questions have been answered and that all necessary tools and guidelines for practitioners have been made available would, as it is often the case in such research projects, overcome the reality. But for sure, through the present project, significant progress has been made, the initial objectives have been reached and the practitioners have nowadays at their disposal design approaches, at different levels of sophistication, allowing checking the robustness of composite car parks under localised fire.

It has been demonstrated herein that the procedures presented within the RFCS project ROBUSTNESS can be adapted to the scenario considered here, by considering new phenomena. Accordingly, the present project confirms that these design procedures could be generalised to different scenarios and could be contemplated for implementation in the codes when the procedures will be fully generalised; however, some developments are still needed (as highlighted within the present project) in order to propose a full analytical approach.

VIII. List of figures

IX. List of tables

X. List of acronyms and abbreviations

η_{fi}	Reduction factor for design load level in the fire situation
δ_N	Elongation of a plastic hinge
Δ_A	Vertical displacement at the top of the lost column
$\Delta_{max.}$	Maximum displacement capacity of the hydraulic jack
Δ_s	Elongation of the reinforcement across the cracks forming in the slab when submitted to the loss of one of its support
$f_{ck,cube}$	Concrete cube strength
θ_{M+max}	Connection rotation corresponding to the maximum sagging bending moment
θ_{Fmax}	Connection rotation corresponding to the maximum reaction load
2D	Two dimensional
3D	Three dimensional
a	Slab length
A (%)	Steel elongation after fracture
A	Cross-sectional area
ARCELORPROFIL	Arcelormittal Belval & Differdange
b	Slab width
Cl 10.9	Class 10.9
Col.-B	Bottom column
CSTB	Centre Technique Industriel de la Construction Métallique
CTICM	Centre Scientifique et Technique du Bâtiment
d	Depth for uniform slab
d1	Thickness of the cover
d2	Thickness of the rib
Displ.	Displacement
E	Elastic modulus
F	Flange

F1	Load cell F1
F2	Load cell F2
F3	Load cell F3
F4	Load cell F4
F5	Load cell F5
FCTUCOIMBRA	Faculdade de Ciencias e Tecnologia da Universidade de Coimbra
FEM	Finite Element Method
F-HJ	Loads measured by the hydraulic jack at the column top
F_{max}	Maximum load capacity of the hydraulic jack/Maximum reaction load
FSE	Fire Safety Engineering
G_F	Concrete fracture energy
G_k	Characteristic value of a permanent action
GC	Gravity centre
ICST	Imperial College of science, technology and medicine
K	Lateral restraint stiffness of the equivalent spring
kg	Kilogram
kN	Kilo-Newton
K_N	Axial stiffness of a plastic hinge
kNm	Kilo-Newton meter
k_ε	Reduction factor multiplying the relative emissivity of steel surfaces in order to take account of the position and shadow effects in the numerical simulations
L	Length of structural member or Left
l_x, l_y	Lengths of the beams of the substructure when submitted to significant membrane forces
l_{0x}, l_{0y}	Initial lengths of the beams of the substructure
m	Meter
M	Bending moment
mm	Millimeter
M^+_{max}	Maximum sagging bending moment

Mpa	Mega-Pascal
M_{x1}, M_{x2}, M_{y1}, M_{y2}	Bending moment in plastic hinges (1 is for sagging, 2 for hogging)
N	Axial force
N_0	initial compression effort in the column that disappears
n_{cold}	Number of cold stories above the lost column
$N_{Ed,fi,20°C}$	Axial force design value for the fire situation
N_x, N_y	tension forces in the beams of the directly affected part (x= for primary frame, y= for secondary one)
P	Pressure transducer or concentrated load acting on one floor of the substructure ($P = Q/n_{cold}$)
q	Uniformly distributed load $[N/m^2]$ acting on the slab at the last storey of the car park
Q	Concentrated load acting on the substructure (composed only with beams of the directly affected part), simulating the loss of the column
q_{limit}	maximum uniformly distributed load $[N/m^2]$ that can sustain the slabs when submitted to the loss of one of its support
$Q_{k.1}$	Characteristic value of the leading variable action
R	Right
rad	Radian
Re (MPa)	Steel yield strength
Rm (MPa)	Steel tensile strength
Rot	Rotation
s	Distance from the top of the slab to the location of reinforcement
SG	Strain gauges
SLS	Serviceability Limit States
t	Thickness of steel deck
T	Test
T_s	Forces in the reinforcement across the cracks forming in the slab when submitted to the loss of one of its support
U	Vertical displacement at the top of the lost column (= the same as Δ_A)

U_c	Central deflection of the slab at the upper storey of a car park
$U_{c,limit.}$	Maximum central deflection of the slab for which the reinforcement across the cracks fails
ULGG or ULg	University of Liège
ULS	Ultimate Limit States
Vert.	Vertical
W	Web
w1	Width of the rib bottom
w2	Width of the rib top
WP	Work Package
P0	Initial column axial force under the ambient condition
Pt	Axial force of the heated column

XI. List of references

Abaqus (2011). Analysis User's manual, v6.11, Dassault Systems Simulia Corp., Providence, USA.

Abaqus Theory Manual & Users Manuals (2007), Version 6.7, Hibbitt, Karlsson and Sorensen, Inc. USA.

ADAPTIC user manual, Version 1.3b, Izzuddin, March, 2009.

Bailey CG (1995). Simulation of the structural behaviour of steel-framed buildings in fire. PhD thesis, The University of Sheffield, UK.

CEB (1990). "CEB-FIP – Model Code", Comité euro-international du béton, Design code, Thomas Telford Services Ltd.

Chapman J.C., and Balakrishnan S. (1964). "Experiments on composite beams", The Structural Engineering, 42:11, 369–83.

Comeliau C., Demonceau J.-F., Huvelle C., Jaspart J.-P. (2012), "Simplified approach". Internal Report, University of Liège

Demonceau J.-F. (2008), "Steel and composite building frames: sway response under conventional loading and development of membrane effects in beams further to an exceptional action", PhD Thesis realised at the ULg.

Department of Defense (DoD) (2009). "Unified Facilities Criteria, Design of Buildings to Resist Progressive Collapse". USA, July.

EN 1090-2:2008, "Execution of steel structures and aluminium structures, Part 2: Technical requirements for steel structures", 2008.

EN 1992-1-1:2004, "Eurocode 2: Design of concrete structures - Part 1-1: General rules and rules for buildings", European committee for standardization, December 2004.

EN 1992-1-2:2004 – "Eurocode 2: Design of concrete structures – Part 1-2: General rules – Structural fire design", European committee for standardization, December 2004.

EN 1993-1-1:2005 – "Eurocode 3: Design of steel structures – Part 1-1: General rules and rules for buildings", European committee for standardization, May 2005.

EN 1993-1-2:2005 – "Eurocode 3: Design of steel structures – Part 1-2: General rules – Structural fire design", European committee for standardization, April 2005.

Fang C. "Robustness of steel-composite structures against localised fire". PhD Thesis. Department of Civil Engineering, Imperial College, University of London, London, UK (to be submitted).

Fang C., Izzuddin B.A., Elghazouli A.Y. and Nethercot D.A. (2011). "ROBUSTFIRE Internal report - Behaviour of a multi-storey composite car park under a real localised fire – parametric studies and development of simplified temperature distribution", Internal Report, Imperial College London.

Fang C., Izzuddin B.A., Elghazouli A.Y., Nethercot D.A., and Obiala R. (2010). "ROBUSTFIRE Internal report - Behaviour of a multi-storey composite car park under a selected real localised fire scenario", Internal Report, Imperial College London.

Fang C., Izzudin B., Elghazouli A., Nethercot D., Gernay T., Demonceau J.-F., Franssen J.-M., Robustfire Report, Benchmark study for floor slabs

Franssen J.-M. (2000). "Failure temperature of a system comprising a restrained column submitted to fire", Fire Safety Journal, 34, p191-207.

Franssen J.-M. (2005). "SAFIR. A Thermal/Structural Program Modelling Structures under Fire", Engineering Journal, A.I.S.C., Vol 42, No. 3, 143-158, 2005.

Franssen J.M., Cooke G.M.E., Latham D.J. (1995). “Numerical Simulation of a Full Scale Fire Test on a Loaded Steel Framework”, Journal of Constructional Steel Research, 35, 377-408.

General Services Administration (GSA) (2003). “Progressive Collapse Analysis and Design Guidelines for New Federal Office Buildings and Major Modernization Projects”. USA, June.

Huang Z., Burgess I.W., Plank R.J. (1999). “The influence of shear connectors on the behaviour of composite steel-framed buildings in fire”, Journal of Constructional Steel Research, 51, 219-237.

Izzuddin B.A. (1991). Nonlinear Dynamic Analysis of Framed Structures, PhD Thesis, Imperial College, University of London.

Izzuddin B.A., and Elnashai A.S. (1993a). “Adaptive Space Frame Analysis – Part I: A Plastic Hinge Approach”, Structures and Buildings, Proceedings of the Institution of Civil Engineers, 99, 303-316.

Izzuddin B.A., and Elnashai A.S. (1993b). “Adaptive Space Frame Analysis – Part II: Distributed Plasticity Approach”, Structures and Buildings, Proceedings of the Institution of Civil Engineers, 99, 317-326.

Izzuddin B.A., Tao X.Y., and Elghazouli A.Y. (2004). “Realistic Modeling of Composite and Reinforced Concrete Floor Slabs under Extreme Loading. Part I: Analytical Method”, Journal of Structural Engineering, ASCE, 130:12, 1972-1984.

Izzuddin B.A., Vlassis A.G., Elghazouli A.Y. and Nethercot D.A. (2008). “Progressive Collapse of Multi-Storey Buildings due to Sudden Column Loss – Part I: Simplified Assessment Framework”, Engineering Structures, 30:5, 1308-1318.

Izzudin B.A., Omer E., Elghazouli A.Y. (2010). “Failure of unrestrained lightly reinforced concrete slabs under fire, Part 1: Analytical Models”, Engineering Structures.

Jaspart et al. (2009). “Deliverable I: Definition of the problem and selection of the appropriate investigation ways”, Robustness of car parks against localised fire, Grant Agreement Number RFSR-CT-2008-00036.

Lemaire F. (2010), “Etude du comportement 3D de structures en acier ou mixtes lors de la perte d’une colonne”, Master Thesis realised at the ULg.

Luu N.N.H. (2009), “Structural response of steel and composite building frames further to an impact leading to the loss of a column”, PhD Thesis realised at the ULg.

Malvern L.E. (1969). “Introduction to the mecanics of a continuous medium”, Englewood Cliffs, NJ: Prentice-Hall.

Omer E., Izzuddin B.A., and Elghazouli A.Y. (2010). “Failure of Unrestrained Lightly Reinforced Concrete Slabs under Fire, Part II: Verification and Application”, Engineering Structures, 32, 2647-2657.

Omer E., Izzudin B.A., M. ASCE, Elghazouli A.Y., M. ASCE (2009). “Failure of Lightly Reinforced Concrete Floor Slabs with Planar Edge Restraints under Fire”, Journal Of Structural Engineering.

Vlassis A.G., Izzuddin B.A., Elghazouli A.Y. and Nethercot D.A. (2008). “Progressive Collapse of Multi-Storey Buildings due to Sudden Column Loss – Part II: Application”, Engineering Structures, 30:5, 1424-1438.

Wainman D.E., and Kirby B.R. (1988). “Compendium of UK standard fire test data, unprotected structural steel — 1”, Ref. No. RS/RSC/S10328/1/87/B. Rotherham (UK): Swinden Laboratories, British Steel Corporation.

XII. Signed technical annex

EUROPEAN COMMISSION
RESEARCH DIRECTORATE-GENERAL

Research Fund for Coal and Steel

ANNEX I
Form 1-1
OBLIGATORY AT THE SUBMISSION STAGE

TECHNICAL ANNEX

Project acronym: ROBUSTFIRE

Proposal No[2]: RFS-PR-07039

Contract No: RFSR-CT-2008-00036

TITLE: Robustness of car parks against localised fire

PROJECT OBJECTIVES

This project aims at developing an assessment approach and design guidance dealing with the robustness of steel composite car parks under localised fire. Towards this goal, the following project objectives have been identified:

1. Review current practice and state of the art in the design and assessment of car parks subject to localised fire, and propose potentially robust structural schemes for subsequent investigation.

2. Develop and validate detailed numerical models as well as simplified analytical models of the fire response of critical structural components, including columns, connections and beams.

3. Propose a system level approach for simplified analytical modelling of steel composite car parks under localised fire, and verify against validated numerical modelling.

4. Develop a robustness assessment approach for steel composite car parks under fire, to be event-independent as far as possible, and propose relevant and practical design guidance.

5. Demonstrate using a real case study the accuracy and practicality of the developed analytical models, robustness assessment approach and corresponding design guidance.

1/174

EUROPEAN COMMISSION
RESEARCH DIRECTORATE-GENERAL

Research Fund for Coal and Steel

ANNEX I
Form 1-2
OBLIGATORY AT THE SUBMISSION STAGE

WORK PACKAGE DESCRIPTION

WP No	1

Work package Title	Definition of the problem and selection of the appropriate investigation ways	Number of man hours[29]
WP Leader (full name & acronym)	ULg (1)	600
Contractor (s) (full name & acronym)	IC (2)	300
	FCTUC (3)	301
	APLR (4)	500
	CSTB (5)	450
	GREISCH (6)	200
	CTICM (7)	157
Total		2510

1 – Objectives

- Definition of the car park structures (constitutive elements, connection types, loading, bracing systems …), of the specific design requirements and of the risks to be possibly encountered in terms of localised fire (destruction of one column or more than one column according to the position of the column in the structure, intensity and duration of the fire …).
- Identification of the distribution of temperatures within the affected part of the structure all along the event on the basis of previous research works performed, in particular within past RFCS projects.
- Selection of the philosophy to be followed so as to derive robustness requirements and related design recommendations (indirect methods, direct methods – alternate load path method or specific load resistance methods - …).
- Identification of the appropriate scenario(s) to be considered later on in the studies and of the related situations

2 - Work programme and distribution of tasks with indication of participating contractors

Work programme

2.1 Review of available knowledge on:

- car park typologies in Europe;
- design procedures for car parks in "normal" conditions of use;
- design requirements for car parks as far as fire and robustness are concerned;
- existing publications on robustness aspects (loss of a column);
- existing publications on localised fire in car parks.

2.2 Definition of the structures and the related safety requirements

- Selection of the studied typology (including fabrication and erection aspects).
- Selection of the scenario characteristics (intensity of the fire, various possible locations of the fire, number and nature of the affected elements …).
- Definition of global design requirements to be fulfilled as far as fire and robustness are concerned.

Distribution of tasks

- All the contractors have imperatively to be involved in this first work package.
- Each contractor will obviously contribute more to some items according to their expertise:
  - Fire aspects: FCTUC (3), Ulg (1), APLR (4), CTICM (7)
  - Robustness aspects: IC (2), ULg (1)
  - Design aspects: APLR (6)
  - Fabrication and erection aspects: APLR (4)
  - Design requirements: CSTB (5), CTICM (7)

3 - Interrelation with other work packages (please give WP No)

This first work package is aimed at clearly define, as expressed above, the type of structure to be considered, the exceptional event to accommodate and the related loading situations. On this basis, the works to be carried out in WP2 and WP3 and will be more precisely defined, as well the nature of the case study to be work out in WP5.

4 - Deliverables and milestones

A report (DI) summarising the whole work will be produced in a rather short time (6 months) so not to delay the progress of works in WP2 and WP3, and in particular the definition of the experimental tests to be carried out.

3/12

EUROPEAN COMMISSION
RESEARCH DIRECTORATE-GENERAL

Research Fund for Coal and Steel

ANNEX I
Form 1-2
OBLIGATORY AT THE SUBMISSION STAGE

WORK PACKAGE DESCRIPTION

WP No	2

Work package Title	Structural individual response of the affected structural elements	**Number of man hours**[29]
WP Leader (full name & acronym)	FCTUC (3)	2900
Contractor (s) (full name & acronym)	ULg (1)	1600
	IC (2)	1400
	APLR (4)	530
Total		6430

1 – Objectives

- The main objective is to acquire the required knowledge on the behavioural response of the individual frame structural elements directly affected by the localised fire and the resultant reduction of carrying capacity of the heated column:
    - heated column in compression and bending;
    - heated beam subjected to bending and axial force (membrane effects);
    - heated beam-to-column joints subjected to bending and axial force (membrane effects).

  The complexity of the studies results from the specific loading situation (non uniform field of temperatures in the cross-sections and along the elements as well as development of membrane forces as a consequence of the partial or total loss of the column).
- More precisely, three approaches will be combined according to the needs (experimental, numerical and theoretical) with the aim, at the end, to derive behavioural models for elements at two different levels:
    - "sophisticated level" (FEM models);
    - "simplified" level (models for designers).

2 - Work programme and distribution of tasks with indication of participating contractors

As said before, three research directions are intended to be followed:

2.1 Experimental tests

Tests on joints subjected to a thermal loading (fire) and to forces (bending and tension) are to be carried out. Tests on columns and beams will not be carried out as FEM models look appropriate to predict their behavioural response. All tests will be carried out by FCTUC (3) where specific experimental facilities are available. The other partners [(1), (2) and (4)] will contribute to the design of the tested specimens and to the detailed examination of the results. The tests specimens will be fabricated in the shop of APLR in Luxembourg. Tensile tests will also be performed in order to assess the real mechanical properties of the steel.

About seven tests on joints are planned:

- Level of temperature 1: *three* tests (for three different values of the M/N ratio)
- Level of temperature 2: *two* tests (for two different values of the M/N ratio)

- Level of temperature 3: *one* test where the joint is only subjected to axial tension force (present complete lack of information for this specific situation)
- Level of temperature 4: one test where the sequence of loading will be as close as possible to what the joint would experience in the actual frame – variable M/N ratio all along the loading)

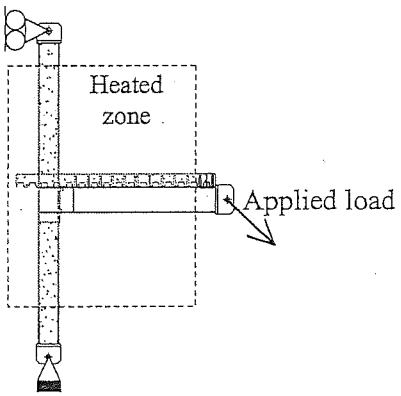

2.2 Numerical simulations

Numerical simulations will be carried out by the three partners to predict the behavioural response of the three individual affected members (columns, beams and joints – with beam, plate or shell elements). The use of various software (FINELG, SAFIR, ADAPTIC, LUSAS) will first require a benchmark study to be carried out so as to ensure the consistency of the results. The experimental tests will then be used to validate the FEM simulations. Finally parametric studies will be performed so as to investigate the influence of various parameters on the response of the elements (acting forces, distribution of temperatures and level of temperatures). All WP3 partners (3) will be similarly involved in these works.

2.3 Theoretical investigations

From the results of the tests and from those of the parametrical studies, engineering models will be developed. For joints, such models already exist at ULg for composite joints subjected to bending and axial force. They will have to be extended to integrate the thermal loading. For beams and columns, the challenge will be to integrate in existing models the effect of the non uniform distribution of temperatures along their length. The reduction of the floor to a grillage of composite beams is also a challenge which will have to be faced. The distribution of the works is expected to be as follows:

- Joints: ULg (1)
- Beams: IC (2)
- Columns: FCTUC (3)

3 - Interrelation with other work packages (please give WP No)

The geometry of the studied beam, column and joint elements, as well as the loading conditions all along the event and (thermal and mechanical) result from WP1. Present WP aims at making available sophisticated and simplified behavioural models, which will later be used in WP3 to investigate the response of the whole structure (considered as an assembly of individual beam, column and joint components).

4 - Deliverables and milestones

As an outcome of WP2, two main deliverables are identified:

- Development of sophisticated behavioural models (DII)
- Development of simplified behavioural models (DIII)

The first ones are of particular importance as they are the only ones able to follow as closer as possible the reality. This allows considering them as references in research, to use them with full confidence for parametrical studies and finally to used them as a direct design tool for complex structures for which the use

by the designer of simplified behavioural models would be questionable.

The simplified models are models which can be more easily used in practice and which could possibly be later on implemented in design guides or codes and which allow the designer to assess the behaviour of the structure in a rather easy and direct way, i.e. in agreement with his requirements in terms of efficiency and competitiveness.

For evident reasons of sequence, the development of sophisticated behavioural models will precede the development of the simplified behavioural models.

EUROPEAN COMMISSION
RESEARCH DIRECTORATE-GENERAL

Research Fund for Coal and Steel

ANNEX I
Form 1-2
OBLIGATORY AT THE SUBMISSION STAGE

WORK PACKAGE DESCRIPTION

WP No	3

Work package Title	Study of the structural response under selected scenario(s)	Number of man hours[29]
WP Leader (full name & acronym)	IC (2)	1600
Contractor (s) (full name & acronym)	ULg (1)	1600
	FCTUC (3)	1265
	APLR (4)	600
Total		5065

1 – Objectives

- The main objective of WP3 is to integrate the knowledge acquired on *elements* in WP2 in a structural model which would allow to predict the response of the *whole frame* subjected to the localised fire. This test is of an extreme importance as the robustness aims at ensuring the global stability of the car park even if a part of it is strongly damaged.
- More precisely now:
  - the way to run FEM simulations of the whole frame subjected to the exceptional loading will have first to be clearly defined;
  - practical behavioural models for the whole frame will have to be developed for daily practice.

2 - Work programme and distribution of tasks with indication of participating contractors

Work programme

2.1 Restraint and resistance against progressive collapse brought by the unaffected part of the structure

When the column subject to fire looses partially or totally its carrying capacity, the undamaged part of the structure "tends to restraint the upper floor to fall down". This stiffness but also the resistance that the undamaged part of the structure may exhibit are keys aspects which will have to be intensively studied. Evaluation models for these restraints are here to be developed.

2.2 Specific study of the 3D slab response

The concrete slab plays an important role which has to be assessed first and then modelled. This topic is already addressed in WP2, but here the effect of the continuity of the slab over the whole car park floor wil be more specifically studied.

2.3 Development of a frame behavioural model

In this model, the frame restraints studied in the sub-task 2.1 here above and the behavioural models developed in WP2 will be combined in a model aimed at identifying the hopefully remaining stability and resistance of the damaged car-park. As a particular aspect, the development of catenary actions in beams and joints will be characterised (tying force, ductility required, beam deflections ...).

2.4 Derivation of robustness requirements

Through 2.3, the request in terms of resistance and ductility, everywhere in the damaged frame, will be known. By comparing these demands to the available resistance and ductility that the frame components may offer, robustness requirements will be derived.

Distribution of tasks

The four contractors involved in WP3 will joint their efforts to reach the listed objectives. Obviously, they will bring into the works their expertise in structural engineering and the knowledge individually gained in WP2 on beams, columns and joints.

3 - Interrelation with other work packages (please give WP No)

The development on WP3 of a behavioural model for the whole frame is the natural continuation of WP1 (definition of the structure and of the related scenarios) and of WP2 (study of individual frame components). **Anyway, in order to plan the tests within WP 2, some preliminary knowledge on the global structural response and 3D slab behaviour is required what explains that Task 3.1 and 3.2 start at the same time than WP2.**

4 - Deliverables and milestones

Two deliverables may be expected as an outcome of WP3:

- Guidelines for the FEM simulation of car parks under localised fire leading to the partial or total loss of a column. (DIV)
- Behavioural models predicting the response of these structures by means of "practice-oriented" approaches. (DV)

4/12/10

EUROPEAN COMMISSION
RESEARCH DIRECTORATE-GENERAL

Research Fund for Coal and Steel

ANNEX I
Form 1-2
OBLIGATORY AT THE SUBMISSION STAGE

WORK PACKAGE DESCRIPTION

WP No	4

Work package Title	Derivation of design recommendations adapted to the industrial request for design efficiency as well as for easy fabrication, erection and control	Number of man hours[29]
WP Leader (full name & acronym)	ULg (1)	1000
Contractor (s) (full name & acronym)	IC (2)	500
	FCTUC (3)	300
	APLR (4)	600
	CSTB (5)	660
	GREISCH (6)	200
Total		3260

1 – Objectives

- In WP3, robustness requirements for car parks subjected to exceptional localised fire will have been derived. For each particular car park being studied, the specific requirements applicable to the structure and its scenarios are have to be expressed before the check of the structural integrity of the damaged structure is carried out. This approach is certainly the most exact one, but will for sure require a huge amount of time and care. Another approach, more adequate to daily practice should therefore be proposed; this is the objective of WP4 in which so-called "event independent" criteria will be derived.
- Just an example: the check of the sufficient ductility of the composite connections would normally imply to compare the required ductility (evaluated by means of the frame behavioural model developed in WP3) to the available joint ductility. Instead of that, practical design guidelines and recommendations on how to select the joint detailing - before any frame analysis is done (i.e. in the first design steps) - could be proposed which would ensure the sufficient ductility of the joints in case of localised fire, but obviously in a well-defined field of application (typology of the frame, number of storeys …).
- In WP4, this second approach would be selected and appropriate design recommendations are to be developed and proposed.

2 - Work programme and distribution of tasks with indication of participating contractors

Work programme

The work within WP4 is organised as an interaction between two activities:

2.1 Derivation of practical recommendations

In this part, the practical "event-independent" recommendations are derived and suggested to comments and reviews before being possibly reworked.

2.2 Critical appraisal of the practical recommendations

Here the practical applicability and suitability of these recommendations is discussed from several points of view: safety, design, fabrication, cost, erection

9/12

Distribution of tasks

The distribution of tasks is based on interactions between scientific institutions and industrial ones, so to ensure that "best practice" tools are developed at the end. The following share of the work is therefore contemplated:

- Derivation of recommendations: ULg (1), IC (2) and FCTUC (3)
- Critical review: APLR (4), CSTB (5) and GREISCH (6)

In the scope of the critical review, APLR will define an Advisory committee composed of engineering offices dealing with fire engineering coming from all over Europe (Members of the Secure with steel Network). The practical recommendations will be analysed and discussed in order to be in phase of the day to day business of structural fire engineering.

3 - Interrelation with other work packages (please give WP No)

WP4 is the natural continuation of WP2 and WP4, but in leading aspects are not only the scientific ones, but also those more directly related to practice: design, fabrication, erection …

4 - Deliverables and milestones

The work will proceed according to a "way and back" approach; this should finally lead to the proposal of a set of practical design recommendations for the design of car parks in which accidentally a column could be affected by a localised fire. A chapter of the final report (DVI) will be devoted to the presentation of these recommendations. The drafting of a complete and independent publication on the subject would require a huge extra work which could not, for time aspects mainly, be properly achieved within the present project. So a prolongation aiming at valorisation and diffusion of the outcome of the present project will possibly be contemplated at the end of the three years.

10/12

EUROPEAN COMMISSION
RESEARCH DIRECTORATE-GENERAL

Research Fund for Coal and Steel

ANNEX IV
Form 1-2
OBLIGATORY AT THE SUBMISSION STAGE

WORK PACKAGE DESCRIPTION

WP No	5

Work package Title	Case study	Number of man hours[29]
WP Leader (full name & acronym)	GREISCH (6)	1170
Contractor (s) (full name & acronym)	CSTB (5)	780
	APLR (4)	300
	FCTUC (3)	300
	IC (2)	450
	ULg (1)	500
	CTICM (7)	600
Total		4100

1 – Objectives

- Selection of a particular case study (typology, dimensions, loading, types of members and joints …) used as a reference all along the duration of WP5.
- Design of the structure according to Eurocodes under "normal" loading.
- Application of the sophisticated frame behavioural model developed in WP3.
- Application of the sophisticated simplified behavioural model developed in WP3.
- Definition of the robustness requirements specific to the selected structure.
- Application of the "event-independent" robustness requirements.
- Interaction between "scientific" partners and "practice-oriented" partners with the aim to improve the practical applicability of the "event-independent" robustness requirements. Moreover a special attention will be paid the adequacy of the requirements with the requests of the control offices in charge of the checking of the safety aspects under normal and exceptional loading.

2 - Work programme and distribution of tasks with indication of participating contractors

Work programme

2.1 Definition of the study case and its design according to the Eurocodes under "normal" loading conditions

2.2 Application of the robustness behavioural models

- Sophisticated models for components and frame
- Simplified models for components
- Simplified models for to the elements

2.3 Application and progressive improvement of the "event-independent" robustness requirements

Distribution of works

All contractors will contribute to this activity, each of them bringing its own expertise:

- Development aspects: ULg (1), IC (2) and FCTUC (3)
- Construction aspects: APLR(4) + Advisory committee
- Design: GREISCH (5)
- Safety and control aspects: CSTB (6), CTICM (7)

3 - Interrelation with other work packages (please give WP No)

As soon as WP1 will be finalised, WP5 will start, in parallel with WP2, WP3 and WP4. This will allow, all along the development process, to ensure a full adequacy between the scientific works, their outcome and the design practice. So it is expected that the proposed design recommendations will fit well to the requests of the construction parties (design office, constructor, control offices ...)

4 - Deliverables and milestones

A chapter of the final report (DVI) will be dedicated to the presentation of the case study. It will address the various aspects of the problem, including design, fabrication, erection, control aspects.

12/12

EUROPEAN COMMISSION
RESEARCH DIRECTORATE-GENERAL

Research Fund for Coal and Steel

ANNEX IV
Form 1-3
OBLIGATORY AT THE SUBMISSION STAGE

PROGRAMME BAR CHART (TASK, PARTNER, DELIVERABLES, MILESTONES)

Work packages	*Work packages' title*	*Deliverables*	Hours on project/ Contractor(s)							1st year				2nd year				3rd year			
			1	2	3	4	5	6	7	I	II	III	IV	I	II	III	IV	I	II	III	IV
WP 1	**Definition of the problem and selection of the appropriate investigation ways**	DI	600	301	300	500	450	200	157												
Task 1.1	Review of knowledge		200	101	100	200	200	100	57												
Task 1.2	Definition of the structures and of the related requirements		400	200	200	300	250	100	100												
WP 2	**Structural individual response of the affected structural elements**	DII and DIII	1600	1400	2900	530	-	-	-												
Task 2.1	Experimental tests		-	-	1300	230	-	-	-												
Task 2.2	Numerical simulations		800	700	800	150	-	-	-												
Task 2.3	Theoretical investigations		800	700	800	150	-	-	-												
WP 3	**Study of the structural response under selected scenario(s)**	DIV and DV	1600	1600	1265	600	-	-	-												
Task 3.1	Restraint and resistance against progressive collapse brought by the unaffected part of the structure		500	-	-	-	-	-	-												
Task 3.2	Specific study of the 3D slab		-	500	365	-	-	-	-												
Task 3.3	Development of a frame behavioural model		500	500	450	300	-	-	-												
Task 3.4	Derivation of robustness requirements		600	600	450	300	-	-	-												

1 2 3 4 5 6 7

WP 4	**Derivation of design recommendations adapted to the industrial request for design efficiency as well as for easy fabrication, erection and control**	**DVI**	**1000**	**500**	**300**	**600**	**660**	**200**	**-**											
Task 4.1	Derivation of practical recommendations		1000	500	300	-	-	-	-											
Task 4.2	Critical appraisal of the practical recommendations		-	-	-	600	660	200												
WP 5	**Case study**	**DVI**	**500**	**450**	**300**	**300**	**780**	**1170**	**600**											
Task 5.1	Definition of the design case and its design according to Eurocodes under "normal" loading conditions		100	50	50	200	100	1000	100											
Task 5.2	Application and progressive improvement of the "even-independent" robustness requirements		400	400	250	100	680	170	500											
Total Hours on project			**5300**	**4250**	**5066**	**2530**	**1887**	**1570**	**760**											

XIII. Appendices

XIII.1. Appendix: Work Package 2 - Structural individual response of the affected structural elements: experimental tests

XIII.1.1. Objectives of the tests performed at Coimbra

The main objective of the experimental tests was to observe the combined bending moment and axial loads in the heated joint when catenary action develops in the frame after the loss of the column. The effect of the localised fire (that led to the column loss) was simulated by the application of elevated temperatures in the composite joint zone. According to previous experimental works performed in real composite steel-concrete open car park structures subjected to fire, a majority of the temperatures measured in the beam bottom flanges were lower than 500ºC; however temperatures of 700ºC were observed in recent tests performed in France (Deliverable I). Seven beam-to-column frames were tested in Coimbra: one reference test at ambient temperature; five tests at 500ºC or 700ºC; and a demonstration test, for which the frame was subjected to an increase of the temperature up to the failure of the column. The effect of the axial restraint to beam coming from the unaffected part of the building was also studied: two tests without axial restraints to the beam; two tests with total axial restraint to the beam; and three tests with realistic axial restraint to the beam. Table 6 presents the objectives of each test.

Table 6. Objectives of the seven experimental tests of sub-frames subject to the loss of a column

Test	Objectives
1	Derivation of the joint M-N curve at ambient temperature – Realistic axial restraint to the beam. *Due to testing problems, this test was performed without any axial beam restraint (see §XIII.1.5.2), and only the joint properties at ambient temperatures were derived.*
2	Derivation of the joint properties at 500ºC – No axial restraint to the beam
3	Derivation of the joint properties at 700ºC – No axial restraint to the beam
4	Derivation of the joint M-N curve at 500ºC – Total axial restraint to the beam
5	Derivation of the joint M-N curve at 700ºC – Total axial restraint to the beam
6	Derivation of the joint M-N curve at 700ºC – Realistic axial restraint to the beam
7	Demonstration of the real joint behaviour of a sub-frame subjected to the loss of a column due to a localised fire – Realistic axial restraint to the beam

XIII.1.2. Extracted sub-frame and testing arrangement

The two dimensions sub-frame was selected from the fifth floor of the typical composite steel-concrete car park building (designed in WP5). Because of the restrictions from the laboratory dimensions, the beam length was reduced from 10 m in the real building to 3 m in the sub-frame to be tested. Figure 57 presents the seven beam-to-column frames tested in Coimbra, including the studied axial restraint to the beam.

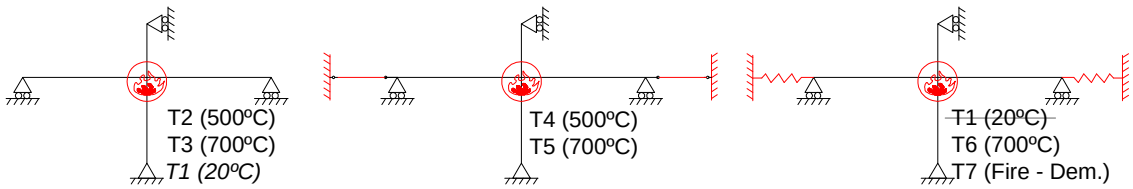

Figure 57. Seven experimental tests

Each sub-frame was defined by two unprotected composite beams IPE 550 steel cross-sections, grade S355, and one unprotected HEB 300 cross-section steel column, grade S460 (Figure 58). A reaction frame perpendicular to the plane of the sub-frame supported the hydraulic jack which was linked by a

pin to the top of the column. The column base was hinged and fixed to a reinforced concrete footing. When the axial restraint to the beam was simulated, the beams restraints were connected to the two strong walls via horizontal HEB 300 cross-section beams. The hydraulic cylinder located at the column base (except for the last test 7) simulated the progressive loss of the column. This cylinder kept a constant vertical displacement of the column during the application of the initial loads and the increase of temperatures, and was finally taken out by decreasing the oil pressure in order to simulate the column loss. A smaller steel profile HEB 140 cross-section was used at the column base in order to facilitate the concreting: the composite sub-structure was located at the floor level. In test 7, this bottom HEB 140 column was also heated.

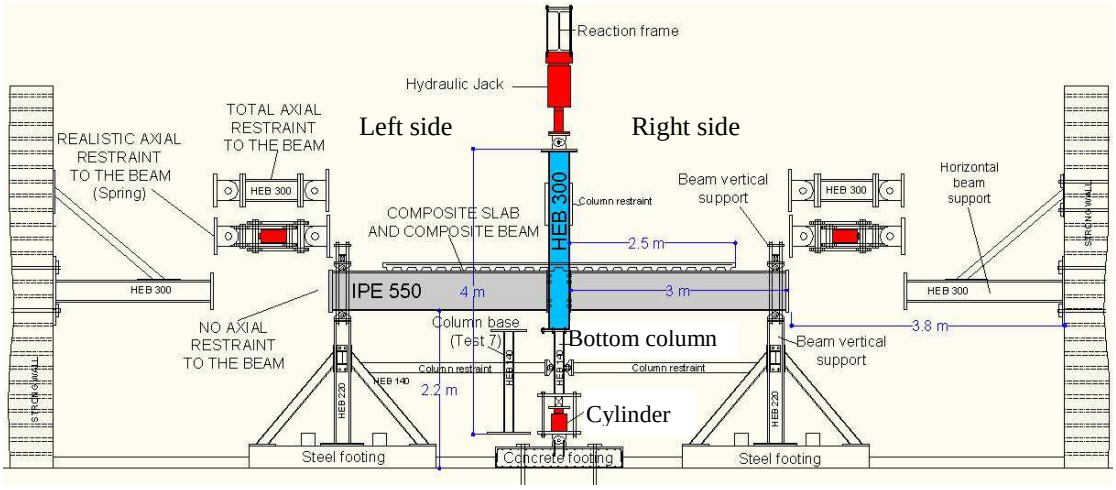

Figure 58. General layout, longitudinal view

The out-of-plane column rotation was prevented at the base (Figure 58) and near the connection (Figure 59). The restraint system allowed vertical movement and also prevented any horizontal displacement of the connection in the plane or out of the plane of the sub-frame. However, in tests 3 and 7, the restraints at the column base were not used.

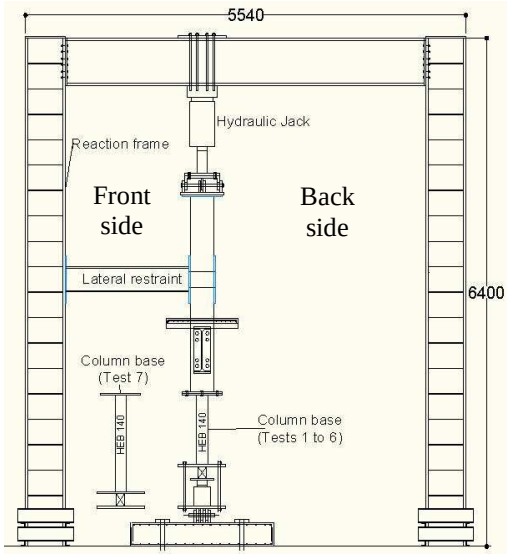

Figure 59. General layout, lateral view

The joint configuration is shown in Figure 16 (§VII.4.8.2). Bolts M30, cl. 10.9, and a steel end-plate of 15 mm thick, S355, were used. In order to ensure the composite behaviour of the beam-to-column joint, ten steel rebars of diameter 12 mm were placed in the composite slab at each side of the column. The composite slab was of steel deck and light-weight in-situ concrete composite floor, and had 900 mm width, 1 mm thick steel sheeting and reinforced concrete C25/30. In practice, the ribs of the steel sheeting should be installed parallel to the beam span (main joint). But in the laboratory, the ribs were positioned perpendicularly to the beam in order to allow the concreting. Nevertheless, difficulties were

experienced during concreting and the average total slab thickness was 130 mm instead of the 120 mm defined in WP5. Constructional longitudinal (8 mm diameter) and transversal rebars (6 mm diameter) were added notably to respect the maximum spacing defined by Eurocode 4 part 1.1. The steel beam was fully connected to the composite slab by 22 shear studs (diameter = 19 mm; height = 100 mm). The beam was not composite all along its length (Figure 58); in order to apply the initial hogging bending moment, a steel beam is considered to apply the restraint to the vertical displacements at the beam supports (Figure 58). This structural consideration was accepted because the reduced slab length was sufficient for the anchorage of the steel rebars included in the behaviour of the composite joint.

XIII.1.3. Description of the loading sequence

XIII.1.3.1. Tests 1 to 6

Each test, from test 1 to test 6, was divided into 3 main steps (see Table 7): step 1 - application of an initial hogging bending moment in the joint, step 2 - heating of the joint zone up to 500ºC or 700ºC (except for test 1 at 20ºC), and step 3 - simulation of the loss of the column and increase of the sagging bending moment up to the failure of the joint.

Table 7. Outline of the tests 1 to 6

Step 1	**Step 2**
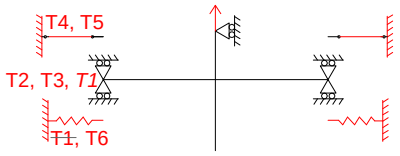	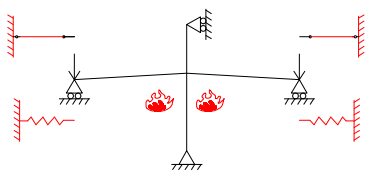
Hogging bending moment	Fire (except for test 1 at 20ºC)
Step 3	
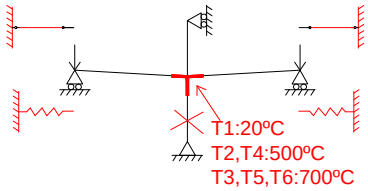	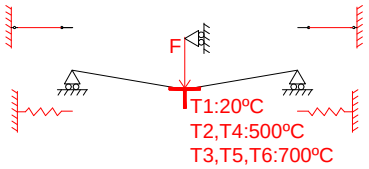
Loss of the column	Sagging bending moment

Step 1 simulated the internal loads in the connection as in the real car park building; a hogging bending moment equal to 450 kNm was applied in the joint for the test 1 at ambient temperature; this value was calculated in a simple 2D model in Abaqus (2007), considering the loads at the service limit state (SLS) defined during the design of the car park building in WP5. According to Eurocode 1 part 1.2, effects of actions under fire may be deduced from those determined in normal temperature design, by calculating the reduction factor η_{fi}, resulting in a target hogging bending moment of 236 kNm for tests 2 to 6:

$$\eta_{fi} = \frac{G_k + 0.5Q_{k.1}}{1.35G_k + 1.5Q_{k.1}} = 52{,}53\%$$

where $G_k = 26.4\ kN/m$ and $Q_{k.1} = 26.7\ kN/m$.

During step 2, temperatures increased with a linear rate equal to around 300ºC/hour. The increase of temperatures stopped and step 3 began once temperatures in beam bottom flanges were equal to 500ºC in tests 2 and 4, and 700ºC in tests 3, 5 and 6. Finally, temperatures were kept constant during the entire step 3, for which the progressive loss of the column was simulated by removing the cylinder from the column base (Figure 58). Then, the vertical load at the column top was increased in the downward direction in order to increase the sagging bending moment in the joint and to reach the joint failure. During the increase of the sagging bending moment, the column was assumed to be completely failed.

XIII.1.3.2. Test 7

The load path and the loads values were chosen in order to reach: i) the buckling of the bottom part of the column due to the increase of temperatures (steel profile HEB 140, S355); ii) the progressive collapse of the sub-frame after the loss of the column (due to safety conditions in laboratory, a sudden failure should not happen after the loss of the column). As shown in the Table 8, the following load path was planned: step 1 - application of an initial hogging bending moment in the joint (236 kNm); step 2 - application of a constant load (250 kN) at the column top; step 3 - heating of the joint zone and the bottom column respectively up to 400ºC and 800ºC; step 4 - heating of the joint zone up to the failure.

Table 8. Outline of the test 7

Step 1	**Step 2**
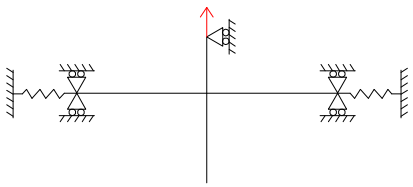	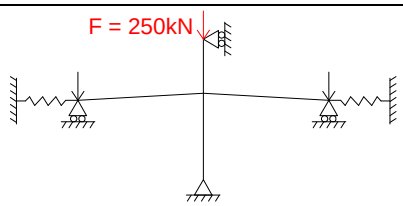
Hogging bending moment	Mechanical loading (250 kN)
Step 3	**Step 4**
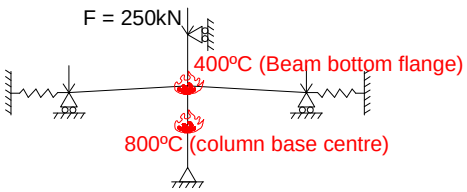	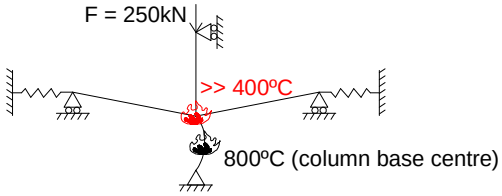
Heating of the column base up to the loss of the column	Heating of the joint up to the total failure of the frame

The mechanical loading of the sub-frame was applied at the column top by the hydraulic jack, and was kept constant during the entire test (steps 2 and 3). First, the temperature was increased up to: i) 800ºC in the bottom part column in order to reach the critical temperature of the steel profile and the complete loss of the column; ii) 400ºC in the joint (measured in the beam bottom flanges). The joint temperature was limited in order to avoid the joint failure once the column fails, and was based on the previous tests. Finally, after the column loss, the joint temperature was increased up to the failure of the sub-frame. The load at the column top (250 kN) and the temperature in the column base (800ºC) were kept constant.

XIII.1.4. Mechanical and thermal loadings

Steel temperatures were increased using Flexible Ceramic Pad (FCP) heating elements (concrete is not heated). In tests 2 to 6, the heated zone consisted of a length of 0.6 m of beam at each side of the joint, of the bolts and of 1 m of column (Figure 60); in test 7 (demonstration test), the column base was heated and the heated zone of the joint was reduced to 0.4 m. Servosis hydraulic jack ($F_{max.}$ = 1000 kN; $\Delta_{max.}$ = 280 mm) was used to apply the mechanical loading at the column top.

In order to define the required capacities of the load cells, displacement transducers and hydraulic jack, preliminary numerical simulations were performed and estimated the global behaviour of the sub-structures to be tested in the laboratory. The non-linear finite element package Abaqus, v6.7 was used to perform the structural model. Beam and shell elements were used to model beam/column, and concrete slab respectively. A static general analysis was performed with thermal and mechanical loadings. No initial imperfections were applied, but geometrical and material non linearities were taken into account. Materials temperature dependent properties were defined according to Eurocode 3 part 1.2 and Eurocode 2 part 1.2. The thermal expansion coefficient was defined constant equal to 1.4 x 10^{-5} /ºC and 1.8 x 10^{-5} /ºC for steel and concrete respectively.

Figure 60. Heated connection zone using Ceramic Pad Heating elements in tests 2 to 6

XIII.1.5. Beam axial restraints

The effect of the axial beam restraint coming from the unaffected part of the building was studied, and three different restraints stiffness's were considered: tests 2 and 3 - no axial restraint to the beam; tests 4 and 5 - total axial restraint to the beam; and tests 1, 6 and 7 - realistic axial restraint to the beam. When no restraint was applied, the beams were free to the axial movement.

XIII.1.5.1. Total restraint

The beam was totally restrained in the axial direction due to a steel profiles HEB 300 that linked the end of the tested beams to strong walls. Each restraint was pinned and allowed the rotation. The axial force was deduced from the strains measured by five strain gauges: two on the top flange, two on the bottom flange and one on the web; in order to know the reaction force direction, the rotation was deducted from the vertical displacements measured by displacements transducers.

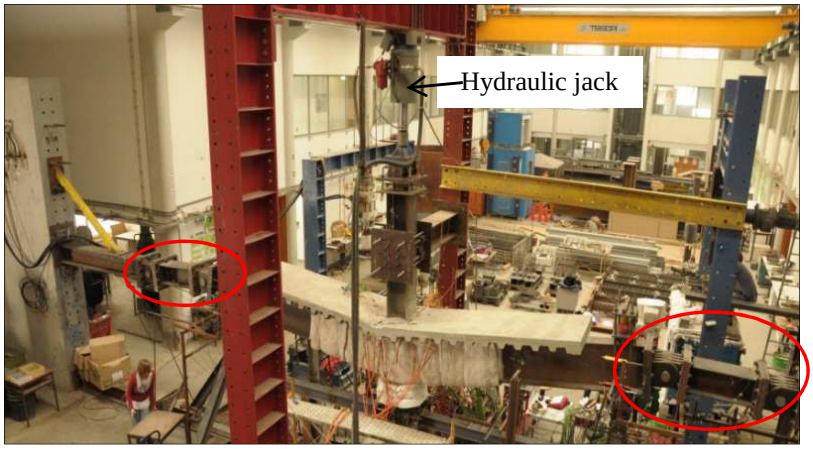

Figure 61. Total axial restraints to the beam (at the end of test 5)

XIII.1.5.2. Spring restraint

The realistic axial restraint to the beam provided by the part of the building not directly subjected to the localised fire and to the loss of the column was initially estimated by a simple elastic analysis performed in the software Abaqus v6.7: five column locations were simulated. A horizontal unitary force was applied at the beam-to-column connection level at the extremity of the sub-structure subjected to the loss of the column, and the displacement was measured. The smaller computed lateral restraint K of the equivalent single spring was 64.4 kN/mm. During the tests, two springs were applied at each beam ends. The stiffness of each spring was equal to two times the stiffness of the equivalent

single spring calculated in Abaqus: 2K (128.8 kN/mm). In the laboratory, the spring restraints were simulated using hydraulic cylinders. The two restraints were working separately using two separated hydraulic circuits: a cylinder to apply the load at the sub-frame and a hydraulic pump to adapt the oil pressure in the cylinder. Each spring restraint was controlled manually: the displacement measured by displacement transducers was read in the data logger, and the oil pressure (measured by pressure transducers) was adapted at the hydraulic pump in order to modify the load applied by the cylinder. The cylinder had the ability to work in tension (max. load of 435 kN) or in compression (max. load of 933 kN), whereas the hydraulic pump was limiting the maximum oil pressure (500 bars) that could be sent to the cylinder, and the force that could be applied by the system was limited to 654 kN in compression and 304 kN in tension. Figure 62 shows the spring restraint made with the double acting long stroke cylinder and a system of transversal bars and steel plates.

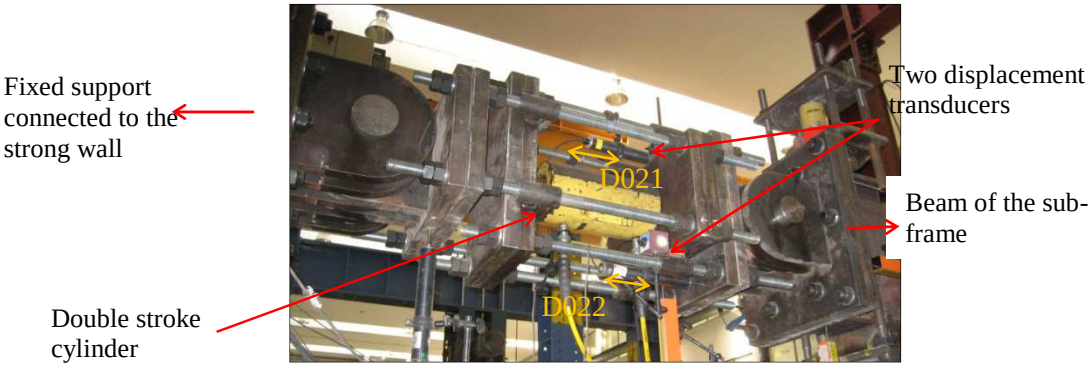

Figure 62. Spring restraint (left)

Even the smaller value of the spring stiffness calculated in the real building (129 kN/mm) would lead to a very low displacement (2.6 mm) at the maximum load able to be applied (654 kN). So the spring stiffness considered for the tests was reduced to 50 kN/mm.

Three tests should have been performed with spring axial restraint to beam: test 1 at ambient temperature, test 6 at elevated temperature (700ºC) and finally the demonstration test 7. In order to simplify the test 1 (20ºC), it was assumed that the spring restraints should only apply the tensile loads once the column loss happened and the catenary action developed. This assumption was based on the fact that the test was performed at ambient temperature without any dilatation of the beams, so no compression loads should be developed at the beams ends. An initial tensile load was applied in the springs in order to allow the beginning of the control (see deliverable II, section II). However, after the column loss (step 3), the beams ends were moving outwards instead of moving inside like it was planned, and the spring restraints should had worked in compression, but this was not possible because it was not planned. This was only after the failure of two bolts that one beam end begun to apply tensile forces at the restraint. In conclusion, the reference test could be considered as performed without any restraint to the beam. Indeed, the spring was linked to the beam at the gravity centre (GC) of the steel beam section (IPE 550) but not at the GC of the CO section: so when the beam rotated, the measured displacements at the GC of the steel beam end showed an outward movement (Figure 63). Tests 6 and 7 were performed with the spring restraints working in compression for the most part of the test.

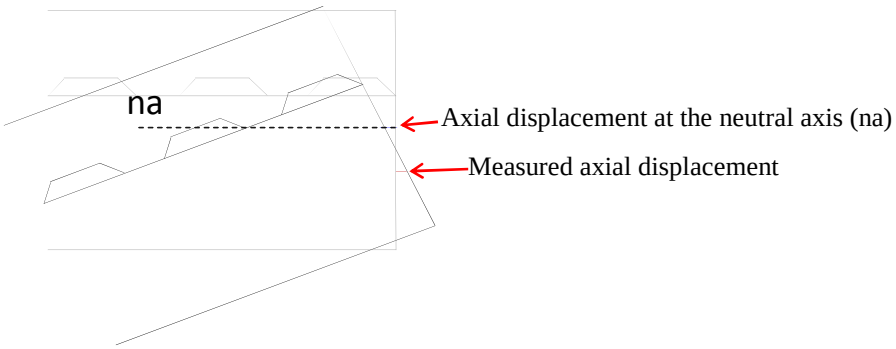

Figure 63. Rotation of the beam extremity and outward displacement of the geometrical centre of the steel beam section

XIII.1.6. Instrumentation of test specimens

XIII.1.6.1. Load cells

Figure 64 presents the measured reaction loads for each test. Load cells F1 and F2 were placed at the top of each beam because they were considered to apply the initial hogging bending moments. The load cell F3 was located at the bottom of the column; the load cell F-HJ was included in the hydraulic jack at the column top and measured the applied load; load cells F4 and F5 were added to the lateral restraint of the column base. The reaction loads from the axial restraints to beams were measured by: i) pressure transducers in case of the spring restraints; ii) strain gauges in case of the total restraints.

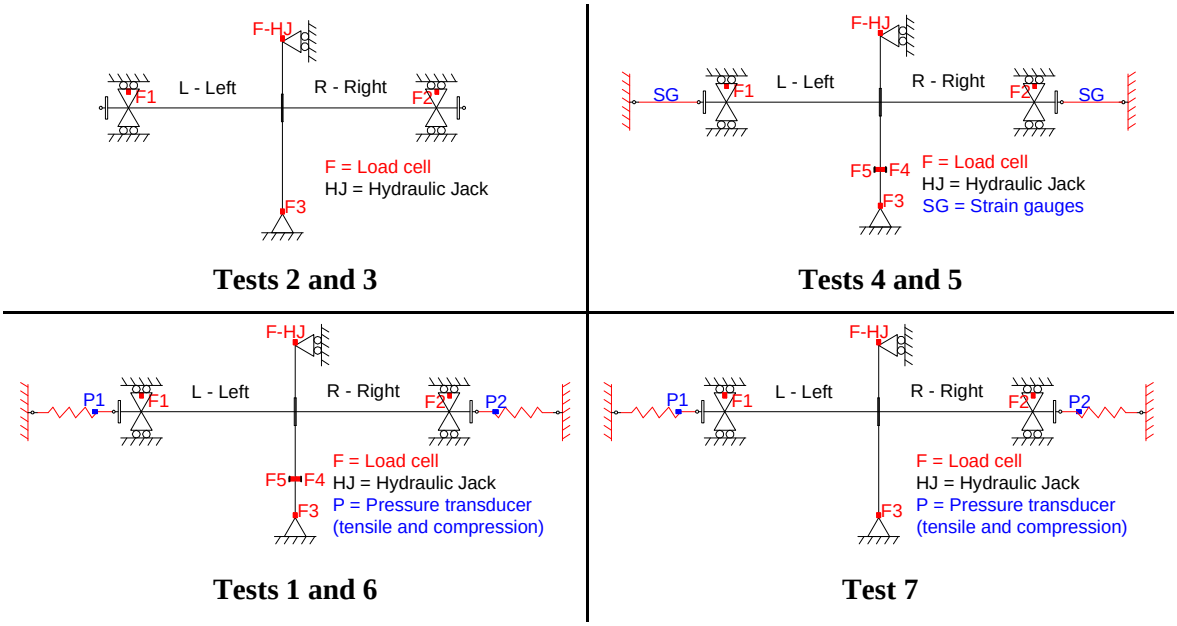

Figure 64. Load cells, pressure transducers and strain gauges to measure the reaction loads

XIII.1.6.2. Displacement transducers

Around 30 displacement transducers were used in order to measure the displacements and deformations of the specimen (Figure 65) and to check the residual displacements of the auxiliary structures, such as footings, frames, etc… Displacement transducers of 200 mm, 100 mm and 50 mm, and wire transducers of maximum deflection 1000 mm were used.

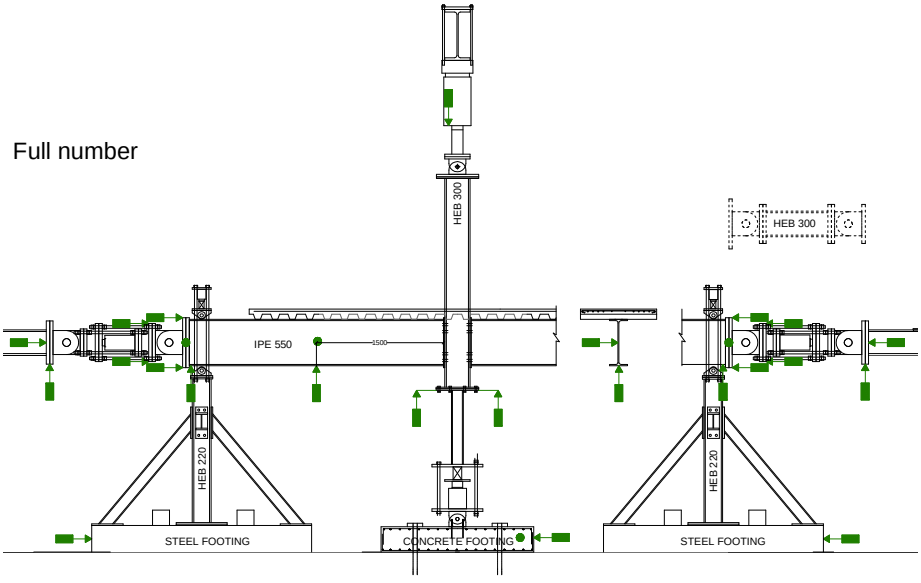

Figure 65. Displacement transducers

XIII.1.6.3. Thermocouples

A total of around 90 (70 for tests 4, 5 and 6) thermocouples of K type with two 0.7 mm wires measured the temperature in the elements: end-plates, bolts, beams, column, and composite slab. The thermocouples of the beams were applied as shown in Figure 66 at 250 mm, 500 mm and 1000 mm from the end-plate. In test 7, as the heated zone of the beam was reduced, and the bottom column was heated, the arrangement of thermocouples was slightly different (see deliverable II, section II). Figure 67 shows, as an example, the thermocouples located on the steel members of the test 5. Additional thermocouples were also measured temperatures in the composite slab.

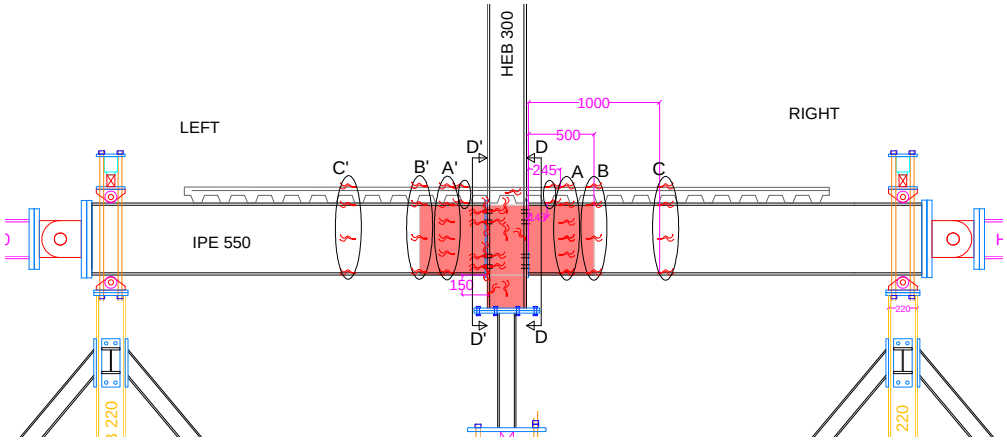

Figure 66. Instrumentation (thermocouples) of the heated zone for tests 2, 3, 4, 5 and 6

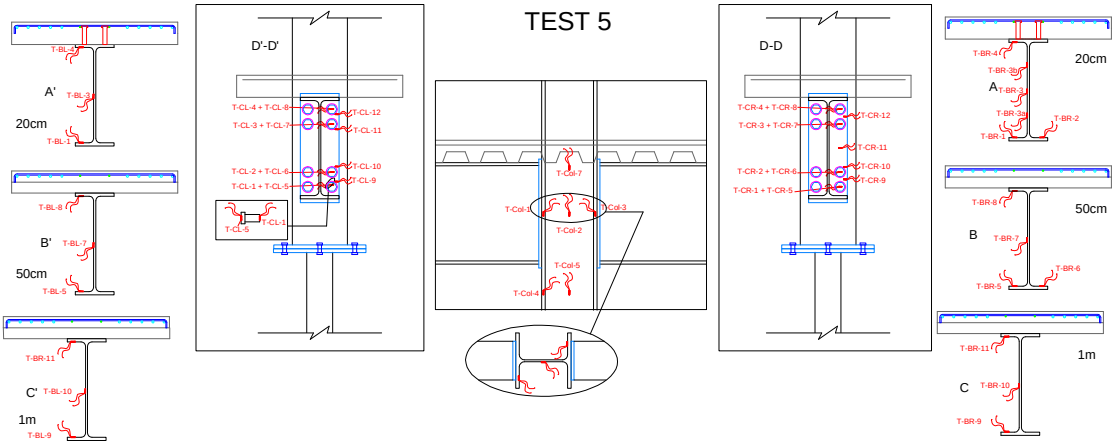

Figure 67. Thermocouples at the steel beams, column and joint of the test 5

XIII.1.6.4. Strain gauges

Around 50 strain gauges were stocked on the beam axial restraints on flanges and web of the HEB 300 profiles to measure the strains and to derive the stresses and the axial load from the total beam restraint (Figure 68). For the reference test 1 at ambient temperature, strain gauges were located into bolts, at 50 cm from each beam extremity, on the column web and on the steel rebars in the composite slab (Figure 69).

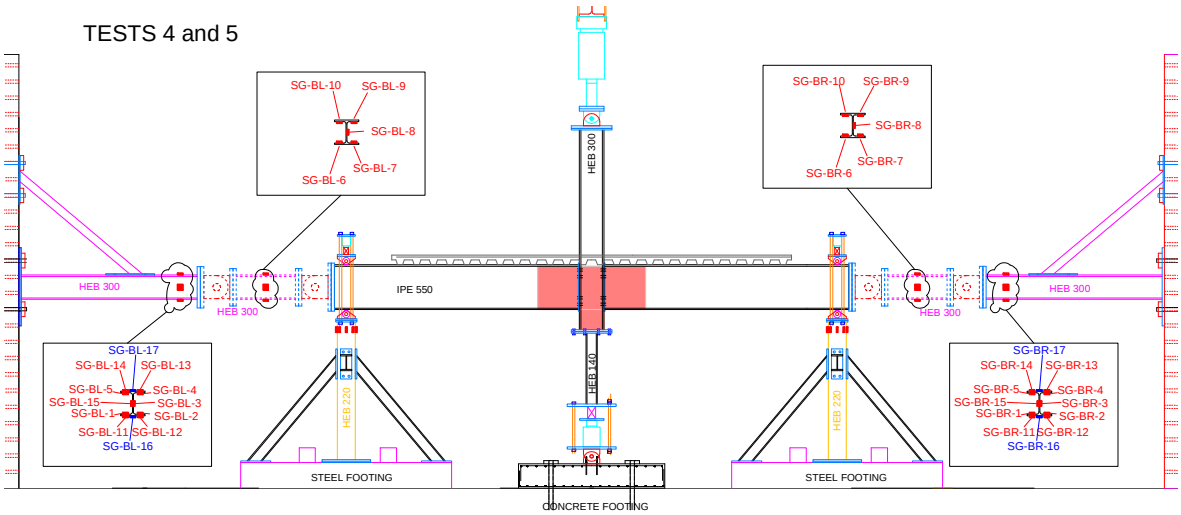

Figure 68. Strain gauges at the beam axial restraints (tests 4 and 5)

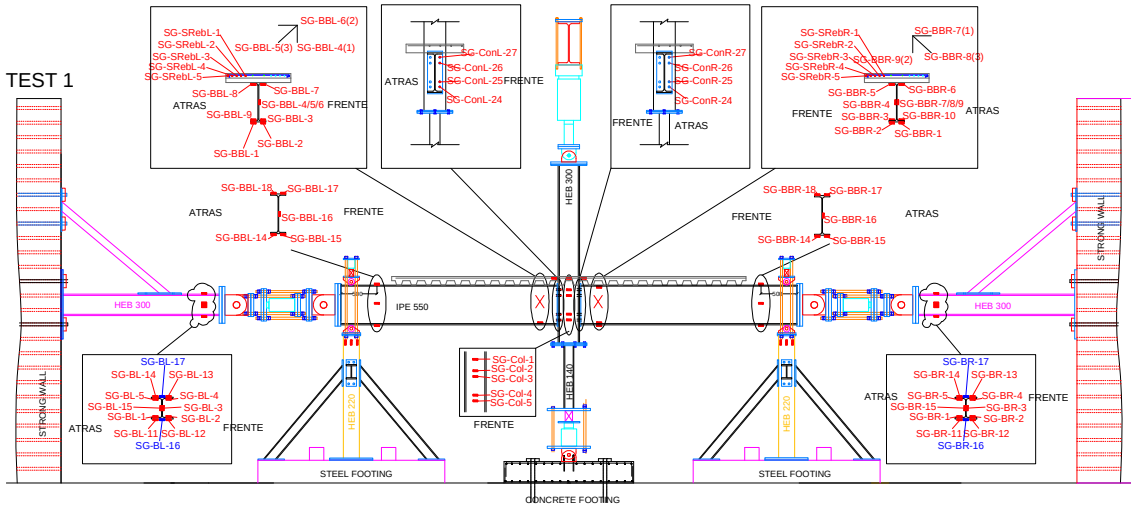

Figure 69. Strain gauges used for the test 1 at ambient temperature

XIII.1.7. Control tests

Control tests were performed in order to determine material properties of the steel joint components and concrete slab for the calibration of the numerical and analytical models against the test results. Detailed results are available in deliverable II, section II.

XIII.1.7.1. Tensile tests of the steel coupons

Mechanical properties of the steel from the beam, the column and the end-plate were defined by 38 tensile coupon tests. From the steel profiles, the coupons were extracted from the webs and flanges, and three tensile tests were performed for each temperature: 20ºC, 500ºC and 700ºC. In the case of the steel end-plate, only two coupons were performed and tested at ambient temperature. Steady-state tests were considered, for which the coupon was heated up to a specific temperature and then tested in tension (constant displacement speed). The yield strength *Re* (MPa), the tensile strength *Rm* (MPa) and the elongation after fracture *A* (%) for each test, were defined according to NP EN 10002-1: 1996 and NP EN 10002-5: 1991. Figure 70 shows the stress-strain curves from the tensile tests performed at 20ºC, 500ºC and 700ºC, respectively for steel coupons extracted from the web and the flanges of the IPE 550 steel profile. Figure 71 show the stress-strain curves from the two tensile tests performed for the end-plate at ambient temperature.

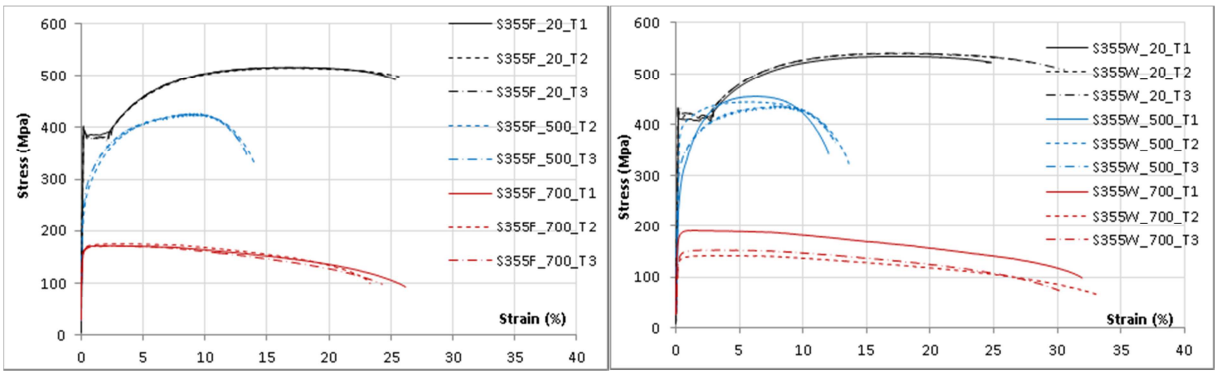

a) b)

Figure 70. Stress-strain curves at 20ºC, 500ºC and 700ºC for steel S355 - IPE 550 (a) flange (F) and b) web (W))

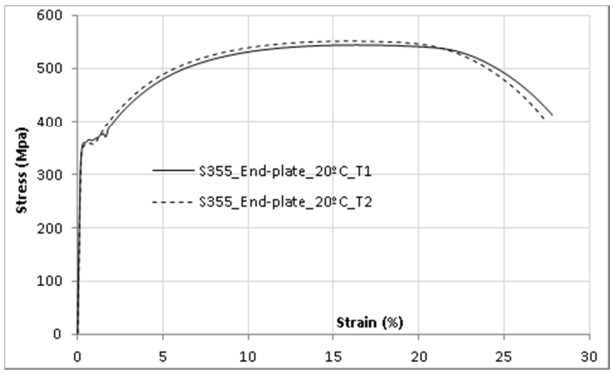

Figure 71. Stress-strain curves at 20ºC for steel S355 – End-plate 15 mm thick

Figure 72 shows the stress-strain curves from the tensile tests performed at 20ºC, 500ºC and 700ºC, respectively for steel coupons extracted from the web and the flange of the HEB 300 steel profile.

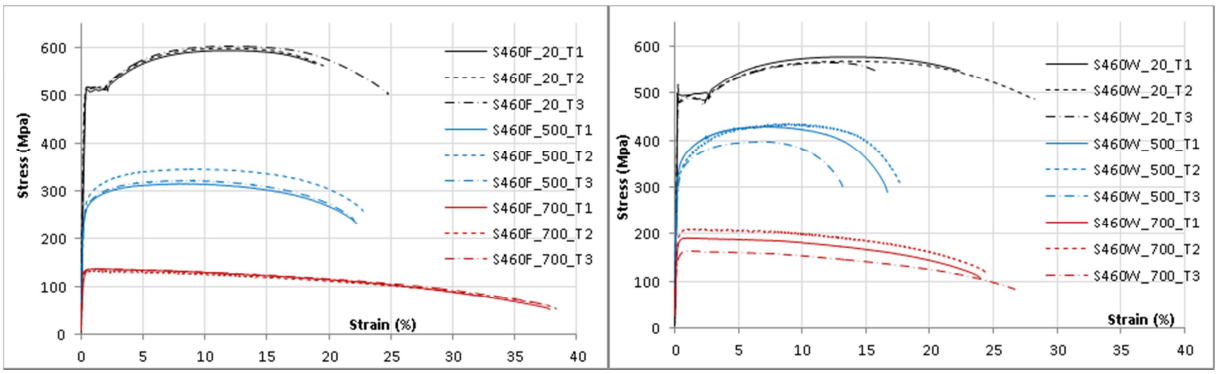

a) b)

Figure 72. Stress-strain curves at 20ºC, 500ºC and 700ºC for steel S460 - HEB 300 (a) flange (F) and b) web (W))

XIII.1.7.2. Tensile tests of the bolts

Mechanical properties of the bolts M30 10.9 were defined by 15 tensile coupon tests. Three tensile tests were performed at ambient temperature, and two tests were performed at each temperature equal to 200ºC, 400ºC, 500ºC, 600ºC, 700ºC and 800ºC. Steady-state tests were performed. Unfortunately, these tests were performed at the end of the project, and results were not used in the calibrations of the numerical and analytical models.

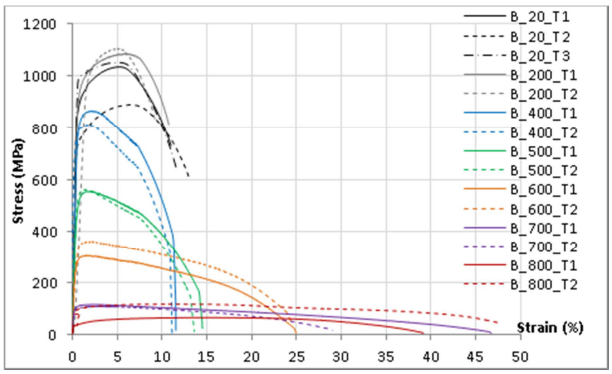

Figure 73. Stress-strain curves of bolts M30 10.9 at 20ºC, 200ºC, 400ºC, 500ºC, 600ºC, 700ºC and 800ºC

XIII.1.7.3. Compression test of the slab concrete

Compression tests on 24 concrete blocks were performed. Three tests were performed after 7 days, 14 days, 28 days and then the day of tests 3, 4, 5, 6 and 7. The concrete properties C25/30 at 28 days were confirmed according to NP EN 206-1 2007: i) the average of each three tests cube strength ($f_{ck,cube}$ = 35 MPa) was higher than the C25/30 characteristic cube strength plus 1 (31 MPa) and was smaller than the C30/37 characteristic cube strength plus one (38 MPa); ii) each individual value was higher than the C25/30 characteristic cube strength minus 4 (26 MPa).

XIII.1.8. Comparisons between the seven experimental tests

In order to simplify the comparisons between tests, only one connection from the joint is taken into account, which is either the connection where bolts failed, or, in case of no bolt failure, the connection the most deformed: left connection for tests 1, 2, 3, 5 and 7 and right connection for tests 4 and 6.

XIII.1.8.1. Summary results of tests 1 to 6

Figure 76 shows the evolution of the connection bending moment *versus* the joint rotation, and Figure 77 shows the total vertical reaction load at the column *versus* the vertical displacement measured at the column top. The hogging bending moment was initially reached during step 1, followed by a variation of this moment during the increase of temperatures in step 2. As described in Section XIII.1.3.1, this initial hogging bending moment should have reach -450 kNm at ambient temperature (test 1) and -236 kNm for the tests at elevated temperatures (tests 2 to 6). The target initial hogging bending moment was well reached in tests 1, 4 and 6, but some difficulties were faced in the laboratory, and this bending moment was higher of around 75% in tests 3 and 5, and lower of 14% in test 2. At the beginning of step 2, reaction loads increased due to the dilatation of the structure; the reaction forces reached a minimum value and the minima hogging bending moments reached around -500 kNm in tests 1, 3, 5 and 6, and around -357 kNm in tests 2 and 4. After that, these reaction loads decreased because of: i) the steel properties degradation due to high temperatures (higher than 600ºC in the webs of the steel beams) in tests 3, 4, 5, and 6; ii) the slight loss of the column support in test 2 due to oil losses in the bottom cylinder (see deliverable II, section II). Beams bottom flanges temperatures reached 500ºC in tests 2 and 4, and 700ºC in tests 3, 5 and 6: Figure 74 shows the temperatures measured during test 2. At about 40 min., during step 2, the temperature increase rate was modified from the maximum rate to 300ºC/hour, which created a peak in temperatures curves. Finally, 500ºC was reached in the beam bottom flanges, whereas the temperature increased faster in the web because of the reduced thickness. Temperatures in beams top flanges were much lower because they were only heated by heat transfer from web, which was reduced by the composite slab protection. During step 3, the temperature was well kept constant in the beam bottom flanges. Concrete temperatures did not rise above 200ºC. The loss of the column was really progressive as the hydraulic jack at the column top imposed a constant displacement rate. Concrete crushing in compression was the first failure observed under sagging bending moment, but this failure was really progressive; first the concrete crushed against the column flanges (Figure 75a), and then the entire slab width failed (Figure 75b, c).

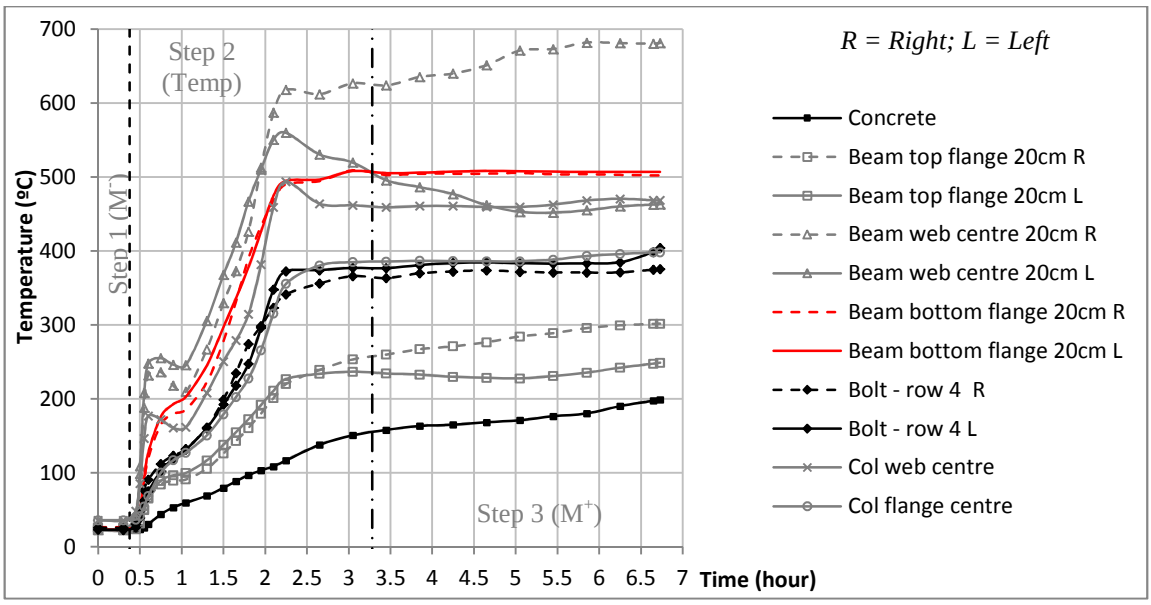

Figure 74. Evolution of the temperatures during test 2

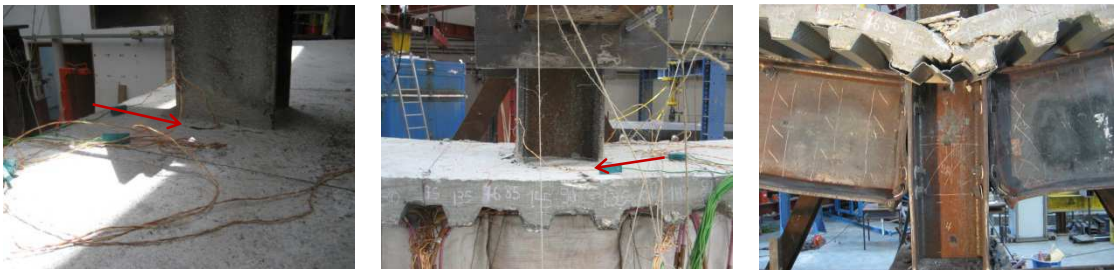

a) b) c)

Figure 75. Concrete crushed: a) against the column flanges; b) along the entire slab width; c) at the end of the test (front view of test 6)

Bolts failures happened in tests 1, 2 and 6 (respectively under 47.5 mrad, 73.6 mrad and 83.3 mrad of connection rotation); the other tests were ended because the maximum vertical displacement of the hydraulic jack at the column top was reached. An "unloading-reloading" was performed at the beginning of the step 3 for tests 3, 4 and 5, and it allowed a better characterization of the elastic stiffness of the joint. In tests 1 and 6, this "unloading-reloading" was not performed because of the difficulties to manually control the spring restraints at the extremities of the beams.

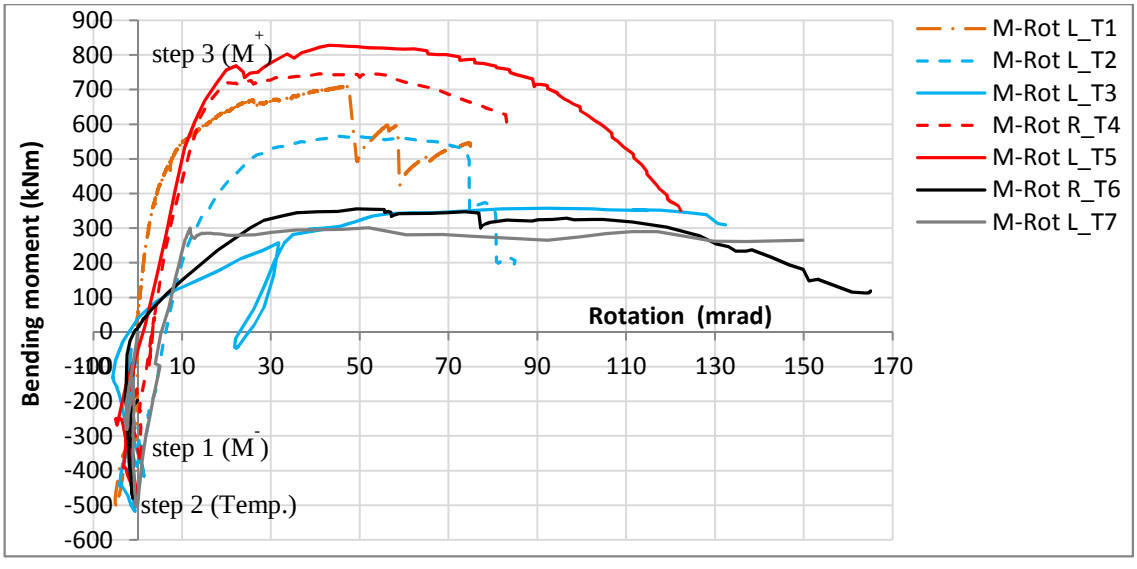

Figure 76. Joint bending moment vs rotation at the connection

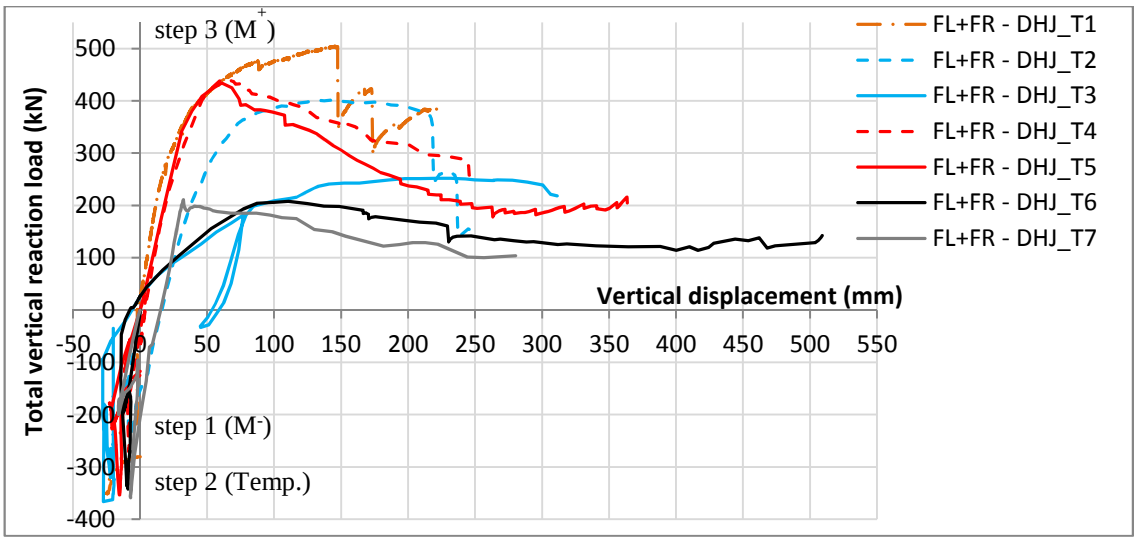

Figure 77. Total reaction load vs vertical displacement measured at the column top

The evolution of the bending moment at the joint *versus* the beam axial load is presented in Figure 78 for tests 1, 4, 5, 6, and 7. In the following comparisons of the results, the test 1 is considered as performed without any restraint to the beam (see § XIII.1.5.2). The restraints were connected to the beams since the beginning of the test. During step 1, the loads and displacements created by the application of the initial hogging bending moment were not enough to develop axial forces to the beams. During step 2 and at the beginning of step 3, the beam extremities were moving outwards and the restraints worked in compression; then compression loads decreased during step 3, and tensile loads were reach at the end of the test 6.

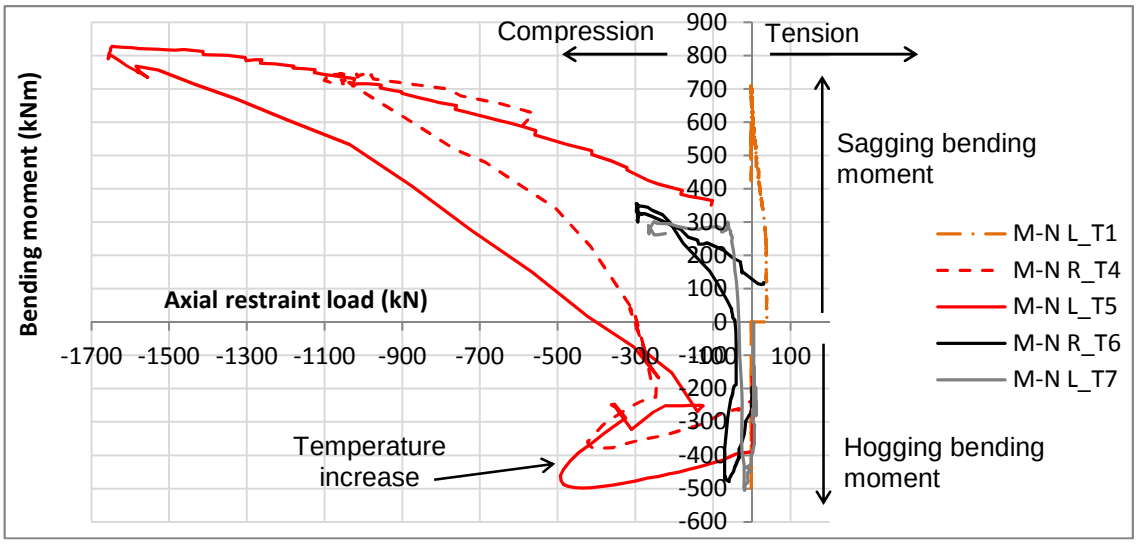

Figure 78. Joint bending moment vs axial loads at the joint

It was observed that the maximum axial compression load was reached: i) for a vertical displacement of the joint varying between 100 mm to 210 mm (Figure 79); ii) once the concrete from the slab was crushed in compression in tests 4 and 5. In test 6, the maximum axial compression load was not reached due to the limitation of the hydraulic system at 300 kN in compression (Figure 80), but it can be assumed that the maximum value would correspond to the 1st bolt failure.

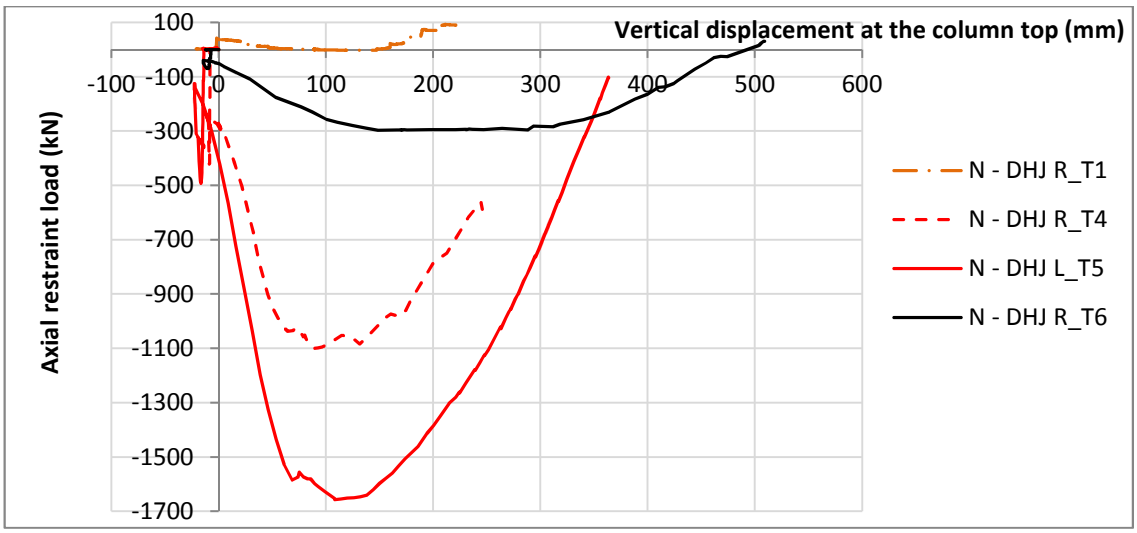

Figure 79. Vertical displacement measured at the column top vs axial loads

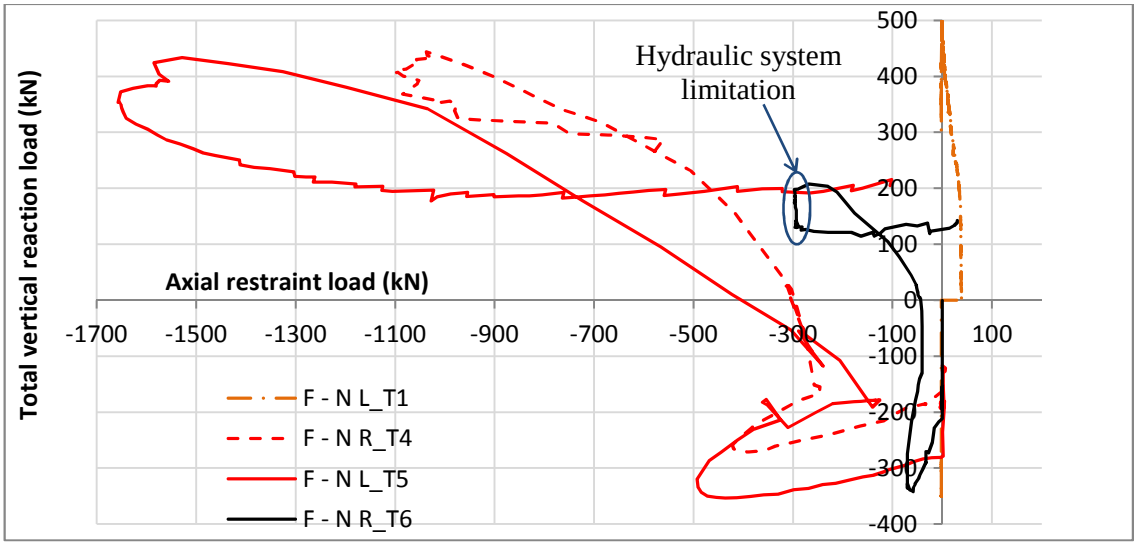

Figure 80. Total reaction load vs axial loads at the joint

Finally, Figure 81 and Figure 82 show the final deformations for tests 1 to 3 (without axial restraint to the beam), and tests 4 to 6 (with axial restraint to the beam). The steel end-plates deformed in the bottom and centre part in all tests, even at ambient temperature, and showed a high ductility. Due to high stresses/deformations, a crack at the base steel end-plate, just above the weld, appeared at the end of the test 1 at ambient temperature. Moreover, the localised deformation mode observed at the steel end-plate centre should happened because of the joint configuration: i) 4 bolt rows and quite a high space between the rows 2 and 3 (260 mm), ii) the end-plate (15 mm) was thinner than the column flange (19 mm), and iii) an initial deformation noticed just after the bolts pre-loading (0.6 mm was measured for the reference test). Moreover, it seems that the beam web was pulling the end-plate due to the sagging bending moment (tensile loads at the bottom part), and the deformation of the end-plate was amplified where it was not linked by bolts to the column flange: in the bottom part and in the centre of the end-plate.

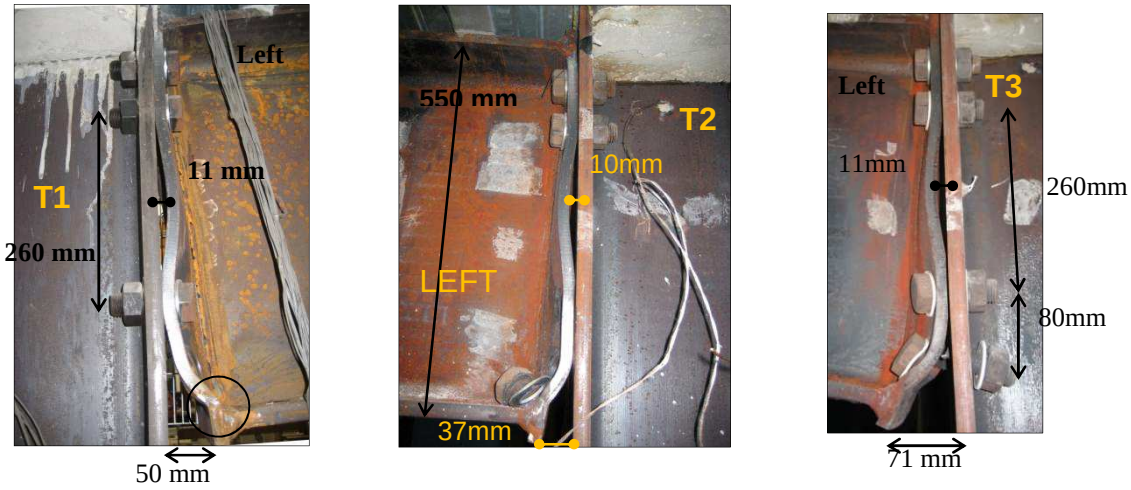

Figure 81. Deformations of the connections for tests 1, 2 and 3

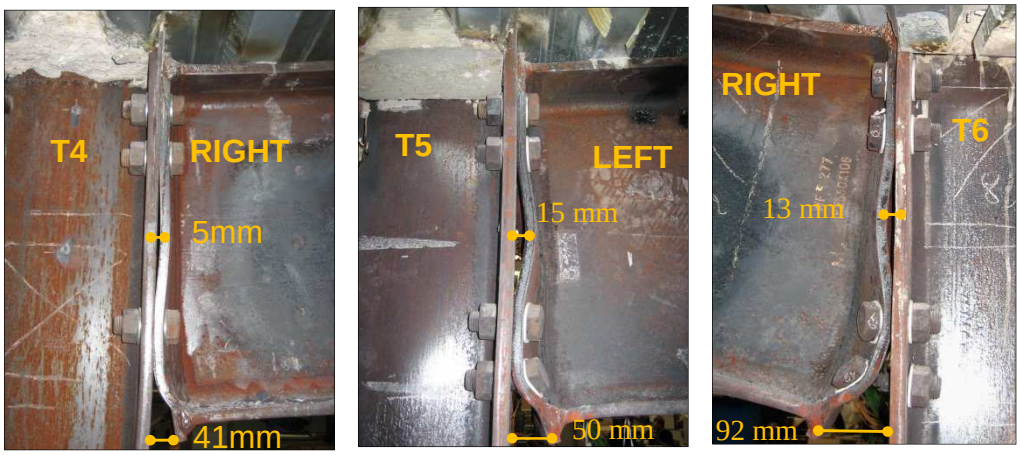

Figure 82. Deformations of the connections for tests 4, 5 and 6

Figure 83 presents the bolts failed in tests 1, 2 and 6. It could be noticed that the bolt failure in test 6 (at around 600ºC) was characterized by a smoother failure than in tests 1 or 2, for which temperatures (respectively 20ºC and around 400ºC) were not yet sufficient to decrease the steel properties.

Figure 83. Bolts failed in tests 1, 2 and 6

XIII.1.8.2. The demonstration test (test 7)

The objective of the demonstration test was to reveal the real behaviour of the sub-frame joint when subjected to a localised fire which leads to the loss of a column. Four main loading steps were defined by: step 1 – Initial hogging bending moment; step 2 – Mechanical loading (constant gravity load of 250 kN); step 3 – 1st increase of temperatures and column loss (400ºC in beams bottom flanges and 800ºC in the bottom column); and step 4 – 2nd increase of temperature and failure of the sub-frame. The bending moment/rotation, load/displacement and bending moment/axial loads curves were presented in Figure 76, Figure 77 and Figure 78, respectively. The hogging bending moment was initially reached during step 1 (-281 kNm). During step 2, the hydraulic jack increased the load at the column top up to reach

+250 kN; however, due to clearances at the column base, the total load at the column reduced from -200 kN to -96 kN, and consequently the hogging bending moment was reduced to -134 kNm. In step 3, the beams were heated up to 400ºC in the bottom flanges, and joint components and column reached lower temperatures (Figure 84); the bottom column was heated up to 800ºC. First reaction loads increased under thermal dilatations effects and reached a maximum value of -359 kN (bending moment equal to -505 kNm); then the bottom column reached its maximum resistance capacity under 578ºC and failed. The failure of the column was really progressive, and was defined as the moment at which the vertical reaction load came back to its initial value at the beginning of the step 3 (95.6 kN). At the end of the step 3, the total load was equal to +211 kN, and the column top came down 25 mm; Figure 85 presents the evolution of the vertical displacements *versus* time. The sagging bending moment increased up to 300 kNm, and the compression axial loads to the beams reached 61 kN.

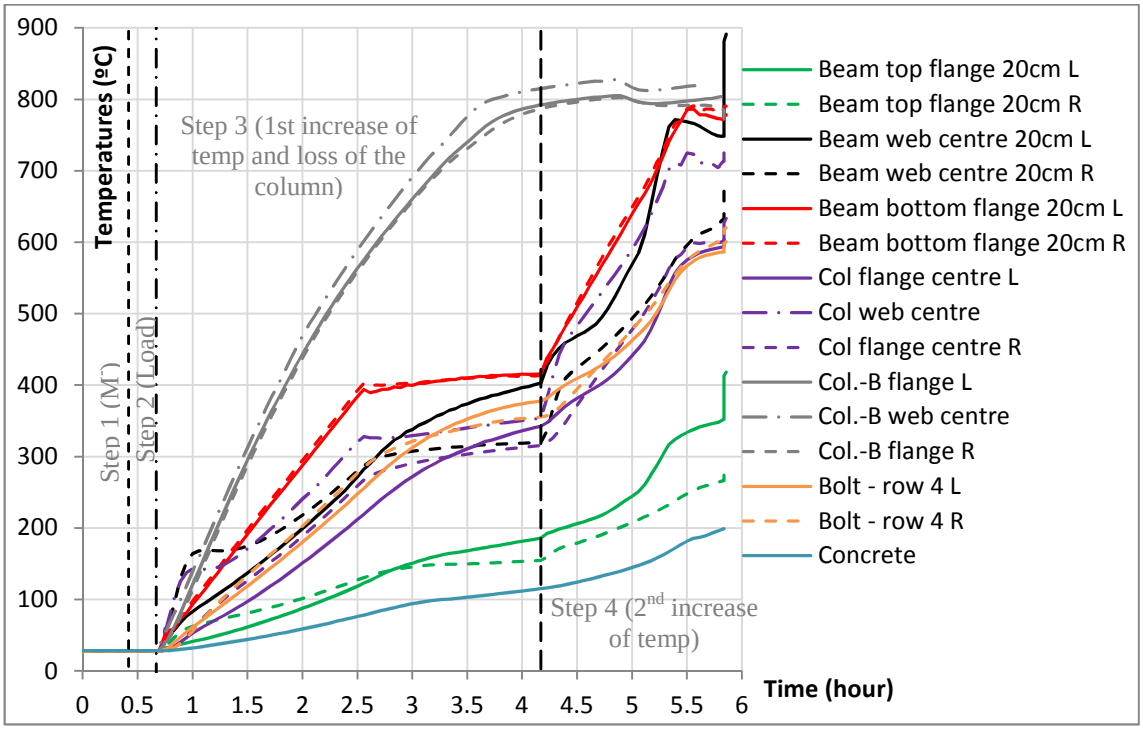

Figure 84. Evolution of the temperatures during test 7 (in beams at 200 mm from the connection, in column centre, in bottom column HEB 140 (Col.-B), in row 4 bolts and in concrete rib in contact with the steel beam)

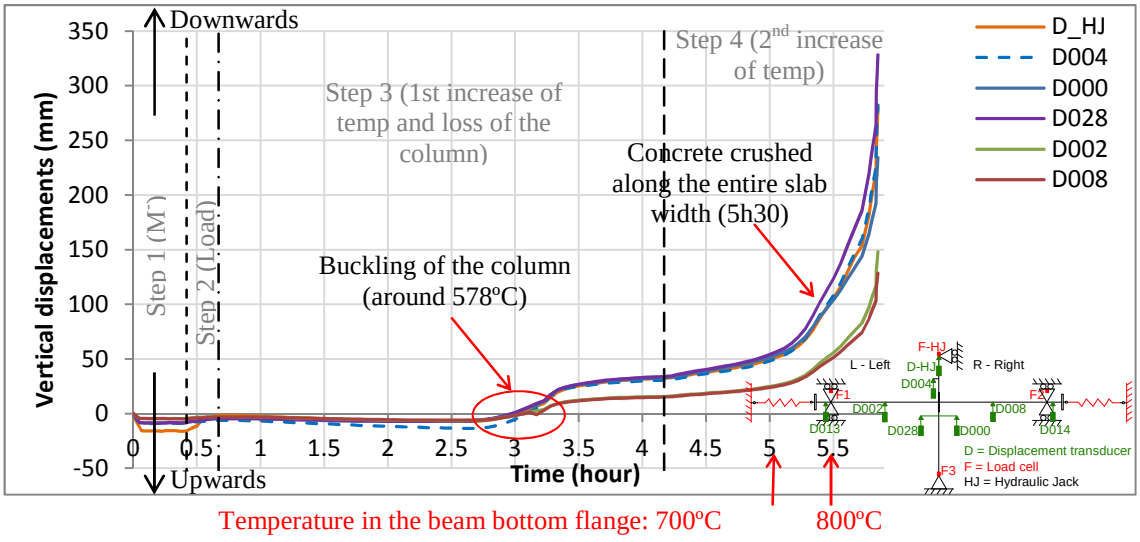

Figure 85. Evolution of the vertical displacements during the entire test 7

During step 4, the temperature in the joint increased under the constant load (250 kN) applied at the top of the column and reached 770ºC in the beam bottom flange: the concrete slab began to crush against

the column flange; the vertical displacement increased faster (Figure 85), and once the concrete slab was completely crushed, beam bottom flanges temperature reached 800ºC and the sub-frame completely failed. The test was stopped at a vertical displacement equal to 280 mm, at 150 mrad and 37 mrad of connection left and right rotations, the total vertical reaction load was 104 kN, and axial loads at the spring restraints were reduced from 266 kN to 222 kN after the concrete crushing. The sagging bending moment was slightly decreased from 290 kNm to 265 kNm. The day after the test, the failure of three bolts from the left connection was observed: two bolts at the row 4 and one bolt at the row 3 (Figure 86a), but the failures were not detected on bending moment/rotation and load/displacement curves. The steel end-plates deformed in the bottom and centre part, and due to high stresses/deformations, a crack at the base steel end-plate, just above the weld, appeared. Figure 86b shows the final deformation of the sub-frame.

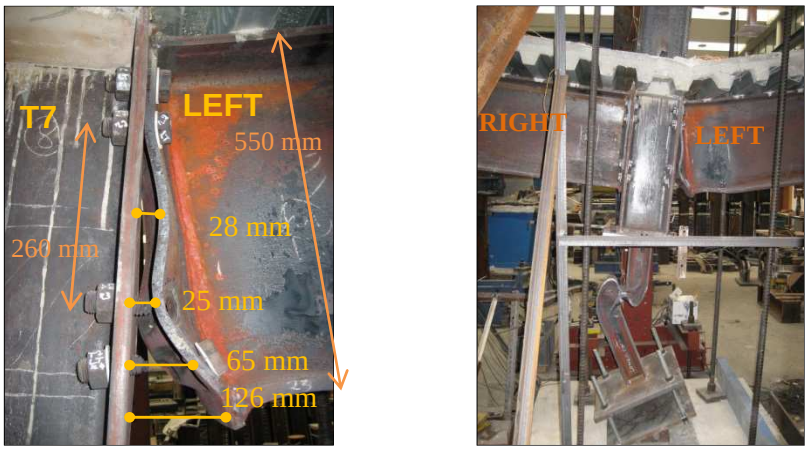

a) b)

Figure 86. a) Deformations of the left connection, and b) final deformation of the frame (test 7)

XIII.1.8.3. Effects of the temperature

In the tests performed without axial restraint to the beam (tests 1, 2 and 3), the maximum reaction load (F_{max}) and the corresponding maximum bending moment (M^{+}_{max}) decreased by 20% at 500ºC, and by 50% at 700ºC. Under these maxima loads, the connection rotation (θ_{M+max}) was more or less equal at 20ºC and 500ºC, but was increased by 97% at 700ºC (Table 9).

Table 9. Comparisons of the results: maximum sagging bending moment M^{+}_{max} (tests 1, 2 and 3)

No axial restraint	**T1**	**T2**	**T3**	**Diff. T1-T2 (%)**	**Diff. T1-T3 (%)**	**Diff. T2-T3 (%)**
Temperature	20ºC	500ºC	700ºC			
M^{+}_{max} (kNm)	710.1	565.0	357.1	-20.4	-49.7	-36.8
Max. vert. load F_{max} (kN)	504.4	401.5	252.0	-20.4	-50.0	-37.2
Vert. displ. (mm)	145.6	143.6	220.3	-1.4	51.2	53.4
Rotation θ_{M+max} (mrad)	46.9	49.5	92.3	5.5	96.6	86.5

In test 1, just after the increase of the jack stroke (performed after the concrete crushing), loads continued to linearly increase, and leaded to a maximum sagging bending moment equal to 710 kNm, which is 21% higher than the theoretical value calculated in Section VII.4.8.3 (588 kNm).

Table 10 presents the initial stiffness of the load/displacement curves (Figure 77) estimated just after the column loss, or at the reloading curve in case that the “unloading-reloading” was performed. It can be observed that the initial stiffness of tests 3 and 6 (700ºC) were much lower than the other ones, but the reloading performed in test 3 showed a higher realistic stiffness (8 kN/mm); unfortunately, the “unloading-reloading” could not be performed in test 6, and the real stiffness is unknown. In comparison to the ambient temperature result (test 1), the effect of the temperature affects the initial

stiffness and decreases it by 36% at 500ºC (test 2) and by 49% at 700ºC (test 3); the initial stiffness was also decreased by 21% between tests 2 (500ºC) and 3 (700ºC).

Table 10. Initial stiffness of the load/displacement curve after the column loss

TEST	Temp. (ºC)	Restraint (kN/mm)	Initial stiffness (kN/mm)	Reloading stiffness (kN/mm)
T1	20	0; 50	15.7	---
T2	500	0	10.1	---
T3	700	0	2.6	8.0
T4	500	Total	13.9	18.5
T5	700	Total	11.3	12.3
T6	700	50	2.9	---
T7	400; 800	50	10.9	---
		Average	11.2	

Table 11 presents the maximum rotations corresponding to the 1st bolt failure (tests 1, 2 and 6) or to the end of the test if no bolt failure was identified (tests 3, 4, 5, 7). In test 1, the first bolt failed for 49 mrad of rotation (503 kN); in test 2, the first bolt failed at 74 mrad of rotation (352 kN), and no bolts were failed at 132 mrad of rotation in test 3 (311 mm of vertical displacement). In comparison to test 1 at 20ºC, the rotation was then increased by 55% at to 500ºC (test 2), and by at least 179% at 700ºC (test 3). The rotation corresponding to the maximum sagging bending moment θ_{M+max} was increased by 64% at the 1st bolt failure in test 2 and by 53% in test 6.

Table 11. Maxima connection rotation for each test, and the corresponding values of the vertical reaction load, axial force, sagging bending moment, and vertical displacement

TEST	Temp. (ºC)	Axial restraint (kN/mm)	Vertical reaction load (kN)	Vert. displ. (mm)	Axial load N (kN)	Bending moment (kNm)	Max. Rotation (mrad)	
T1	20	0; 50	502.5	147.5	-1.3	707.4	47.5	*1st bolt failure*
T2	500	0	375.1	215.5	0.0	527.9	73.6	*1st bolt failure*
T3	700	0	218.1	311.4	0.0	309.1	132.4	*end of the test*
T4	500	Total	253.8	245.8	-588.0	592.6	89.4	*end of the test*
T5	700	Total	204.5	363.8	-104.5	351.1	122.3	*end of the test*
T6	700	50	161.0	229.5	-293.6	343.9	83.3	*1st bolt failure*
T7	400; 800	50	104.1	280.2	-222.0	265.1	149.8	*end of the test (3 bolts failed)*

In tests 4 and 5, during the increase of the temperatures (step 2), the axial and vertical loads increased more in test 5 than in test 4 (Figure 78), due to the higher dilatations under 700ºC. During step 3, for a same axial compression load, the sagging bending moment in test 5 at 700ºC was lower than in test 4 (500ºC) because of the reduced steel properties. In test 5, under the maximum bending moment reached in test 4 (746 kNm), the axial load from the restraint was 58% higher. Table 12 shows that the maximum bending moment reached in test 5 was 11% higher than in test 4; at this point, the vertical reaction load was 5% lower in test 5, but the compression axial restraint was 66% higher; the rotation and vertical displacement were respectively 22% and 15% lower in test 5. Test 5, under higher steel temperatures, reached higher bending moment/axial restraint load than test 4 certainly because of the non-uniform concrete slab thickness in test 5. Indeed, during the concreting of test 5, a support situated near the column (back side) fell down, which created a higher thickness of the slab on this side (the slab

thickness on the front side extremity was 60 mm, whereas the slab thickness on the back side extremity was 100 mm). As the concrete was only slightly heated, the concrete properties were not decreased by temperature, and the compression resistance of the joint was increased by the slab thickness, even under higher steel temperatures.

Table 12. Comparisons of the results: maximum sagging bending moment M_{+max} (tests 4 and 5)

Total axial restraint	**T4**	**T5**	**Difference (%)**
Temperature	500ºC	700ºC	
M^+_{max} (kNm)	746.4	828.0	10.9
Vert. load F_{max} (kN)	355.6	336.5	-5.4
Axial load N (kN)	-990.7	-1646.7	66.2
Vert. displ. (mm)	154.7	132.2	-14.5
Rotation θ_{M+max} (mrad)	54.9	43.0	-21.5

Tests 4 and 5 are also compared together in relation to the maximum vertical reaction load (Table 13). It can be observed that both reached the same vertical reaction load, under more or less the same vertical displacement and rotation, but with more 47% of compression load from axial restraints in test 5 (700ºC).

Table 13. Comparisons of the results: maximum vertical reaction load F_{max} (tests 4 and 5)

Total axial restraint	**T4**	**T5**	**Difference (%)**
Temperature	500ºC	700ºC	
M^+ (kNm)	719.6	756.6	5.1
Max vert. load F_{max} (kN)	443.6	433.6	-2.3
Axial load N (kN)	-1037.6	-1528.2	47.3
Vert. displ. (mm)	64.4	61.0	-5.2
Rotation θ_{Fmax} (mrad)	20.6	19.9	-3.3

XIII.1.8.4. Effect of the axial restraints to the beams

Tests 2 and 4 were both performed under 500ºC in the beams bottom flanges, respectively without any axial restraint to the beam and with total axial restraint to the beam. In test 4, the maximum reaction load was 11% higher (Table 14), the vertical displacement under maximum reaction load was 55% lower, the bending moment was 27% higher and the rotation was 58% lower than in test 2.

Table 14. Comparisons of the results corresponding to the maximum vertical reaction load F_{max} (tests 2 and 4)

500ºC	**T2**	**T4**	**Difference (%)**
M^+ (kNm)	no	total	
Max vert. load F_{max} (kN)	565.0	719.6	27.4
Axial load N (kN)	401.5	443.6	10.5
Vert. displ. (mm)	0.0	-1037.6	---
Rotation θ_{Fmax} (mrad)	143.6	64.4	-55.2
M^+ (kNm)	49.5	20.6	-58.4

The maximum bending moment reached 565 kNm in test 2, whereas in test 4, the maximum bending moment was increased by 32%, for a rotation only 11% higher (Table 15).

In test 2, the first bolt failed at 74 mrad of joint rotation (216 mm of vertical displacement). Under the same rotation in test 4, the total reaction load was 17% lower, the bending moment was 32% higher and

the axial compression load restraint was equal to 773 kN. So, due to the compression load from the axial restraint to the beam, the joint was able to resist to a higher sagging bending moment without any bolt failure. Indeed, the compression load from the axial restraint combined with sagging bending moment, moved the neutral axis of the connection downward, allowing the development of additional compression loads in the concrete slab, and reduction of the tensile loads in the bottom bolt rows. Once the concrete crushed against the column slab and along the entire slab width, tests 4 and 5 were still able to continue to deform without failure: between the maximum sagging bending moment and the end of the test, the rotation increased by 113% in test 4 and by 184% in test 5.

Table 15. Comparisons of the results: maximum sagging bending moment M^{+}_{max} (tests 2 and 4)

500ºC	**T2**	**T4**	**Difference (%)**
Restraint	no	total	
M^{+}_{max} (kNm)	565.0	746.4	32.1
Vert. load F_{max} (kN)	401.5	355.6	-11.4
Axial load N (kN)	0.0	-990.7	---
Vert. displ. (mm)	143.6	154.7	7.7
Rotation θ_{M+max} (mrad)	49.5	54.9	10.8

Between tests 3 and 6, the maximum bending moment (Table 16) was not affected by the axial restraint to the beam (difference of 0.5%); however, the corresponding rotation was 40% lower in test 6. Between tests 3 and 5, the maximum bending moment increased considerably (by 132%); the corresponding rotation was 53% lower in test 5. The same conclusions can be made for tests 5 and 6.

Table 16. Comparisons of the results: maximum sagging bending moment M^{+}_{max} (tests 3, 5 and 6)

700ºC	**T3**	**T6**	**T5**	**Diff. T3-T5 (%)**	**Diff. T3-T6 (%)**	**Diff. T5-T6 (%)**
Restraint	no	50 kN/mm	total			
M^{+}_{max} (kNm)	357.1	355.5	828.0	131.8	-0.5	132.9
Vert. load F_{max} (kN)	252.0	198.0	336.5	33.5	-21.4	70.0
Axial load N (kN)	0	-297.3	-1646.7	---	---	453.8
Vert. displ. (mm)	220.3	148.7	132.2	-40.0	-32.5	-11.1
Rotation θ_{M+max} (mrad)	92.3	55.1	43.0	-53.4	-40.3	-22.0

The effect of the axial restraint affects the initial stiffness and increases it by 83% at 500ºC (from test 2 to test 4) and by 54% at 700ºC (from test 3 to test 5).

XIII.1.9. References related to the WP2 appendix

Abaqus Theory Manual & Users Manuals (2007), Version 6.7, Hibbitt, Karlsson and Sorensen, Inc. USA.

EN 1991-1-2:2002, “Eurocode 1: Actions on structures – Part 1-2: General actions – Actions on structures exposed to fire”, European committee for standardization, November 2002.

EN 1992-1-2:2004, “Eurocode 2: Design of concrete structures – Part 1-2: General rules – Structural fire design”, European committee for standardization, December 2004.

EN 1993-1-2:2005 – “Eurocode 3: Design of steel structures – Part 1-2: General rules – Structural fire design”, European committee for standardization, April 2005.

EN 1994-1-1:2004. “Eurocode 4: Design of composite steel and concrete structures – Part 1-1: General rules and rules for buildings”. European committee for standardization, December 2004.

Jaspart et al. (2009). “Deliverable I: Definition of the problem and selection of the appropriate investigation ways”, Robustness of car parks against localised fire, Grant Agreement Number RFSR-CT-2008-00036.

NP EN 10002-1 (2006). “Metallic materials – Tensile testing – Part 1: Method of test at ambient temperature”, Instituto Português da Qualidade.

NP EN 10002-5 (2005). “Metallic materials – Tensile testing – Part 5: Method of test at elevated temperature”, Instituto Português da Qualidade.

NP EN 206-1:2007, “Concrete – Part 1: Specification, performance, production and conformity”, Norma Portuguesa, Instituto Português da Qualidade, Portugal, 2007.

XIII.2. Appendix for WP3 – Detailed modelling of reference car park under selected fire scenario

This appendix presents a detailed numerical study on the reference car park subject to the proposed localised fire scenario. The reference car park is modelled using reduced sub-frames under the framework of the multi-level modelling approach. In order to capture the response of the reference structure as accurately as possible with a comprehensive consideration of structural ductility supply for robustness assessment, detailed structural analysis is performed through employing a realistic temperature distribution obtained from detailed heat transfer analysis, and the nonlinear behaviour of joints is comprehensively considered.

XIII.2.1. Verification of multi-level modelling approach

Three modelling levels (A, B and C) can be generally employed for the current fire scenario, as shown in Figure 87. At level A, consideration is given to a whole system of the influenced sub-structure with appropriate boundary conditions representing the surrounding cool structures. Provided that the upper ambient floor systems have similar structure type and applied loading, the assessment model can be simplified to level B, where a reduced model consisting of the fire affected floor-column system and the upper ambient floor system are considered. At this level, the two systems (i.e. fire and ambient) are investigated separately. The derived characteristics of the ambient floors can be incorporated into a nonlinear ‘spring’ applied at the top of the fire-affected floor system. Then emphasis is given to the behaviour of the fire affected floor system with the added spring. Finally, at level C, planar effects within the floor slab are ignored, and grillage models with composite beams are considered instead. The effective width of the slab flange can be obtained through Eurocode 4, 2004 considering shear lag, and the ribs can be ignored in the slab flange along the perpendicular direction.

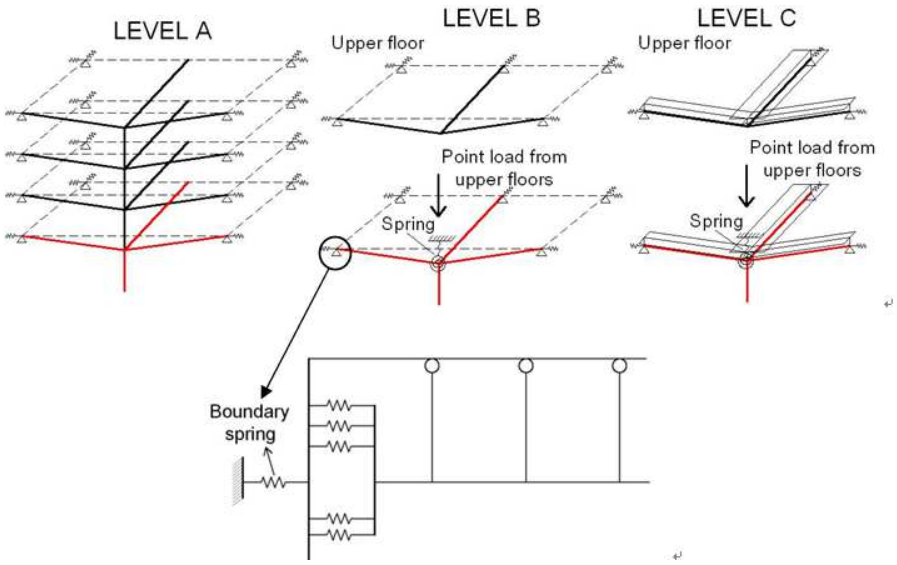

Figure 87. Illustrative descriptions of three model levels

In order to verify the accuracy of the proposed model reduction procedure, a four-storey steel-framed composite structure is established in ADAPTIC, as shown in Figure 88. Joint details are ignored in the model, and beams and columns are assumed to be rigidly connected. All the boundary springs are considered as fully restrained. It is assumed that the internal column at the ground floor experiences a uniform increase in temperature, and this temperature reduces linearly from the column top to room temperature 3m away from the column within the connected steel beams. The slab is considered as fully protected and remains under ambient conditions throughout the heating procedure. This model is then reduced to a level C model comprising the fire floor system and an additional spring. The downward and upward stiffness of one ambient floor is given in Figure 89. In ADAPTIC, the spring is modelled using an element that is capable of simulating the force-displacement relationships with multi-linear approximations. The loads exerted onto the reduced model include a 5kN/m^2 UDL, a point load from the upper three ambient floors and the subsequent thermal load.

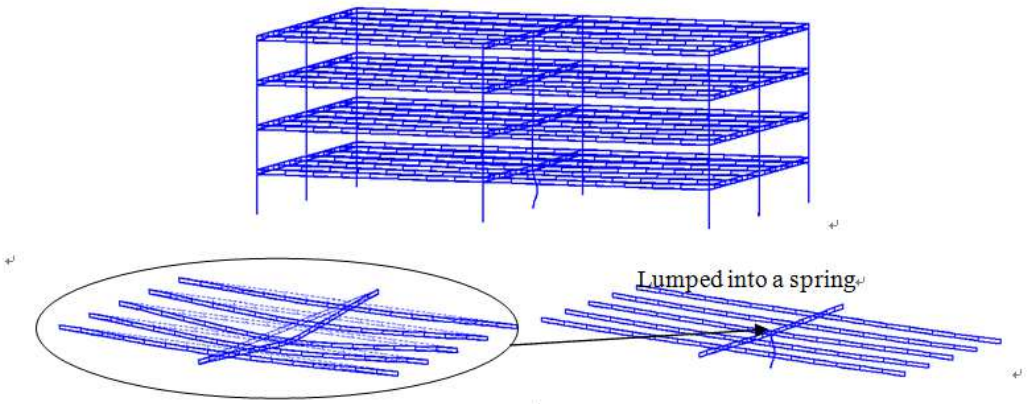

Figure 88. Deflection shape of ADAPTIC model with internal column at 1000ºC

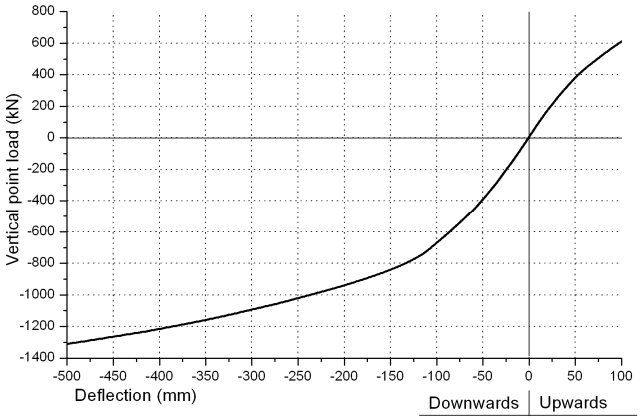

Figure 89. Response of one ambient floor

Figure 90 presents the vertical displacement at the column top for the 4-storey model as well as the reduced system model, while Figure 91 provides the column axial force ratio P_t/P_0 from the two models, where P_t is the axial force of the heated column, and P_0 is the initial column axial force under the ambient condition. The peak column axial force ratio P_t/P_0, the maximum floor deflection, and the critical temperature of the two levels of the models are listed and compared in Table 17, where the critical temperature is defined at the instant when the column internal axial force returns back to its initial value under ambient temperature. It is found that the responses of the two models are very close, which verifies that a reduced system model is capable of capturing the behaviour of the structures subject to localised fire with sufficient accuracy compared with more complex multi-storey models, provided that the response of upper ambient floors is accurately modelled. Therefore, in the ROBUSTFIRE project, reduced substructure models (Levels B and C) are employed for simulating the reference building.

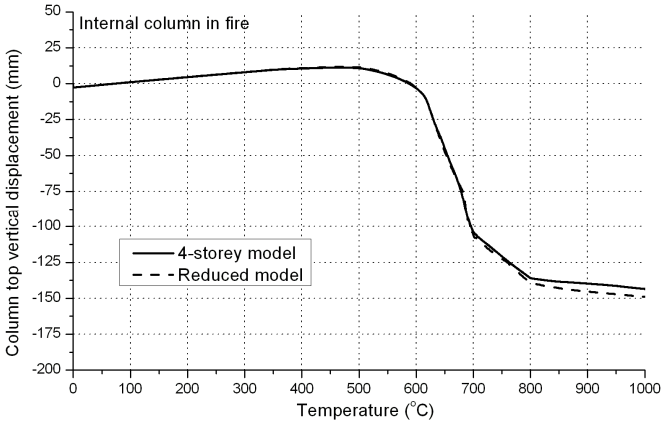

Figure 90. Variation of vertical displacement at column top

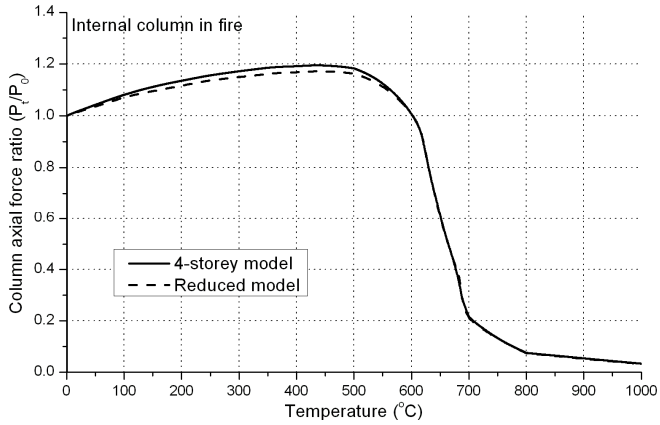

Figure 91. Variation of column axial force

Table 17. Comparison of key results between two models

Structural response	Full 4-storey model	Reduced system model	Discrepancy
Maximum column axial force ratio P_t/P_0	1.195	1.172	1.92%
Vertical deflection at 1000°C(mm)	143.5	148.9	3.76%
Critical temperature (°C)	601.8	602.5	0.12%

XIII.2.2. Joint modelling, joint failure criteria, and system failure criteria

The component method is employed for joint modelling in the sub-frame model considered in ADAPTIC. The bolt-rows are represented by discrete spring elements, and these are connected by rigid links. The axial springs are defined in terms of stiffness and resistance which are obtained from the characteristics of the corresponding components. In the current model, bilinear curves are employed to model the force-deformation response of each component.

Figure 92 presents the component model developed for the major axis flush end-plate joints. For the four internal bolt-row spring series, the axial property in tension is contributed from four components, namely, column web in tension (cwt), column flange in bending (cfb), bolt in tension (bt), and end-plate in bending (epb). The compressive characteristic for the inner springs is determined by the resistance of the column web in compression (cwc). The two outer spring series are free to be pulled in tension, but in compression the resistance and stiffness are contributed from the beam web/flange in compression (bwfc). Where column web stiffeners are added, the stiffness of the column web in compression (cwc)

can be considered as infinite. Moreover, the column web in shear (cws) is represented by applying an additional spring at the bottom flange of the beam.

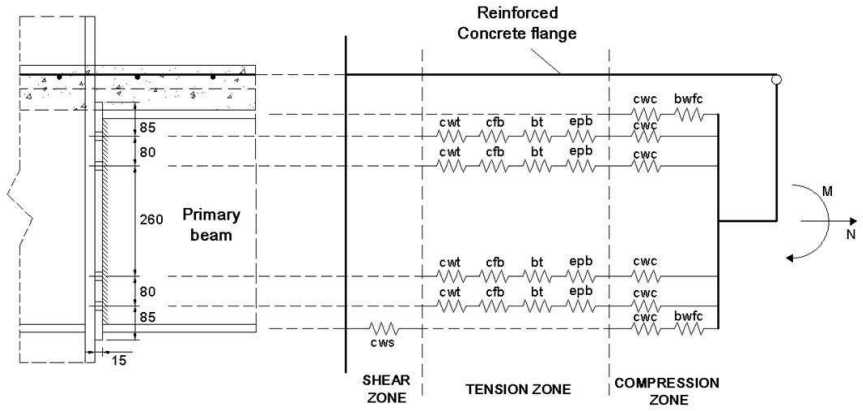

Figure 92. Component model for major axis beam-to-column joint

Minor axis beam-to-column and beam-to-beam joints are mainly designed for resisting shear force, where composite action is not considered in the design. Figure 93 illustrates the mechanical model of the minor axis beam-to-column and beam-to-beam joints. The axial property in the tension zone is contributed from five components, namely, bolts in tension (bt), bolts in shear (bs), angle plate in bending (ab), angle plate in bearing (abr), and beam web in bearing (bwbr). The compressive characteristics for the four inner spring series depend on the properties of bolts in shear (bs), angle plate in bearing (abr), and beam web in bearing (bwbr). The two outer springs are free to be pulled in tension, but in compression the resistance and stiffness are contributed from the beam web/flange in compression (bwfc) and column web in bending (cwb). Moreover, two additional contacts element are adopted to model the 10mm gap between the beam flanges and the column/beam web. The gap between bolts and bolt-holes and the slip friction between bolts and plates are not considered in this component model.

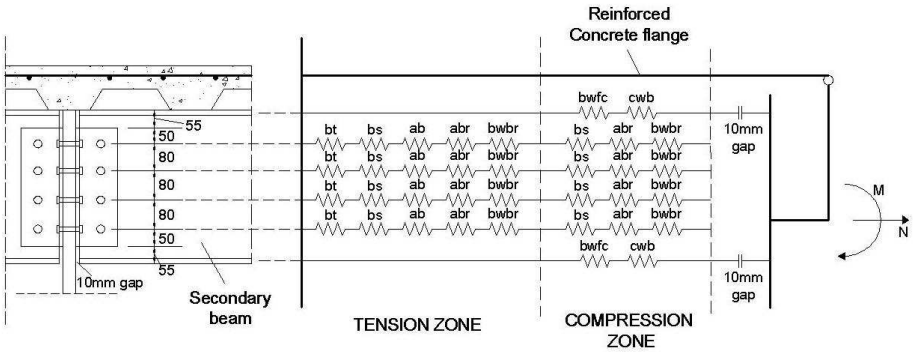

Figure 93. Component model for major axis beam-to-column and beam-to-beam joints

Failure criteria are proposed for the considered joints in this project. A joint is deemed to fail when any of the following conditions are met:

1) The deformation capacity of any steel joint component proposed by Fang et al., 2011 is exceeded.

2) An overall deformation limit of 35mm is exceeded for bolt-rows in cleat joints, or a limit of 25mm is exceeded for bolt-rows in end-plate joints (Owens and Moore, 1992; Jarrett, 1990; Vlassis et al., 2008).

3) For composite joints, the rupture deformation of reinforcement bars based on Anderson et al., 2000 is exceeded.

4) The overall shear force transferred by joints surrounding a column exceeds the overall shear resistance.

Utilising the joint failure criteria defined above, failure definition of the system is determined. Recent research (Vlassis *et al.*, 2009) indicated that the collapse of even one floor can cause severe damage on the floor below for typical existing steel-framed composite constructions, thus triggering progressive collapse. Therefore, the definition of safe structure in this project is based on the avoidance of collapse in any of the affected floors. In other words, structural failure/progressive collapse occurs when the deformation of either the fire affected floor or the upper ambient floors exceeds their respective ductility capacity. In this respect, the failure of any floor system is attributed to the ductility failure of any surrounding ambient joint on that floor, thus failure criteria are defined in terms of whether the ductility limits of the joints are exceeded. If the surrounding ambient joints have sufficient resistance, but the joints directly exposed to fire fail first, the structure is still deemed safe. The defined failure criteria in this study should be on the conservative side, because residual resisting mechanism (e.g. membrane action) may be maintained by the slab after failure of the surrounding joints. Based on this definition of structural failure, the load-deflection response of the spring representing one typical ambient floor with the 2D full slab and the grillage slab is given in Figure 94, where the failure mode of the ambient floor systems is found to be governed by the rupture of ambient joint rebars under hogging moment.

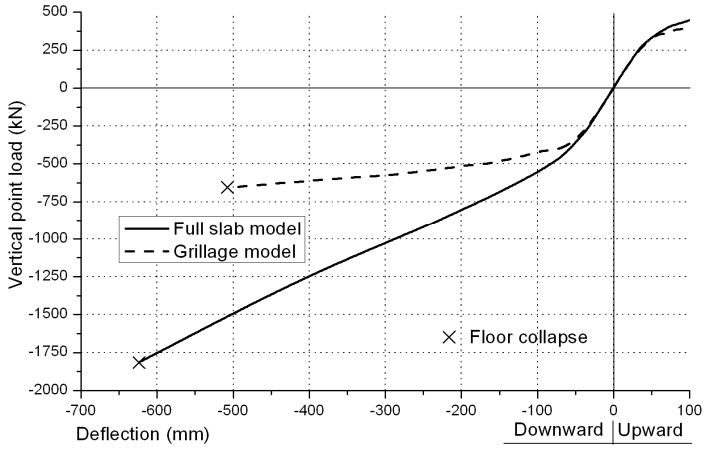

Figure 94. Ductility supply of spring representing one ambient floors

XIII.2.3. Structural robustness assessment

It is recalled that four 'V3 class' cars parking around the internal column is considered as the fire scenario in this project. The interval of the fire spreading from one car to another/other car/s is 12 minutes, and the history of the heat flux on the surfaces of the structural members (e.g. steel beams and composite slab) are captured at 3 minute intervals using the method of Hasemi et al., 1995. The vertical distance between the fire origin and the ceiling is 2.4m, and the fire is assumed to occur at the floor levels 1, 5, or 8.

XIII.2.3.1. Fire at floor level 1

The deflection of the fire affected floor for the grillage model and the full slab model during the considered fire scenario at the ground floor is shown in Figure 95. The structural behaviour predicted by the 2D full slab model shows that buckling of the fire affected column occurs at around 25minutes (column temperature of around 600°C), but this does not directly lead to overall failure of the system, which is largely attributed to the additional resistance provided by the seven ambient floors above the fire affected floor; therefore, the vertical floor deflection is arrested and then stabilized at approximately 300mm without exceeding the ductility supply offered by joints. The corresponding stabilised deflected shape after column buckling of floor level 1 is illustrated in Figure 96.

After column buckling, shear failure (punching shear) of the fire affected beam-to-column joint is observed at a time of 30 minutes. The corresponding failure temperature of the joint and column is 741°C, under which condition the overall shear force resisted by the four fire affected beam-to-column steel connections exceeds their overall elevated temperature shear capacity, as explained in Figure 97. In the current mode, punching shear is assumed to occur when the shear resistance of all the connection surround the internal column is exceeded by the overall shear force, and it is simulated artificially by

abruptly removing the resistance of fire affected connections completely. Figure 97 shows that before the buckling of the column, the fire affected beam-to-column connections are subjected to significant shear forces, but no shear failure is found due to the limited reduction of their shear capacity. When the column buckles, the upper ambient floors have sufficient vertical load resistance to 'pull up' the fire affected floor with a stabilized deflection of 300mm, such that in effect the buckled column can be seen to continue to provide the vertical resistance. In this case the shear force transferred to the upper ambient structure through the steel beam-to-column connections stabilizes at around 600kN (but less than the initial ambient value of 800kN). As the temperature keeps increasing, the shear capacity of the fire affected beam-to-column joint is further reduced, and when it drops below the transferred shear force, first joint failure of the system is triggered by means of punching shear. Initiated by the joint shear failure, the fire affected floor is detached from the upper ambient floors. The final deflection of the individual fire affected floor is then arrested at 740mm but still with sufficient ductility supply provided by the surrounding ambient joints. Since no successive joint failure is observed after the first joint failure (punching shear), progressive collapse of the structure is prevented.

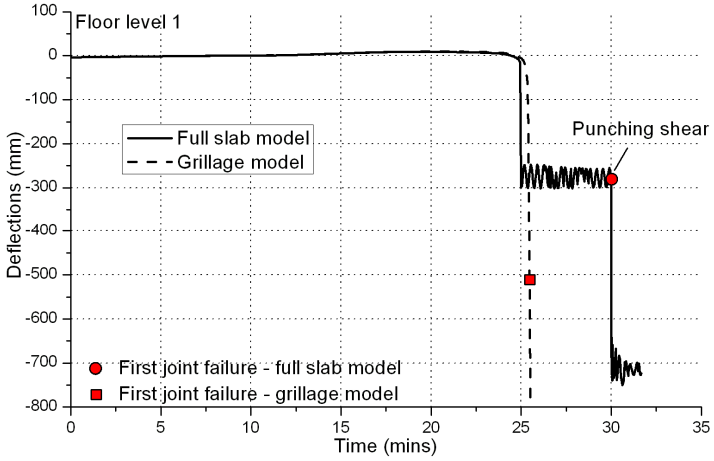

Figure 95. Deflection of fire affected floor for fire at floor level 1

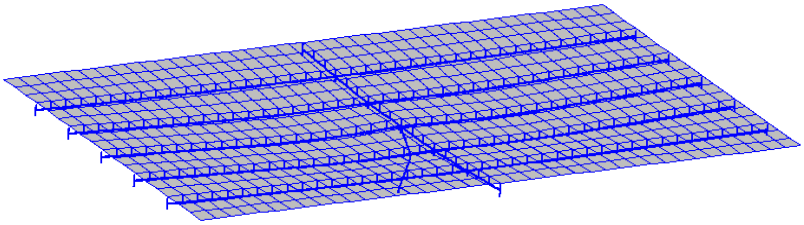

Figure 96. Deflected shape of floor level 1 at time = 25m00s (full slab model)

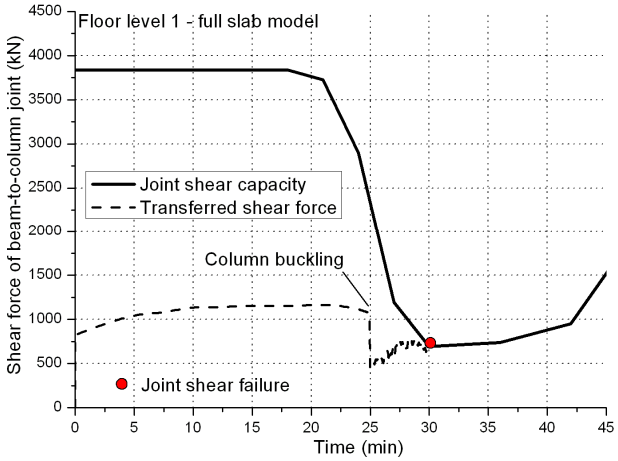

Figure 97. Shear response of fire affected joint for fire at floor level 1 (full slab model)

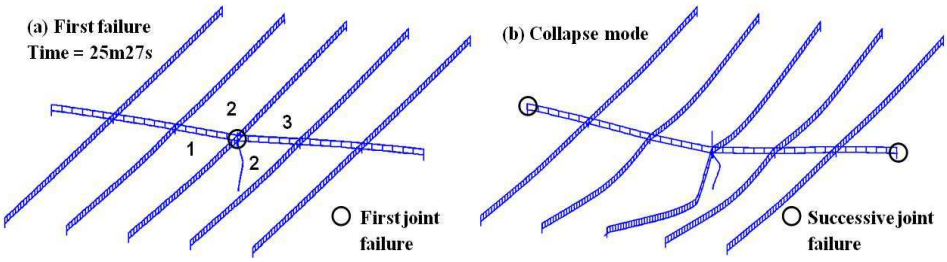

Figure 98. First and successive joint failures of grillage model for fire at floor level 1

On the other hand, the grillage model predicts a less desirable robustness response. Figure 98 illustrates the first failure and the successive collapse mode of the grillage model subject to vehicle fire affecting floor level 1. First joint failure is observed at a time of 25 minutes and 27 seconds in the fire affected major axis beam-to-column joint under sagging moment along with the buckling of the fire affected column, where the elongation of the lowest bolt-row (furthest from the centre of compression) exceeds the maximum limit of 25mm. Soon afterwards, successive joint failure is directly triggered in the surrounding ambient major axis beam-to-column joints due to the ruptures of reinforcement rebar. This progressive collapse mode is a typical 'double-span' failure mechanism which is largely due to the buckling of the fire affected column and insufficient upper ambient floor resistance.

XIII.2.3.2. Fire at floor level 5

Employing the obtained temperature distribution onto the structural model, the deflection of the fire affected floor for the grillage model and the full slab model during the considered fire scenario at floor level 5 is shown in Figure 99.

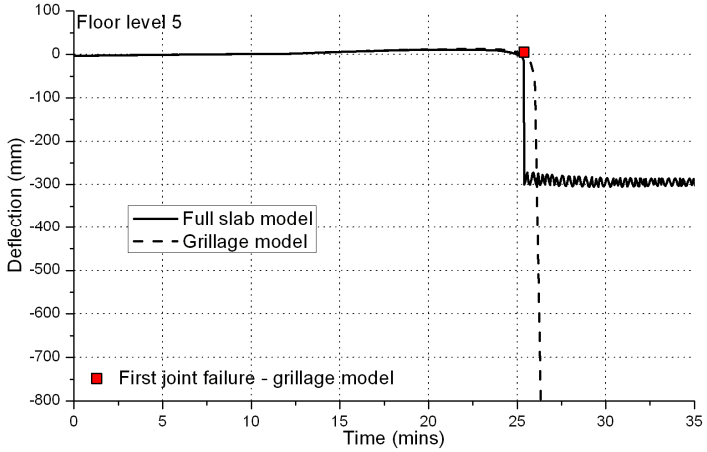

Figure 99. Deflection of fire affected floor for fire at floor level 5

With respect to the full slab model, no joint failure is observed at floor level 5 throughout the whole fire. The fire affected column starts to buckle at a time of 25 minutes and 25 seconds (column temperature of 572°C), where due to sufficient load redistribution capacity of the structural system, a stabilized floor mid-span deflection of about 300mm is maintained. The stabilised deflected shape after column buckling of floor level 5 is illustrated in Figure 100. As the temperature continues to increase, the overall shear capacity of the four fire affected beam-to-column steel connections decreases to around 18% of the ambient capacity at a time of 30 minutes where the peak temperature is achieved, but no shear failure (punching shear) is observed at the fire affected floor, as illustrated in Figure 101. Therefore, sufficient robustness is exhibited of the reference structure subject to fire at floor level 5.

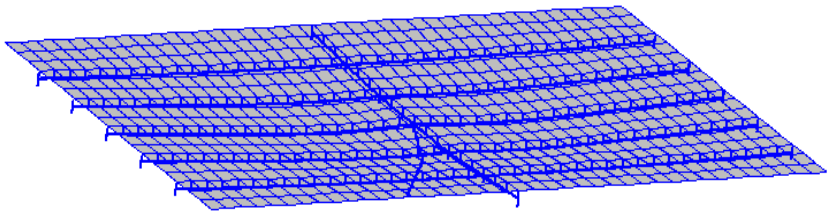

Figure 100. Deflected shape of floor level 5 at time = 25m25s (full slab model)

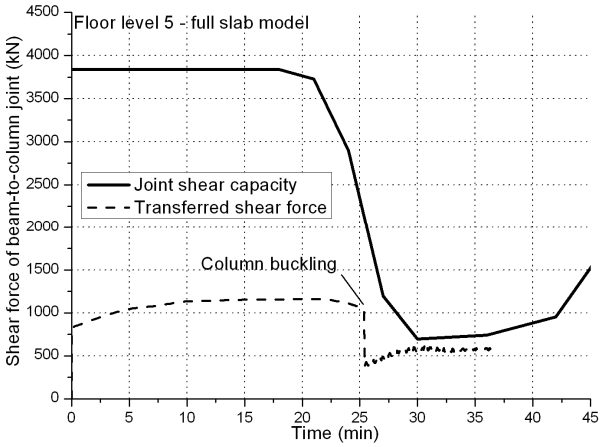

Figure 101. Shear response of fire affected joint for fire at floor level 5 (full slab model)

On the other hand, for the grillage model subject to fire at floor level 5, a poorer performance is observed. Figure 102 shows the first joint failure and the successive collapse mode of the grillage model. The first joint failure is observed at a time of 25 minutes 20 seconds in the fire affected minor axis beam-to-column joint under hogging moment, where the elongation of the highest bolt-row exceeds the maximum limit of 35mm. This is a typical 'single-span' failure type which is due to insufficient ductility offered by the fire affected joint (subject to hogging moment) supporting a single-span beam when the supported fire affected column still maintains its resistance. Successive joint failure is found in the ambient minor axis beam-to-column joints located at the other end of the secondary beam, and at the same time, the fire affected column starts to buckle. The structure exceeds its robustness limit state due to insufficient ductility supply provided by the surrounding ambient joints very soon after the first joint failure. Clearly, the less robust response obtained by the grillage model compared with the full slab model is mainly due to the neglect of 2D slab effects that can greatly contribute to the vertical resistance of floor systems.

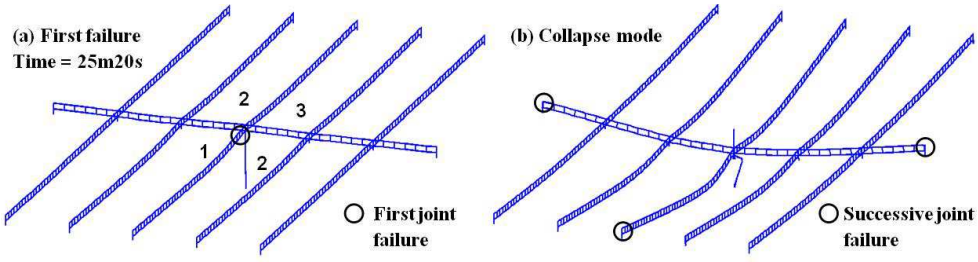

Figure 102. First and successive joint failures of grillage model for fire at floor level 5

XIII.2.3.3. Fire at floor level 8

The considered sub-structural model for floor level 8 is only comprised of the fire affected floor system without the spring representing upper ambient floors. This is different from the models of the other two fire cases at floor levels 1 and 5 where the resistance offered by the upper ambient floors can be relied on. The floor deflections for the grillage model and the full slab model during the considered fire scenario are shown in Figure 103.

For the structural response predicted by the full slab model, first joint failure is observed at a time of 27 minute 10 seconds along with column buckling in the fire affected major axis beam-to-column joint

under sagging moment, which is governed by the 25mm limit of the rupture elongation of the lowest bolt-row (furthest from the centre of compression). It is evident that this first joint failure mode is directly caused by the buckling of the column, and subsequently the fire affected floor system deflects significantly to withstand the vertical loading on its own in double span with the absence of contributions from upper ambient floors. The deflected shape after column buckling of floor level 8 is illustrated in Figure 104.

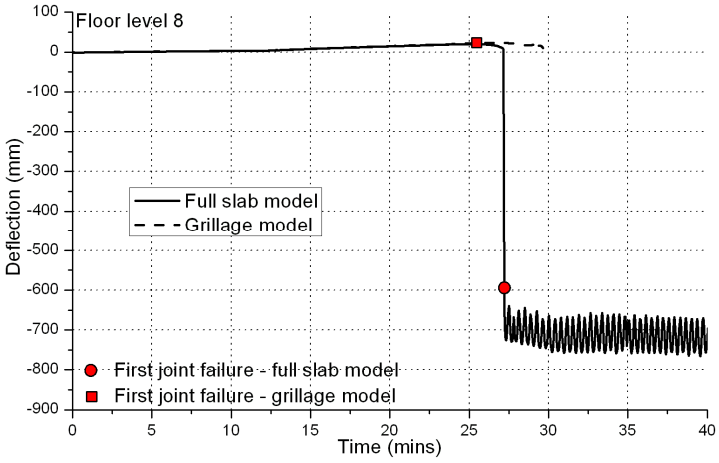

Figure 103. Deflection of fire affected floor for fire at floor level 8

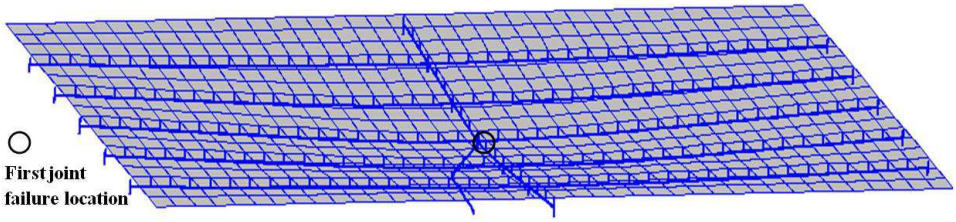

Figure 104. Deflected shape of floor level 8 at time = 25m25s (full slab model)

Importantly, no shear failure (punching shear) is observed in the fire affected beam-to-column joint before column buckling, and this can be explained through Figure 105, where the corresponding transferred shear force and the shear capacity of the fire affected joints are illustrated. Despite a complete loss of the resistance of the fire affected column, which directly leads to the first failure of the fire affected major axis beam-to-column joint, no successive surrounding ambient joint failure is induced in the double-span top floor system bridging over the buckled column. The final floor deflection is arrested at around 750mm without triggering progressive collapse. Therefore, sufficient robustness is exhibited for the reference car park subject to localised fire at the top floor when the full slab model is considered.

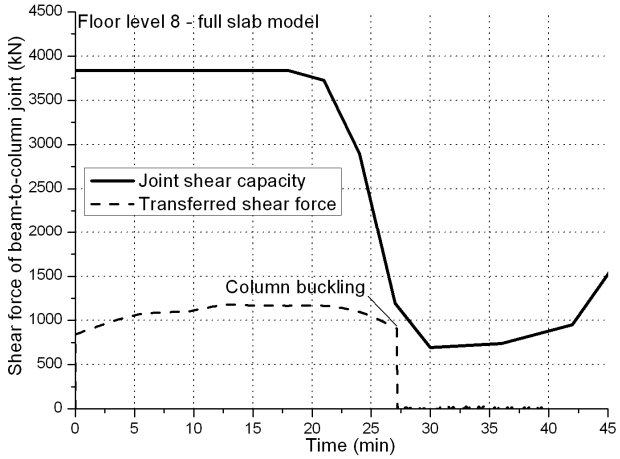

Figure 105. Shear response of fire affected joint for fire at floor level 8 (full slab model)

On the other hand, the grillage model predicts a different first joint failure mode, which occurs before column buckling in the secondary beam where the fire affected minor axis beam-to-column joint fails under hogging moment due to the rupture of the highest bolt-row (the elongation exceeds the maximum limit of 35mm), as shown in Figure 106(a). Afterwards, successive failure is induced in the ambient minor axis beam-to-column joints located at the other end of the secondary beam, as shown in Figure 106(b). No column buckling is observed due to a relatively lightly load resisted by the top floor fire affected column. It should be noted that the collapse stays localised in the failed secondary beam in a 'single-span' manner (i.e. the collapse of the secondary beam only). This is again attributed to the neglect of the 2D slab effect in the grillage model where the contributions from adjacent parts of the floor slab cannot be relied on.

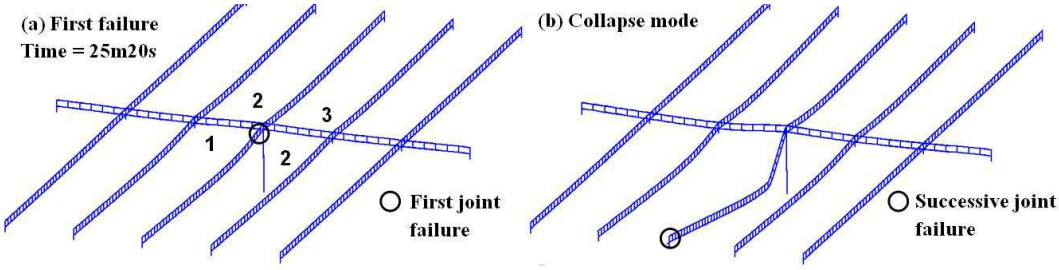

Figure 106. First and successive joint failures of grillage model for fire at floor level 8

XIII.2.4. Concluding remarks

This appendix presents a detailed discussion on the response of the reference car park under the selected localised fire scenario. Multi-level system models are employed for the structural analysis, where detailed 2D slab models and simplified grillage models of the floor systems have been used to investigate the robustness behaviour of the car park. The definition of overall system failure/progressive collapse is based on comparison of the ductility demand against the ductility supply offered by the surrounding joints, where the component method is employed to characterise the nonlinear joint response. Based on the overall structural analysis, the following comments and outcomes are noted:

- Three types of first joint failure are observed in the reference building subject to the selected fire scenario, namely, single-span failure type, double-span failure type and shear failure type (punching shear). For a typical car park structure where 2D slab effects, e.g. slab membrane action, are considered, the single-span failure type due to the failure of the fire affected joint under normal hogging moment before column buckling is less likely to occur. The other two first joint failure types can be more commonly found, and these are typically associated with column buckling and joint shear failure at elevated temperature. In reality, however, shear failure may not be easy to occur since the joint shear capacity in this project is evaluated in a conservative manner, i.e. yield capacity = shear resistance.
- The upper ambient floors can provide an alternative load path for the fire affected floor. Indeed, if the upper ambient floors can resist the redistributed vertical load under a double span configuration with relatively small deflections, and the fire affected floor can resist its load under a single span configuration, no successive collapse is expected unless punching shear occurs, even if the column under fire were to lose its resistance completely due to buckling.
- The grillage model predicts that the reference car park is susceptible to progressive collapse after first joint failure, while the full slab model predicts a more robust structure although first joint failure is also observed. This indicates that grillage approximations which are usually employed for conventional structural designs may be too conservative for structural robustness assessment. Under this circumstance, detailed 2D slab models are recommended for more realistic robustness assessment, particularly for structures where grillage models predict inadequate robustness.
- Based on the structural robustness predicted by the full slab models which indicate low potential for progressive collapse of the reference car park, it can be preliminarily concluded that under the considered fire scenario, typical modern multi-storey steel/composite car parks under unfactored gravity load can exhibit favourable robustness even in the absence of additional water sprinkler systems or anti-fire coatings.

XIII.2.5. References related to the WP3 appendix

Anderson D., Aribert J.M., Bode H., and Kronenburger, H.J. (2000). “Design Rotation Capacity of Composite Joints”. The Structural Engineer, 78:6, 25-29.

Eurocode 3: Design of steel structures – Part 1.8: Design of steel structures-Design of joints, European Committee for Standardization, 2005, May.

Eurocode 4: Design of composite steel and concrete structures – Part 1-1: General rules and rules for buildings. European committee for standardization, 2004, December.

Fang C., Izzuddin B.A., Elghazouli A.Y. and Nethercot D.A. (2011). “Robustness of Steel-Composite Building Structures Subject to Localised Fire”. Fire Safety Journal, 46:6, 348-363.

Hasemi Y., Yokobayashi Y., Wakamatsu T., and Ptchelintsev A.V. (1995). Fire Safety of Building Components Exposed to a Localized Fire – Scope and Experiments on Ceiling/Beam System Exposed to Localised Fire, ASIAFLAM’95, Hong Kong.

Izzuddin B.A., Vlassis A.G., Elghazouli A.Y. and Nethercot D.A. (2008). “Progressive Collapse of Multi-Storey Buildings due to Sudden Column Loss – Part I: Simplified Assessment Framework”, Engineering Structures, 30:5, 1308-1318.

Kuhlmann U., Davison J.B., Kattner M. (1998). “Structural Systems and Rotation Capacity”, Proceeding of COST Conference on Control of the Semi-rigid Behaviour of Civil Engineering Structural Connections, Liege, Belgium, 167–176.

Jarrett N.D. Axial Tests on Beam/Column Connections. (1990). “BRE Client Report CR 55/90”, Building Research Establishment, Garston, Watford, UK.

Owens G.W., and Moore D.B. (1992). “The Robustness of Simple Connections”. The Structural Engineer, 70:3, 37-46.

Vlassis A.G., Izzuddin B.A., Elghazouli A.Y., and Nethercot D.A. (2008) Progressive Collapse of Multi-Storey Buildings due to Sudden Column Loss – Part II: Application, Engineering Structures, 30:5, 1424-1438.